Characterization of the Arabidopsis compact inflorescence (cif) mutant and isolation of CIF1 to ACA10, a P-type IIB CAp2p+s-ATPase gene
by Lynn DeAnn George

A dissertation submitted in partial fulfillment of the requirement for the degree of Doctor of Philosophy in Biological Sciences
Montana State University

Abstract:
A mutant in Arabidopsis, called compact inflorescence (cif), was identified among the T2 progeny of an Agrobacterium transformant. The most apparent aspect of the cif phenotype was a strong reduction in the elongation of internodes in the inflorescence. Elongation and expansion of adult vegetative rosette leaves were also compromised in mutant plants while juvenile vegetative and reproductive organs developed normally.

Thus, cif mutant plants appeared to exhibit a novel, adult vegetative phase-specific phenotype. In hopes of gaining insight into the genetic mechanisms that underlie inflorescence architecture and vegetative phase specific identities, and regulate vegetative phase change, a study of this mutant was undertaken. The specific goals of this project included the following: 1) Characterize the altered development of the compact inflorescence mutant and its relation to plant developmental growth phases; 2) determine the genetic basis for inheritance of the cif trait; 3) through map-based cloning, determine the identity of genes whose altered alleles confer development of the cif phenotype; 4) determine the relationship of the CIF genes to developmental pathways that are known to influence vegetative phase change in flowering plants.

Results of the study confirm the restriction of the cif phenotype to a single plant developmental growth phase and describe the impact on the cif trait of exogenous hormone applications, changes in light quality, and variable photoperiods, compact inflorescence is inherited as a two-gene trait involving the action of a recessive locus, and a naturally occurring dominant locus. These two cif genes appear to be key components of a growth regulatory pathway that is closely linked to phase change. Recombinant frequency mapping of the CIF genes, and final isolation of the cif1-1 and cif1-2 alleles to mutations in ACAl 0, a gene encoding a P-type IIB Ca^2+ ATPase are described, as well as cloning of the ACAl0 gene and transgenic complementation of the cif1-1 mutation. Implications of the cif mutant phenotype in plant calcium signaling are also discussed.

CHARACTERIZATION OF THE *Arabidopsis compact inflorescence (cif)* MUTANT AND ISOLATION OF *CIF1* TO ACA10, A P-TYPE IIB CA^{2+}-ATPASE GENE

by

Lynn DeAnn George

A dissertation submitted in partial fulfillment
of the requirement for the degree

of

Doctor of Philosophy

in

Biological Sciences

MONTANA STATE UNIVERSITY
Bozeman, Montana

April 2003

APPROVAL

of a dissertation submitted by

Lynn DeAnn George

This dissertation has been read by each member of the dissertation committee and has been found to be satisfactory regarding content, English usage, format, citations, bibliographic style, and consistency, and is ready for submission to the College of Graduate Studies.

Robert Sharrock _____ 4/21/03
(Signature) Date

Approved for the Department of Biological Sciences

Jay Rotella _____ 29 April 2003
(Signature) Date

Approved for the College of Graduate Studies

Bruce McLeod _____ 4-29-03
(Signature) Date

STATEMENT OF PERMISSION TO USE

In presenting this dissertation in partial fulfillment of the requirements for a doctoral degree at Montana State University, I agree that the Library shall make it available to borrowers under rules of the Library. I further agree that copying of this dissertation is allowable only for scholarly purposes, consistent with "fair use" as prescribed in the U.S. Copyright Law. Requests for extensive copying or reproduction of this dissertation should be referred to Bell & Howell Information and Learning, 300 North Zeeb Road, Ann Arbor, Michigan 48106, to whom I have granted "the exclusive right to reproduce and distribute my dissertation in and from microform along with the non-exclusive right to reproduce and distribute my abstract in any format in whole or in part."

Signature Lynn Yeargen

Date 4/18/03

ACKNOWLEGMENTS

Foremost I would like to thank my advisor and major professor, Robert Sharrock. Dr. Sharrock has been a constant source of scientific expertise and encouragement throughout my graduate career. It has been a great privilege and pleasure to work in his laboratory. Second, I would like to thank Ted Clack whose technical expertise facilitated most aspects of my research. I would also like to thank Rich Stout for providing me unlimited access to his thermal cycler. I am extremely grateful to the undergraduate students Vanessa Berg and Erin Clifford who spent countless hours collecting tissue and extracting DNA. Finally, I would like to thank my son, Emmett, for being an inspiration to me, and my husband, Eric, for his constant support and encouragement.

TABLE OF CONTENTS

LIST OF TABLES

Table Page

LIST OF FIGURES

Figure Page

ABSTRACT

A mutant in *Arabidopsis*, called *compact inflorescence* (*cif*), was identified among the T_2 progeny of an *Agrobacterium* transformant. The most apparent aspect of the *cif* phenotype was a strong reduction in the elongation of internodes in the inflorescence. Elongation and expansion of adult vegetative rosette leaves were also compromised in mutant plants while juvenile vegetative and reproductive organs developed normally. Thus, *cif* mutant plants appeared to exhibit a novel, adult vegetative phase-specific phenotype. In hopes of gaining insight into the genetic mechanisms that underlie inflorescence architecture and vegetative phase specific identities, and regulate vegetative phase change, a study of this mutant was undertaken. The specific goals of this project included the following: 1) Characterize the altered development of the *compact inflorescence* mutant and its relation to plant developmental growth phases; 2) determine the genetic basis for inheritance of the *cif* trait; 3) through map-based cloning, determine the identity of genes whose altered alleles confer development of the *cif* phenotype; 4) determine the relationship of the *CIF* genes to developmental pathways that are known to influence vegetative phase change in flowering plants.

Results of the study confirm the restriction of the *cif* phenotype to a single plant developmental growth phase and describe the impact on the *cif* trait of exogenous hormone applications, changes in light quality, and variable photoperiods. *compact inflorescence* is inherited as a two-gene trait involving the action of a recessive locus, and a naturally occurring dominant locus. These two *cif* genes appear to be key components of a growth regulatory pathway that is closely linked to phase change. Recombinant frequency mapping of the *CIF* genes, and final isolation of the *cif1-1* and *cif1-2* alleles to mutations in ACA10, a gene encoding a P-type IIB Ca^{2+} ATPase are described, as well as cloning of the ACA10 gene and transgenic complementation of the *cif1-1* mutation. Implications of the *cif* mutant phenotype in plant calcium signaling are also discussed.

CHAPTER 1

A REVIEW OF *Arabidopsis thaliana*, PLANT DEVELOPMENTAL GROWTH PHASES, THE GENETIC REGULATION OF INFLORESCENCE ARCHITECTURE, AND PLANT CALCIUM SIGNALING

Introduction

A mutant in the plant *Arabidopsis thaliana* was identified among the T_2 progeny of an *Agrobacterium* transformant. This mutant, called *compact inflorescence (cif)*, exhibited an altered structure of the flowering bolt, or inflorescence, and onset of the mutant trait appeared to coincide with the transition between two plant developmental growth phases. A detailed characterization of the *cif* phenotype was initiated, as well as recombinant frequency mapping of the genes whose altered alleles confer inheritance of the mutant trait. The study confirmed the association of the *cif* phenotype with a single plant developmental growth phase, and culminated in the molecular isolation of a mutated Ca^{2+} ATPase gene. The following chapter comprises reviews of the model organism used for this study, plant developmental growth phases, the genetic regulation of inflorescence architecture, and plant Ca^{2+} signaling.

Arabidopsis thaliana – A Model Organism for Molecular Genetics

Biology of *Arabidopsis*

Arabidopsis thaliana, a small herbaceous annual of the Brassicaceae or mustard family, was named in 1842. The species name, *thaliana*, honors Johannes Thal, a XVIth-century German physician of Nordausen Thüringen who described *Arabidopsis* in 1577

in his book detailing the flora of the Harz Mountains (Rédei, 1992). Common names are mouse-ear cress and wall cress. In the wild, *Arabidopsis* grows in the moderate temperate climates of the northern hemisphere including Europe, Asia and North America. *Arabidopsis* is not likely indigenous to America though as its distribution coincides with the shipping routes of European grains imported by the settlers (Rédei, 1992). The most likely origination is the Central Asian highlands of the Western Himalayas (Berger, 1965; Rédei, 1970). Wild ecotypes of *Arabidopsis* are most commonly winter annuals with seed germination in the fall, survival through the winter as a vegetative rosette, and transition to flowering in early spring. Many different accessions of *Arabidopsis* have been collected from natural populations and are presently available for experimental analysis. The Columbia and Landsberg ecotypes are the accepted standards for genetic and molecular studies.

In greenhouse conditions, the entire life cycle of *Arabidopsis* is completed in approximately six weeks, and includes seed germination, formation of a vegetative rosette, bolting of the reproductive shoot, flowering, and maturations of seeds. The flowers of *Arabidopsis* are 2-4 mm long, self-pollinate, and can be easily crossed by applying pollen to the surface of the stigma. Each flower has an outer whorl with 4 green sepals, and inner whorls containing four white petals, six stamens bearing pollen, and a central gynoecium. The ovary within the gynoecium develops into a silique that contains 30 to 60 seeds. A single plant may have more than 200 flowers during its life and thus may produce more than 10,000 seeds. Mature plants reach 15 to 20cm in height.

A History of *Arabidopsis* Research

Friedrich Laibach initiated the use of *Arabidopsis* as an experimental organism in 1907 (Rédei, 1992). He conducted the first deductive experiments in *Arabidopsis* including accurately counting the 10 somatic and 5 meiotic chromosomes. Laibach was also first to note that the amount of chromatin in *Arabidopsis* was only about one third that of other members of the Brassicaceae. Laibach's work that most significantly impacted the use of *Arabidopsis* as an experimental organism was published in Botanisches Archiv in 1943 wherein he notes the features of *Arabidopsis* that make it particularly well suited to experimental classical genetics (Rédei, 1992). Some of these features include: 1) small size; 2) rapid generation time (5-6 weeks under optimal growth conditions); 3) ability to grow well in controlled conditions (either on soil or defined media); 4) ease of cross- and self-fertilization; 5) fecundity (up to 10,000 seeds per plant); 6) small chromosome number; and 7) ease of mutagenesis.

George P. Rédei introduced *Arabidopsis* as a model system for plant genetics to the United States in 1965 (Rédei, 1992). Heslot et al. first described the use of ethylmethane sulfonate as a chemical mutagen in 1959, and its great efficiency in *Arabidopsis* was demonstrated by Röbbelen in 1962 and McKelvie in 1963 (Rédei, 1992). *Arabidopsis* research became more prevalent in the early 1980's with the release of a detailed genetic map and publications outlining the value of *Arabidopsis* for research in plant physiology, biochemistry, and development. This was followed by a subsequent advance, the establishment of a transformation system using co-cultivation with disarmed cointegrate agrobacterial vectors by Lloyd *et al.* in 1986 (Rédei, 1992). The discovery

that the size of the *Arabidopsis* nuclear genome is the smallest known among flowering plants (Sparrow et al., 1972; Leutwiler et al., 1984), and that it contains a very low level of dispersed repetitive DNA (Pruitt and Meyerowitz, 1986) prompted the development of *Arabidopsis* as a model system for molecular as well as classical genetics.

The modern era of *Arabidopsis* research began in 1987 with the opening of the Third International *Arabidopsis* Conference at Michigan State University and the subsequent formation of an electronic *Arabidopsis* newsgroup (Meinke, 1998). Numerous researchers experienced in the analysis of other model organisms began to study *Arabidopsis* as a promising model for basic research. An important outgrowth of this increased enthusiasm for *Arabidopsis* research was the drafting in 1990 of a vision statement outlining long-term research goals for the *Arabidopsis* community. These included saturating the genome with mutations, identifying every essential gene, and sequencing the entire genome by the end of the decade (Meinke, 1998). The importance of applying advances with *Arabidopsis* to other plants and to solving practical problems in agriculture, industry, and human health was also stressed. In 1994, several European labs cooperatively began a pilot-sequencing project of the *Arabidopsis* genome (Pennisi, 2000). The project quickly grew to 17 European groups under the coordination of Michael Bevan, a geneticist at the John Innes Centre in Norwich, United Kingdom. In 1996, the sequencing effort expanded to form an international consortium known as the *Arabidopsis* Genome Initiative and included the Institute for Genomic Research (TIGR) in Rockville, Maryland, Cold Spring Harbor Laboratory, Washington University, Stanford University, the University of Pennsylvania, the University of California,

Berkeley, and Kazusa DNA Research Institute in Kisarazu, Japan. This initiative became a model for multinational cooperation and resulted in the sequencing of 118.7 million base pairs of the 125 million base pair *Arabidopsis* genome.

Genetic Analysis

The *Arabidopsis* research community has developed most of the methods and resource materials expected of a model genetic organism. These include simple procedures for chemical and insertional mutagenesis, efficient methods for performing crosses and introducing DNA through plant transformation, extensive collections of mutants with diverse phenotypes, and a variety of chromosome maps of mutant genes and molecular markers. The absence of an efficient system for homologous recombination in *Arabidopsis* is a limitation shared by some other model organisms including *Drosophila melanogaster* and *Caenorhabditis elegans* (*C. elegans*).

Integration of cloned DNA into the *Arabidopsis* genome, or plant transformation, is routinely performed through the use of the pathogenic bacterium *Agrobacterium tumefaciens*, a technique that was pioneered during the late 1980's (Schell, 1987; Horsch et al., 1986; Weising et al., 1988; Zambryski, 1988). *Agrobacterium* is a soil organism that, in nature, induces the tumorous growths of crown-gall disease on susceptible host plants. During the initial stages of tumorigenesis, a defined region of *Agrobacterium* DNA, the T-DNA, is physically transferred from a bacterial plasmid (the Ti plasmid) into the nuclear genome of the infected plant cell. The T-DNA is flanked by 24-bp imperfect direct repeats which are required in *cis* for transfer. A set of genes outside the T-DNA, called the virulence (*vir*) genes, act in trans to promote T-DNA transfer. The T-DNA

contains genes that direct the synthesis of the phytohormones auxin and cytokinin and through the overproduction of these compounds within the transformed plant, uncontrolled cell division characteristic of a tumor results.

Genetic researchers have disarmed *Agrobacterial* strains by deleting the tumor-inducing genes. These disarmed strains are no longer tumorigenic, but are still fully transfer proficient and DNA inserted between the 24-bp repeats will be randomly and stably integrated into the plant genome. Currently, a binary-plasmid system is generally used for *Agrobacterium*-mediated plant transformation. The *vir* genes have been maintained on the Ti plasmid, while the *cis*-acting repeat sequences have been placed on relatively small plant transformation vectors capable of replicating both in *E. coli* and *Agrobacterium.* Between the *cis*-acting repeat sequences are multiple cloning sites that allow the insertion of gene constructs of interest, and a selectable marker gene that confers resistance to specific antibiotics upon transformed plant cells. The most widely used antibiotic resistance gene product is the bacterial neomycin phosphotransferase type II (NPTII) enzyme that detoxifies compounds such as Kanamycin and G418 by phosphorylation. Initially, *Arabidopsis* researchers used wounded tissue or entire seeds as the starting plant material to be transformed. More recently, floral dipping methods, that avoid plant regeneration through tissue culture, have made plant transformation routine (Clough and Bent, 1998). It has been shown that the ovule is the target of T-DNA integration in the floral dipping method (Desfeux et al., 2000). The main drawbacks of T-DNA transformation are the often complex integration patterns of T-DNA, including transfer of vector sequences that flank the T-DNA, multiple insertions,

and the high frequency of concatemeric insertions, which in T-DNA mutagenesis (see below) can complicate the identification of flanking sequences.

Agrobacterium-mediated plant transformation has been used extensively in T-DNA mutagenesis of *Arabidopsis*. Thousands of transgenic lines carrying random T-DNA insertions throughout the genome have been deposited in public stock centers. Many additional lines are being produced at private companies interested in functional genomics. Maize transposable elements introduced through *Agrobacterium*-mediated transformation have also been used extensively for gene disruption in *Arabidopsis*. Chemical mutagenesis, with alkylating agents such as ethylmethane sulfonate (EMS), has also been used extensively for genetic analysis. Mature seeds are the preferred targets for chemical mutagenesis as selfing M1 plants derived from a single experiment can produce millions of progeny seeds homozygous for recessive mutations. Bulk collection and screening of M_2 seeds requires only a small area: 10,000 seeds can be germinated in a single Petri dish, and selection for a particular phenotype among hundreds of thousands of newly germinated seedlings is possible.

The success of *Arabidopsis* as a model organism is primarily due to its amenability to forward genetic screens wherein mutagenized plants are screened for phenotypes of interest. Through insertional and chemical mutagenesis techniques, several thousand mutants of *Arabidopsis* defective in almost every aspect of plant growth including gametogenesis, seed formation, leaf and root development, flowering, senescence, metabolic and signal transduction pathways, responses to hormones, pathogens, and environmental signals, and many cellular and physiological processes

have been identified. Forward genetic screens culminate in the molecular isolation of the mutated gene, allowing the assignment of a developmental function to the wild-type allele. Once a mutation that affects a particular developmental or metabolic pathway has been identified, secondary screens allow further dissection of the pathway that is affected by the mutation. A screen for second-site mutations that enhance (worsen) the phenotype, generally identify genes that act redundantly with the primary mutation or possibly interact physically with the mutant gene product. Alternatively, enhancer mutations may uncover a partially redundant parallel pathway. Suppressor mutations identify interacting proteins, or downstream pathways that become activated by the second-site suppressor.

Genetic screens have also been developed to identify genes that affect epigenetic information including methylation profiles that contribute information for controlling developmental pathways. Unlike other model systems including mouse, *Arabidopsis* tolerates large defects in epigenetic regulation. The *Arabidopsis ddm1* mutant (*decrease in DNA methylation1*) exhibits a reduction in genome-wide cytosine methylation by 70%, but is viable and fertile (Vongs et al., 1993). Thus *Arabidopsis* is particularly well suited for studying epigenetic phenomena.

The availability of reporter genes, in combination with efficient transformation methods in *Arabidopsis,* make biological processes with subtle or hidden phenotypes accessible to forward genetic approaches. Typically, a reporter gene encoding firefly luciferase (LUC), β-glucuronidase (GUS) or green fluorescent protein (GFP) is fused to the promoter of a specifically regulated inducible gene. This allows for observation of

the wild-type expression pattern of the inducible gene. Subsequent mutagenesis of such lines allows screening for a deviation from the wild-type expression pattern and the identification of genetically interacting loci. This type of screen has been used since the late 1980s and has allowed the identification of important genes in the circadian system (Millar, 1995), hormone-signaling pathways (Meier et al., 2001), and in plant responses to biotic (Bowling et al., 1994) and abiotic stresses (Xiong et al., 2001). All of these are extremely difficult to detect in conventional phenotypic screens.

Plants were the first organisms in which the silencing of introduced DNA was observed (Napoli, 1990). Since then, numerous examples have confirmed the specific inactivation of a transgene either at the transcriptional level (transcriptional gene silencing, TGS) or after transcription (post-transcriptional gene silencing, PTGS) (Matzke et al., 2001). In PTGS, the mRNA of a transgene is specifically degraded. If endogenous mRNA, homologous to the transgene RNA, is also present, expression of the endogenous gene will also be silenced, (Matzke et al., 2001). Although gene silencing was initially perceived as an uncontrollable and unwanted source of instability of transgene expression, it offered an entry point for the genetic analysis of silencing mechanisms (Page and Grossniklaus, 2002). Studies of PTGS in *Arabidopsis* led to the establishment of a molecular link between PTGS in plants, Quelling in *Neurospora crassa* and RNA Interference in *C. elegans* (Page and Grossniklaus, 2002).

Reverse genetic research proceeds from genotype to phenotype; different mechanisms are used to silence or alter the expression of a particular gene of interest and the effects of this genetic change on the development of the organism indicate gene

function. Reverse genetic screens depend on the researcher's judgment of the candidacy of a gene by sequence alone and thus are biased and perhaps less likely to lead to new insights than unbiased forward screens. However, the *Arabidopsis* researcher currently has access to very powerful tools for taking the reverse genetics approach. Disruption of a gene itself is generally the most direct way to understand its function. Unlike other model systems, such as yeast or mouse, no efficient methods for targeted gene disruption exist in flowering plants. Transposons or T-DNA are used as more or less random mutagens to create loss-of-function mutations. Because the sequence of the inserted element is known, the gene in which it is inserted can be recovered using various cloning or PCR-based strategies. The Nottingham *Arabidopsis* Stock Centre (NASC), the Salk Institute, the Flanking Sequence Tags (FST) project at Versailles and the Torre Mesa Research Institute (TMRI) all maintain insertion databases that can be searched for known insertions in a gene of interest. The Knockout Facility at the University of Wisconsin, Madison maintains large populations of T-DNA insertion lines and offers a service whereby pools of independent T-DNA lines are screened to obtain a 'knockout' mutation in a gene of interest. Anti-sense technology utilizing PTGS can also be used to effectively "knockout" the expression of a chosen gene (Ruban et al., 2003; Laval et al., 2003).

A powerful tool in reverse genetics, called TILLING (Targeting, Induced Local Lesions IN Genomes), has recently become available to the *Arabidopsis* researcher. TILLING is a high-throughput, PCR-based screen for EMS-induced point mutations within a specific gene (McCallum et al., 2000). The technology is based on an

endonuclease that preferentially cleaves mismatches in heteroduplexes between wild-type and mutant DNAs. Subsequent analysis of cleavage products on a sequencing gel allows the rapid identification of induced point mutations. Unlike insertional mutagenic approaches that generally result in knockout mutations, TILLING provides an allelic series of point mutations in a gene of interest. This approach is especially valuable for analyzing the function of essential genes in which knockout mutations would be lethal.

The *Arabidopsis* Genome

Through an international consortium known as the *Arabidopsis* Genome Initiative, 118.7 megabases of the *Arabidopsis* 125 megabase genome sequence was released in the year 2000, and represents the first complete sequence of a plant nuclear genome (The *Arabidopsis* Genome Initiative, 2000). With the fewest gaps and most substantial extension into centromeric regions, the sequence obtained was also the most accurate sequence available for any organism, over that of *Saccharomyces cerevisiae, C. elegans,* and *Drosophila.* An extensive analysis of the *Arabidopsis* genome sequence was published by The *Arabidopsis* Genome Initiative in the journal *Nature* (2000) **408:** 796-813. A brief summary of that analysis follows.

The *Arabidopsis* genome contains approximately 25,500 genes encoding proteins from 11,000 different families. This functional diversity is similar to that of two other multicellular eukaryotes, *Drosophila* and *C. elegans,* indicating that a proteome of 11,000-15,000 protein types is sufficient for a wide diversity of multicellular life. Only 9% of the proposed 25,500 *Arabidopsis* genes have been characterized experimentally. However, from their similarity to proteins of known function in other organisms, 69% of

Arabidopsis proteins have been assigned a putative function. The *Arabidopsis* genome contains roughly 150 protein families that appear to be unique to plants. *Arabidopsis* genes tend to be compact, with an average gene length of approximately 2,000 kb per gene. *Arabidopsis* genes typically contain coding regions of about 250 base pairs each, punctuated by short introns. The genes are closely spaced, about 4.6 kb apart, indicating that their regulatory regions are also short. The exons in *Arabidopsis* are richer in guanosine and cytosine bases (44%) than are the introns (32%), a feature that is unique to plant genes. Approximately 60% of the *Arabidopsis* genome has been duplicated. The large-scale duplication, but not triplication, suggests that *Arabidopsis* had a tetraploid ancestor. Sequence comparisons between *Arabidopsis* and tomato indicate that this duplication event likely occurred around 112 million years ago. Gene loss and chromosomal rearrangements presumably generated the small genome and five chromosomes of the *Arabidopsis* we know today.

Approximately one-fifth of the intergenic DNA, or 10% of the genome is represented by transposons in *Arabidopsis*. In several cases, genes appear to have been included as 'passengers' in transposable units. *Arabidopsis* telomeres are composed of CCCTAAA repeats and average between 2-3 kb. The *Arabidopsis* genome project gave the first detailed picture of centromeric sequences in a higher eukaryote. *Arabidopsis* centromeres, like those of many higher organisms, contain numerous repetitive elements including retroelements, transposons, microsatellites and middle repetitive DNA. Such repetitive regions are very likely heterochromatic, and are generally viewed as poor environments for gene expression. However, 47 expressed genes were found to lie

within the centromeres of *Arabidopsis*. In several cases, the genes were found residing on islands of unique sequence flanked by repetitive arrays.

The *Arabidopsis* genome sequence also offers unique avenues for studying gene regulation and signal transduction. Consistent with its rather highly methylated genome, *Arabidopsis* possesses eight DNA methyltransferases (DMTs), including a chromomethyltransferase that is unique to plants. Transcription in *Arabidopsis* by RNA polymerases II and III appears to involve the same machinery as is used in other eukaryotes although most transcription factors for RNA polymerase I are not found. Only two polymerase I regulators (other than ploymerase subunits and TATA-binding protein) are found in *Arabidopsis*. Surprisingly, the *Arabidopsis* genome was found to encode atypical subunits for the largest and second largest subunits of polymerase I, II and III. These novelties may endow plant-specific functions. *Arabidopsis* possesses twice as many transcription factors as *Drosophila*, and more than three times as many transcription factors as *C. elegans*. The most widely used signaling pathways in vertebrates, flies, and worms, including Wingless/Wnt, Hedgehog, Nothch/lin12, JaK/Stat, TGF-β/SMADs, receptor tyrosine kinase/Ras and the nuclear steroid hormone receptors are all absent in *Arabidopsis*. However, 340 transmembrane receptor-like kinase (RLK) genes are found in the *Arabidopsis* genome, of which Ser/Thr kinases comprise the largest class. With the exception of CLV1, the ligands sensed by RLKs are essentially unknown, providing a compelling avenue for future research. While there are approximately twenty MAP kinases found in *Arabidopsis*, a higher number than in any other eukaryote, there is potentially only a single heterotrimeric G-protein complex.

With the full genome sequence in hand, the *Arabidopsis* community has recently taken on a more challenging goal yet. A new 10-year project, called the NSF 2010 Project, seeks to determine the function of every *Arabidopsis* gene by the year 2010 (Somerville and Dangl, 2000). To this end, every *Arabidopsis* gene will be inactivated or overexpressed. The resulting phenotypes will be examined by all available criteria, including full-genome mRNA expression profiling and metabolic profiling. Comprehensive information will be available about where and when every gene is expressed; where the protein is localized; how the protein is modified; and with what, if any, other proteins the gene product interacts. Additional goals of the 2010 project include determining the substrates for every protein kinase, and the promoters controlled by each transcription factor. In cases where genes have apparent functional redundancy, the phenotype of the multiple mutant will be determined. It is envisioned that this knowledge will facilitate the development of a virtual plant – a computer model that will use information about each gene product to simulate the growth and development of a plant under many environmental conditions (Somerville and Dangl, 2000).

Phase Change in Flowering Plants

Flowering plants pass through a succession of three major post-embryonic developmental stages, or phases, during their life cycle: juvenile vegetative, adult vegetative, and reproductive (Poethig, 1990; Lawson and Poethig, 1995; Kerstetter and Poethig, 1998). The juvenile vegetative phase begins when the shoot apical meristem generates a stem, true leaves and axillary buds. This phase may last for a few days or

many years, depending on the species, and is distinguished by unique morphological and physiological traits, including leaf shape, trichome distribution, and by the absence of reproductive capacity. The subsequent adult vegetative phase is characterized by changes in these morphological traits and by the development of a competency of the shoot to shift into reproductive growth. Reproductive phase is characterized by the production of flowers in place of leaves. In many flowering plants, including *Arabidopsis*, the transition to reproductive growth is accompanied by the generation of an inflorescence, an elongated scaffold of stem and leaf structures, which supports and presents the reproductive organs or flowers. Although the elongated internodes and small cauline leaves of the inflorescence develop after what is usually considered to be the initiation of reproductive phase, these organs are essentially "vegetative" tissues.

Although progression through two distinct phases of rosette development (i.e. juvenile and adult) is a recognized component of plant life cycles, little is known regarding the genetic basis for the regulation of vegetative phase change (Kerstetter and Poethig, 1998). Goebel (1900) originally proposed that a single morphogenetic program controls the development of all leaf types in flowering plants. He hypothesized that variation in leaf morphology arises because different parts of a leaf primordium are arrested at different points along this pathway (Kerstetter and Poethig, 1998). Much experimental evidence contradicts this early hypothesis however, and supports the modern view that juvenile and adult leaves are specified by distinct developmental programs (Kerstetter and Poethig, 1998). Strong evidence in support of this view comes from the study of phase change mutants in maize. The dominant gain-of-function *Teopod*

mutations result in the prolonged expression of juvenile traits (Evans and Poethig,1995; Poethig, 1988). The expression of adult traits however, including reproductive competence, is unaffected. The leaves of *Teopod2* mutants are morphologically and anatomically intermediate structures, combining features that are normally specific to either juvenile or adult leaves. The phenotypes of the *teopod* mutants suggest that the *TP* genes regulate a juvenile program of leaf identity that operates in parallel to, and to some extent independently of the program that specifies adult traits (Kerstetter and Poethig, 1998).

In recent years, large advancements have been made toward understanding the genetic mechanisms and developmental pathways that control the transition to reproductive growth. Meristem patterning, or the establishment of precise localities of gene expression, is very likely the primary process governing floral morphogenesis (Coen and Meyerowitz, 1991; Weigel and Meyerowitz, 1994). Thus, the specific meristem domain in which the organ originates determines floral organ identity. Like flower development, meristem patterning could also play a major role in determining the identities of juvenile and adult leaves and in vegetative phase change. However, there is strong evidence that argues against a meristem-patterning model in vegetative development. Clonal analyses in maize suggest that there is no cell lineage restriction between juvenile and adult organs of the shoot (Poethig et al., 1986). That adult phase maize shoots can be readily induced to revert to the juvenile phase in culture (Kerstetter and Poethig, 1998) further implies that the shoot meristem does not possess developmentally determined juvenile and adult domains. The development of leaves that

are transitional between the juvenile and adult vegetative phases argues perhaps most strongly against a meristem-patterning model for the specification of vegetative organ identity (Kerstetter and Poethig, 1998). In maize and in *Arabidopsis*, the distal region of transitional leaves often expresses juvenile traits while the basal region expresses adult traits (Goebel, 1900; Bongard-Pierce et al., 1996; Telfer et al., 1997). Such development suggests that upon induction, phase change occurs globally, in all cells of the meristem and in all undetermined cells in preexisting organs. Because leaves mature basipetally, regions at the tip of preexisting leaves are likely to have already become determined for the previous developmental state, whereas basal regions of the leaf will still have the capacity to switch to the new state. Hence, this model suggests that vegetative phase change comprises global changes in gene expression throughout the meristem and undetermined regions of preexisting organs such that organ identity is determined temporally depending on maturation of the shoot, rather than spatially (Kerstetter and Poethig, 1998).

To date, no *Arabidopsis* genes have been identified that are differentially expressed between the juvenile and adult phases of vegetative growth. Furthermore, little is known regarding the signaling mechanisms that trigger the global changes in gene expression that likely result in vegetative phase change (Kerstetter and Poethig, 1998). Relatively few phase-associated mutations have been described in *Arabidopsis*, all of which affect the timing of the phase transitions rather than the development of phase-specific organ morphologies. Most phase mutants in maize also exclusively affect the timing of phase transitions.

Genetic Regulation of Inflorescence Architecture in Flowering Plants and Mutants Affecting Internode Elongation and Inflorescence Development

As outlined above, *Arabidopsis* exhibits separate vegetative and reproductive growth phases. The vegetative phase, called the rosette, is characterized by the production of leaves in a spiral with very little stem elongation between leaves. A group of parental cells at the center of the rosette, termed the shoot apical meristem (SAM), provides the initials that differentiate into leaf and stem cells. Upon transition to the reproductive phase, the SAM begins to produce flowers in place of leaves. In most angiosperms, this transition is accompanied by dramatic elongation of internodes within the stem/shoot system resulting in the production of a showy, flower-bearing bolt called the inflorescence. Elongation of internodes is accomplished via numerous cell divisions in the apical region of the internode coupled with extensive cell enlargement. These processes occur after the SAM has moved slightly upward, and thus are considered a phase of development distinct from the generation of inflorescence initials by the SAM (Steeves and Sussex, 1989). *Arabidopsis* exhibits a high degree of internode elongation in both the primary inflorescence stem and in lateral branches such that an extended bolt called a compound raceme is produced.

Elongation of inflorescence internodes is a trait of particular significance in determining plant reproductive architecture and, hence, in the evolution of flowering plants. Long internodes generate a more conspicuous reproductive structure that functions in the crucial roles of presenting reproductive organs to pollinators and dispersal of seeds. Moreover, the vast array of inflorescence designs observed among

flowering plants results in large part from the differential elongation of inflorescence internodes. Bradley et al. (1996b) have proposed the existence of at least three pathways in *Antirrhinum* that determine inflorescence traits, including internode length, cauline leaf morphology, hairiness of the stem, and phylotaxy. Two of these pathways were shown to be independent of genes that control floral meristem identity, such as *Floricaula*, the homolog of *Leafy* in Arabidopsis (Bradley et al., 1996a), drawing a distinction between inflorescence and floral development.

Different inflorescence traits have also been strongly selected for during the domestication of many crop plant species. For example, modification of inflorescence branching patterns and apical dominance by allelic variation at the *teosinte branched* locus has been shown to be a major component of the evolution of cultivated maize from its wild ancestor teosinte (Doebley et al., 1997). This finding in maize illustrates the importance of genetic variation in relatively few critical regulatory genes in the origins of cultivated plant architectures.

Despite their importance in plant morphogenesis, the mechanisms through which specific plant cells are signaled to divide and expand and how these mechanisms are regulated at developmental transitions is poorly understood. Attempts have previously been made to isolate mutants of *Arabidopsis* that maintain normal vegetative growth and normal floral meristem identity but exhibit altered inflorescence development. One candidate for such a mutation is *erecta*, found in the common Landsber *er* strain, which produces plants with reduced height, somewhat clustered flowers, and short petioles and siliques (Torii et al., 1996). The *ERECTA* locus has been cloned and encodes a receptor-

like protein kinase that is expressed in the shoot apical meristem and in organ primordia (Tori et al., 1996; Yokoyama et al., 1998). Recently, more loci similar to *erecta*, called *corymbosa*, have been identified (Komeda et al., 1998). A large screen of mutagenized *Arabidopsis* for mutants with short flower stalks resulted in the identification of the *acaulis* mutants (Tsukaya et al., 1993; Hanzawa et al., 1997). The *ACAULIS5* gene has recently been shown to encode a spermine synthase (Hanzawa et al., 2000). However, all of these mutants are quite pleiotropic in their effects, altering growth of juvenile and adult vegetative tissues, overall plant stature, and in some cases, the number of flowers produced and the development of fruits. Hence, the *ERECTA, CORYMBOSA,* and *ACAULIS* loci are likely to be important generally in signaling appropriate growth regulation during organ formation in the plant, but are not restricted in their activities to a specific phase of plant development.

Calcium Signaling in Higher Plants

Calcium as a Signaling Molecule in Plants

Plant cells use a variety of messengers in signaling pathways including Ca^{2+}, lipids, pH, and cyclic GMP. No single messenger however, has been demonstrated to respond to more stimuli, both biotic and abiotic, than has cytosolic free Ca^{2+} (Sanders et al., 1999). Biotic stimuli that alter Ca^{2+} levels include the hormones abscissic acid and gibberellin, fungal elicitors, and nodulation factors. Abiotic stimuli include light (with red, blue, and UV/B irradiation each acting via different receptors and leading to distinct developmental responses), low and high temperature, touch, hyperosmotic stress, and

oxidative stress (Sanders et al., 2002). Calcium signals are generated through the opening of ion channels that allow the flow of Ca^{2+} from an area in which the ion is present at a relatively high concentration to an area of lower concentration. Plant cells generally maintain a very low cytosolic level of calcium, on the order of micromolar concentrations, whereas the extracellular fluid contains relatively high levels, on the order of millimolar concentrations. Although the electrochemical potential across the membranes of organelles is likely to be less negative than that across the plasma membrane, a number of intracellular compartments also serve as important reservoirs of Ca^{2+} ions. While the endoplasmic reticulum, mitochondria, and chloroplasts have all been shown to sequester Ca^{2+}, the large lytic vacuole of mature plant cells is the principal intracellular Ca^{2+} store (Sanders et al., 1999; Sanders et al., 2002). Maintenance of low cytosolic Ca^{2+} ion concentrations is achieved by either the ATP-driven removal of Ca^{2+} through pumps, or by the proton motive force-driven removal by carriers. The interplay between influx of Ca^{2+} through channels, and efflux from pumps and carriers determines the profile of a Ca^{2+} spike.

To date, the best understood calcium signal transduction pathway in plants controls the opening and closing of stomata by guard cells within the epidermis (Geisler, 2000). Here, voltage-gated Ca^{2+} release channels, and inositol 1,4,5-triphospahate and cADP-ribose-sensitive calcium release pathways function in the generation of calcium signatures (Geisler et al., 2000). The specific transduction events involved in stomatal closure that occur downstream from calcium however are not known. In general, the initial perception of a calcium signal occurs through the binding of calcium to many

different calcium sensors. Ca^{2+} sensors in plant systems can be divided into two types, sensor relays and sensor responders (Sanders et al., 2002). Sensor relays, such as calmodulin, undergo a calcium-induced conformational change (sensing) that is relayed to an interacting partner. The interacting partner then responds with some change in its enzyme activity or structure (for example, calmodulin stimulation of a calcium pump). In contrast, sensor responders undergo a calcium-induced conformational change (sensing) that alters the protein's own activity or structure. A primary class of Ca^{2+} sensor responders is the calcium-dependent protein kinase (CDPK) family. Most of the known calcium-stimulated protein kinase activities in plants are associated with CDPKs. Despite their major role in plant Ca^{2+}-signaling, CDPKs are found only in some protozoans and are absent from the genomes of *Saccharomyces cerevisiae*, *C. elegans*, *Drosophila*, and humans (Cheng et al., 2002). Four distinct domains typify CDPK family members: an N-terminal variable domain, a protein kinase domain, an autoinhibitory domain, and a calmodulin-like domain. The calmodulin-like domain contains Ca^{2+}-binding EF hands that allow the protein to function as a Ca^{2+} sensor (Cheng et al., 2002). Under the basal condition of low free Ca^{2+}, the autoinhibitory domain acts as a pseudosubstrate and is bound by the kinase domain, keeping substrate phosphorylation activity low (Harmon et al., 1994). Upon binding Ca^{2+} via the EF hand motifs, CDPKs undergo conformational changes that release the pseudosubstrate from the catalytic site, activating the protein. Little is known about the function of the N-terminal variable domain. It has been proposed that this region contains subcellular targeting information (Harper et al., 1994). Many plant CDPKs have a Gly residue at the

second position (Cheng et al., 2002). This N-terminal residue can be modified by covalent attachment of myristic acid, which promotes protein-membrane and protein-protein interactions. The *Arabidopsis* genome is predicted to encode 34 different CDPKs and the precise biological function(s) of most of these enzymes is not known (Cheng, 2002). By definition, sensor responders function through intramolecular interactions, whereas sensor relays function through bimolecular interactions. These two different modes of decoding calcium signals are used extensively in plants to provide many pathways by which calcium can trigger a diverse number of responses (Sanders et al., 2002).

Why Calcium?

Metabolism in all cells requires the presence of orthophosphate (P_i) and phosphorylated organic compounds, particularly for cytosolic reactions associated with the transduction of free energy (Sanders et al., 1999). Together, Ca^{2+} and P_i have a low solubility product, which indicates that at relatively high calcium concentrations, the availability of soluble P_i decreases drastically. For this reason, mechanisms for reducing cytosolic Ca^{2+} concentrations to a level well below the millimolar concentrations present in seawater would have arisen early in evolution (Sanders et al., 1999). Indeed, transport systems that export Ca^{2+} from the cytosol are present in all cells to sustain steady state values of cytosolic Ca^{2+} in the submicromolar range. Such mechanisms for maintaining Ca^{2+} homeostasis would have been ideal for subsequent evolution of Ca^{2+} based signaling pathways (Sanders et al., 1999). Specifically, the elevation of cytosolic Ca^{2+} levels by a

factor of 10 or 20 can occur more rapidly than would be possible for ions or solutes that are maintained at millimolar levels (Sanders et al., 1999).

The chemistry of Ca^{2+} also lends itself to signal transduction (Sanders et al., 1999). The ability of a Ca^{2+} ion to coordinate numerous uncharged oxygen atoms enables the evolution of protein conformations in which remote domains can participate in calcium binding. It has been shown that calcium-induced conformational changes can elicit downstream events in signaling pathways (McPhalen et al., 1991).

Specificity in Calcium Signaling

As stated previously, changes in cytosolic Ca^{2+} occur during the transduction of a wide variety of abiotic and biotic signals. During the last ten years of calcium signaling research, a single question has pervaded the field (McAinsh and Hetherington, 1998). How can a simple non-protein messenger be involved in a multitude of signal transduction pathways and yet convey stimulus specificity within these pathways? Growing evidence indicates that signal specificity is inherent in the amplitude and frequency of Ca^{2+} waves within the cytosol. The dynamic profile of a calcium wave is determined by the combinatory effects of influx through channels and efflux patterns through pumps and carriers. Research in two nonplant systems (Xenopus oocytes and Dictyostelium) has demonstrated that increasing the abundance or activity of a Ca^{2+} pump can indeed alter signal transduction (Lechleiter et al., 1998; Roderick et al., 2000). Thus, in addition to their housekeeping functions, efflux pathways play an integral role in defining the information encoded in a calcium signal.

Statement of the Problem

A mutant in *Arabidopsis*, called *compact inflorescence* (*cif*), was identified among the T_2 progeny of an *Agrobacterium* transformant. The most apparent aspect of the *cif* phenotype was a strong reduction in the elongation of internodes in the inflorescence. Elongation and expansion of adult vegetative rosette leaves were also compromised in mutant plants while juvenile vegetative and reproductive organs developed normally. Thus, *cif* mutant plants appeared to exhibit a novel, adult vegetative phase-specific phenotype. In hopes of gaining insight into the genetic mechanisms that underlie inflorescence architecture and vegetative phase specific identities, and regulate vegetative phase change, a study of this mutant was undertaken. Results of the study implicate alterations in Ca^{2+} signaling. The specific goals of this project included the following:

1) Characterize the altered development of the *compact inflorescence* mutant and its relation to plant developmental growth phases.
2) Determine the genetic basis for inheritance of the *cif* trait.
3) Through map-based cloning, determine the identity of genes whose altered alleles confer development of the *cif* phenotype.
4) Determine the relationship of the *CIF* genes to developmental pathways that are known to influence vegetative phase change in flowering plants.

CHAPTER 2

THE *Arabidopsis compact inflorescence* GENES: PHASE-SPECIFIC GROWTH REGULATION AND THE DETERMINATION OF INFLORESCENCE ARCHITECTURE

Introduction

Flowering plants go through a succession of developmental stages, or phases, during their life cycle. Three major phases have been described: juvenile vegetative, adult vegetative, and reproductive (Poethig, 1990). The juvenile phase begins when the shoot apical meristem generates a stem, true leaves and axillary buds. This phase may last for a few days or many years, depending on the species, and is distinguished by a variety of unique vegetative traits including leaf shape and trichome distribution, and by the absence of reproductive capacity. The subsequent adult vegetative phase is characterized by a different set of vegetative traits and by a competence of the shoot to shift into reproductive growth. For many plants, reproduction is the last phase in the life of the shoot and is characterized by the production of flowers in place of leaves.

In *Arabidopsis*, the juvenile vegetative phase is marked by the production of small, simple leaves with little or no internode elongation between them (Telfer and Poethig, 1998). The leaf blade and petiole of juvenile leaves are easily distinguished, and the lamina is round in shape with a smooth edge (Telfer and Poethig, 1994). Trichomes are evenly distributed on the adaxial (upper) surface and absent on the abaxial (lower) surface (Telfer et al., 1997). As the shoot shifts into adult phase growth, later leaves gradually take on adult characteristics including an elongated shape with the lamina and

petiole becoming less distinct, and the outer edge of the leaf blade becoming serrate (Telfer and Poethig, 1994). Adult vegetative leaves also bear trichomes on the abaxial surface, as well as the adaxial surface (Telfer et al., 1997). These differences in leaf anatomy are accompanied by a competence of the shoot to respond to floral inducers (McDaniel et al., 1992; Shannon and Meeks-Wagner, 1991). Although distinct organ types are generated during the juvenile and adult phases of vegetative development, intermediate organs that exhibit traits of both phases are typical during the transition from juvenile to adult growth. This suggests that expression of the juvenile and adult developmental programs overlaps during the progressive maturation of the shoot, and that the two programs are not mutually exclusive.

The reproductive phase in *Arabidopsis* is characterized by the production of flowers in place of leaves. The flowers are displayed on a highly elongated and branched bolt. Together the elongated bolt and the flowers that it supports are collectively known as the inflorescence. During production of the inflorescence, the shoot apical meristem initially generates nodes bearing small cauline leaves with secondary inflorescence meristems in the leaf axils. Later, the meristem generates leafless nodes with floral meristems that produce individual flowers. The lower internodes of the inflorescence that subtend cauline leaves elongate dramatically as the inflorescence grows. Although they develop after what is usually considered to be the initiation of reproductive phase, the elongated stem internodes and the small cauline leaves of the inflorescence are essentially "vegetative" tissues.

This report describes a mutant of *Arabidopsis* called *compact inflorescence.* The *cif* trait is specific to the growth pattern of adult vegetative leaves and vegetative portions of the inflorescence with the most striking aspect being a lack of internode elongation in apical inflorescence internodes such that a cluster of flowers is produced, rather than the wild-type raceme. Elongation and expansion of adult vegetative leaves is also compromised in *cif* plants. The *cif* phenotype is inherited as a two-gene trait requiring homozygosity for a recessive mutant allele of one gene, *CIF1*, and either heterozygosity or homozygosity for a dominant allele of a second unlinked gene, *CIF2.* Although the growth pattern of adult vegetative tissues is dramatically affected in mutant plants, the proper identity of organs is maintained, as well as the timing of organ production and of the phase transitions. Additionally, development of juvenile vegetative organs is indistinguishable from that of wild type, and *cif* plants exhibit normal floral meristem identity and are fully fertile. Thus, *cif* plants harbor mutations in two genes that appear to regulate the growth pattern of adult vegetative tissues, specifically in response to the juvenile to adult phase transition.

Results

Isolation of the *cif* Mutant

The *compact inflorescence* phenotype was identified among the T_2 progeny of an *Agrobacterium* transformant in the ecotype No-0. Figure 2.1 shows the phenotype of *cif* mutant plants, the most striking feature of which is the generation of a cluster of flowers at the apex of the inflorescence, rather than the wild-type raceme. *cif* plants produce

normal flowers that are fully fertile (inset, Figure 2.1), and juvenile rosette development in *cif* is indistinguishable from that of wild type (see below). Therefore, the altered growth responses in *cif* appear to be specific to adult vegetative organs. A backcross of the mutant to the parental ecotype resulted in 3:1 wild-type : *cif* segregation in the F2 generation, indicating the activity of a recessive mutation, the *cif1-1* allele. In crosses to divergent ecotypes however, the action of two genes becomes evident (see The cif Phenotype is Inherited as a Two-Gene Trait). Kanamycin resistance and the *cif* phenotype segregated independently in T_3 seedlings, indicating the mutation is not associated with an intact transgene, and Southern blot analysis confirmed the lack of a T-DNA tag in the mutant (not shown).

Figure 2.1. The *cif* phenotype.
A 38-day old *cif* plant grown in a 16-hour photoperiod. Basal internodes on the primary inflorescence exhibit limited elongation while apical internodes do not elongate, generating a cluster of flowers/fruits. All internodes of secondary inflorescences show extremely reduced elongation. Inset shows the wild-type morphology of *cif* flowers.

Vegetative Development and
Phase Change in No-0 Wild-type

Figure 2.2 shows the rosette morphology of wild-type and *cif* plants. Juvenile development in the *cif* mutant is identical to wild type (Figure 2.2a,b). The late rosette leaves of *cif* plants however clearly exhibit compromised elongation and expansion compared to the late rosette leaves of wild-type plants (Figure 2.2c,d). The abrupt onset of this *cif* leaf expansion phenotype suggested that it might correlate with the juvenile to adult phase transition. In order to more clearly define this phase transition in the ecotype No-0, the rosette leaves of wild-type plants were observed for the presence of morphological features that are characteristic of adult vegetative growth, including an elliptical leaf shape, a serrated leaf margin, and abaxial trichomes. A leaf series showing the progression from juvenile to adult in an individual No-0 rosette is shown in Figure 2.2e. In addition, a plot of leaf lengths for ten No-0 rosettes is shown in Figure 2.3.

When grown under a 16-hour photoperiod, wild-type plants of the ecotype No-0 generate six rosette leaves that are clearly juvenile. These leaves have a round to ovate shape with the broadest point below the middle of the leaf (Figure 2.2a,c,e). The lamina has a smooth edge, is easily distinguished from the petiole, and exhibits evenly distributed adaxial trichomes and no abaxial trichomes (Figures 2.2a,c,e; 2.3a). Leaf 7 also exhibits primarily juvenile traits, although the leaf blade is somewhat elongated in shape and occasionally serrated along the leaf margin (Figure 2.2e). Leaf 8 in No-0 exhibits numerous adult characteristics including a distinctly elliptical shape with the broadest point midway between the ends (Figure 2.2e), and a more sharply serrated leaf

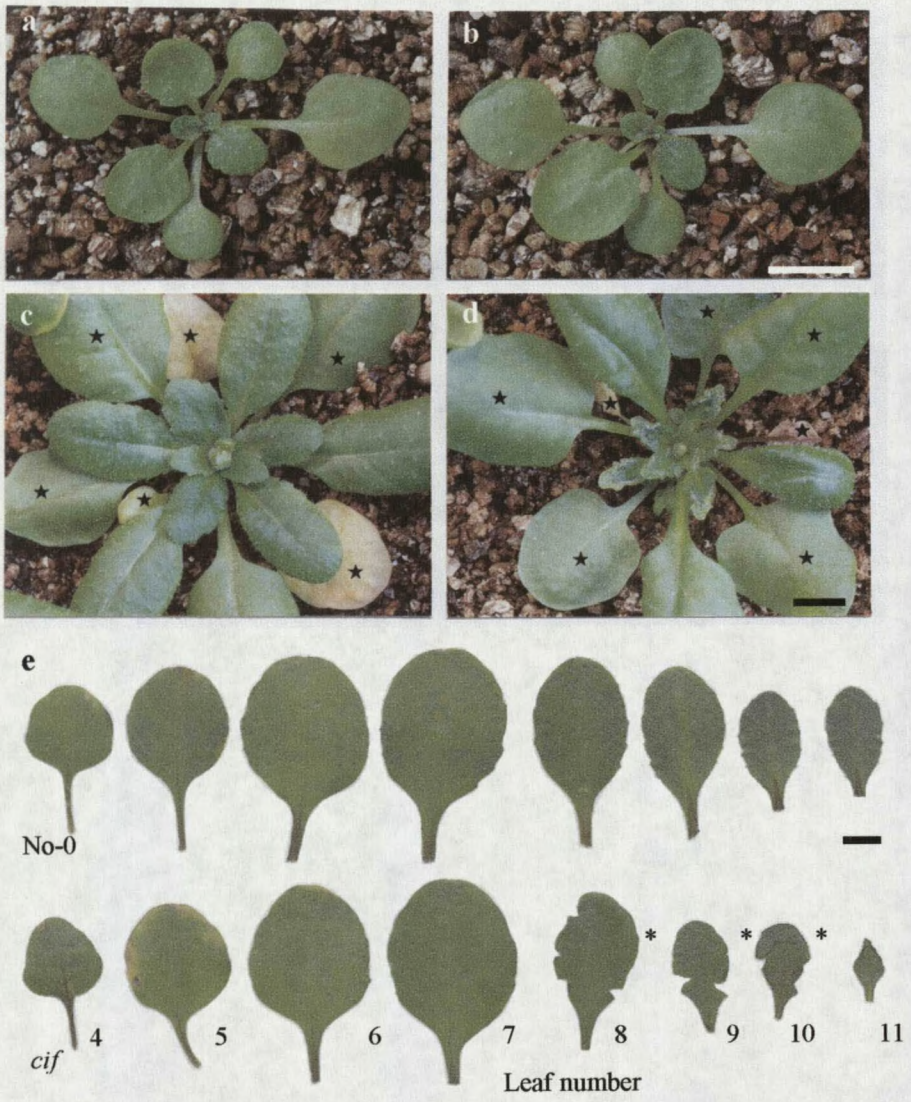

Figure 2.2. Vegetative phase change in No-0 wild type and *cif*.
(a,b,c,d,e) Wild-type and *cif* plants grown in a 16-hour day under fluorescent lights. Wild-type (a) and *cif* (b) plants in the juvenile vegetative phase are indistinguishable. Both have 2 cotyledons and 6 juvenile leaves after 14 days of growth. At 34 days, adult vegetative leaves of *cif* plants (d) exhibit reduced elongation and expansion as compared to wild type (c). Visible juvenile leaves and transitional leaf 7 on (c) and (d) are marked with a star. (e) Rosette leaves from 27-day old individual No-0 wild-type and *cif* plants showing the transition from juvenile to adult growth. Leaves 4, 5 and 6 exhibit juvenile features (the first 3 leaves exhibit a morphology similar to leaf 4, not shown). Leaf 7 is transitional, and leaf 8 exhibits primarily adult characteristics including an elliptical shape and a serrated leaf margin. Leaf 8 is also the first leaf to exhibit the *cif* trait. Scale bars = 5 mm. *Affected leaves of *cif* plants frequently tear when flattened for mounting.

margin (Figure 2.2e). Leaf 8 also shows a less distinct division between the petiole and lamina (Figure 2.2e), and a dense distribution of adaxial trichomes (not shown). Although the 8th leaf in No-0 exhibits numerous adult characteristics, abaxial trichomes do not appear until, on average, the 9th leaf (Figure 2.3a). This suggests that under a 16-hour photoperiod, leaves 7 and 8 are transitional between the juvenile and adult phases of growth, exhibiting some features of both. Adult morphological features become stronger in later rosette leaves with the broadest portion of the leaf blade becoming progressively more distal (Figure 2.2e). Figure 2.3b shows that in a 24-hour photoperiod, the transition to adult growth occurs earlier, with plants of the ecotype No-0 generating leaves with adult characteristics beginning at leaf 6. The appearance of abaxial trichomes in a 24-hour photoperiod is again only roughly correlated with the onset of adult phase growth as abaxial trichomes on average appear on leaf 5, a leaf that is otherwise juvenile in morphology (Figure 2.3b).

The Onset of the *cif* Phenotype
Correlates Closely with the
Juvenile to Adult Phase Transition

Wild-type and *cif* plants exhibit indistinguishable seedling and juvenile vegetative rosette morphologies. Table 2.1 shows that hypocotyls of wild-type and *cif* seedlings are the same length when grown either in the dark or under white light. Figures 2.2 and 2.3 show that in both 16 and 24-hour photoperiods, wild type and *cif* produce the same number of juvenile leaves and that these leaves are the same lengths and shapes. The areas of *cif* juvenile leaves are also comparable to wild-type leaf areas (Table 2.1). Moreover, Figure 2.4 shows that wild-type and mutant plants initiate juvenile rosette

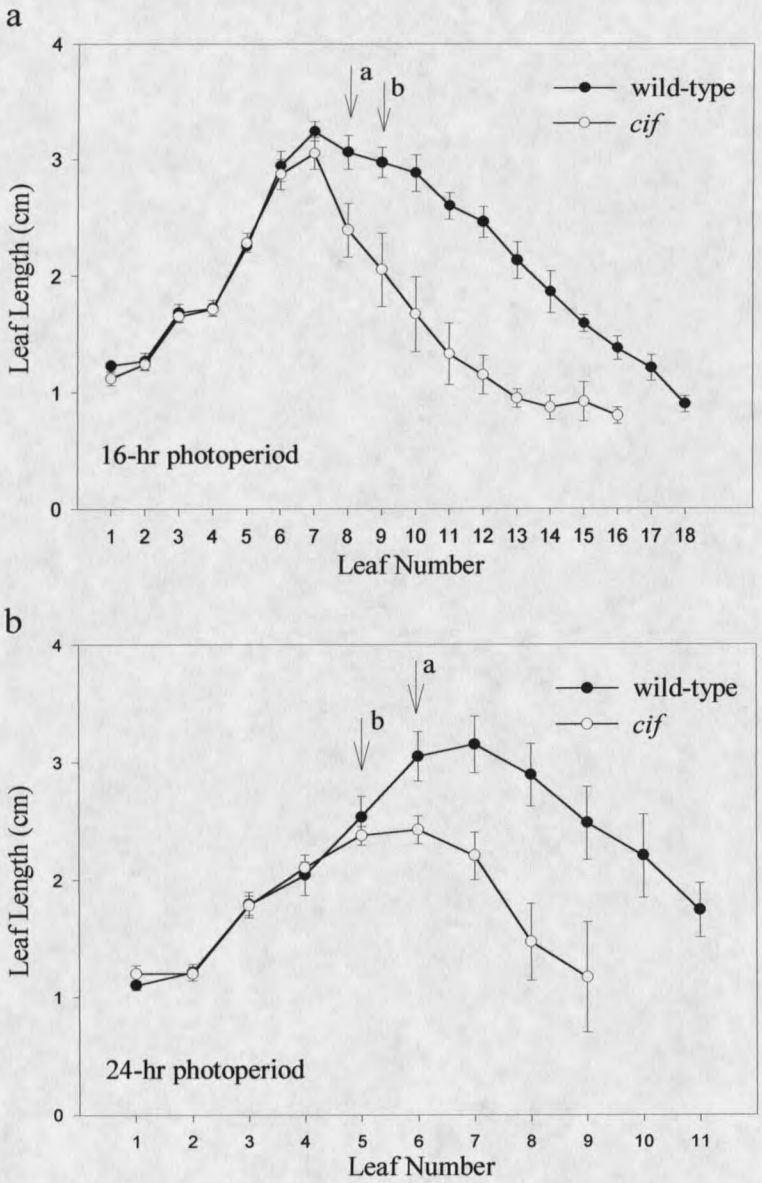

Figure 2.3. Vegetative leaf development in No-0 wild type and *cif*.
(a) Juvenile and adult leaf lengths of wild-type and *cif* plants at flowering (34 days). Plants were grown in a 16-hour photoperiod of fluorescent light. The leaves of 10 wild-type and 10 *cif* plants were measured and observed for adult leaf characteristics. The first leaf with primarily adult characteristics is indicated by arrow (a). The first leaf with abaxial trichomes is indicated by arrow (b). Error bars represent one standard error of the mean. (b) Juvenile and adult leaf lengths of 8 wild-type and 8 *cif* plants at flowering (20 days). Plants were grown in a 24-hour photoperiod of fluorescent light. Symbols are the same as in panel (a). The last two adult leaves of *cif* plants could not be detected at flowering in either experiment.

leaves at the same rate. Thus, the juvenile vegetative phases of wild-type and *cif* plants appear to be identical.

Table 2.1. Measurements of No-0 wild-type and *cif* plants

	Wild-type		*cif*	
Hypocotyl length - dark grown (mm)	8.5 ± 0.77	(*n*=40)	8.5 ± 0.63	(*n*=36)
Hypocotyl length - light grown (mm)	2.4 ± 0.17	(*n*=20)	2.3 ± 0.24	(*n*=20)
Area of the 5th juvenile leaf (cm^2)	1.4 ± 0.21*	(*n*=10)	1.5 ± 0.61*	(*n*=10)
Area of the 5th adult leaf (cm^2)	1.2 ± 0.36*	(*n*=10)	0.3 ± 0.20*	(*n*=10)
Days to flowering				
16-hr photoperiod (fluorescent)	33.8 ± 1.03	(*n*=11)	33.6 ± 1.35	(*n*=11)
24-hr photoperiod (fluorescent)	19.0 ± 0.60	(*n*=12)	19.2 ± 0.58	(*n*=12)
8-hr photoperiod (fluorescent)	51.3 ± 1.49	(*n*=11)	50.6 ± 1.12	(*n*=17)

*Leaf areas were measured from plants grown in a 16-hour photoperiod under fluorescent lights.
n, number of plants measured.
±, standard deviation.

In a 16-hour photoperiod, both No-0 wild-type and *cif* plants exhibit strong adult leaf characteristics beginning at leaf eight (Figure 2.2e). It is at this transition to the adult phase of growth that the *cif* phenotype becomes apparent. The first few adult rosette leaves of mutant plants do not elongate to wild-type length (Figures 2.2d,e and 2.3a) and are often distinctly down-rolled (Figure 2.2d). Subsequent adult leaves exhibit dramatic reduction in elongation and expansion of the leaf blade (Figures 2.2d, e and 2.3a). Table 2.1 shows that the fifth adult leaf of *cif* plants has only 25% the area of its wild-type counterpart. Nonetheless, the *cif* mutant generates adult leaves at the same rate as wild-type plants, with both plants having the same number of leaves after 25 days of growth (Figure 2.4). Moreover, because the effects of *cif* are more pronounced on later rosette

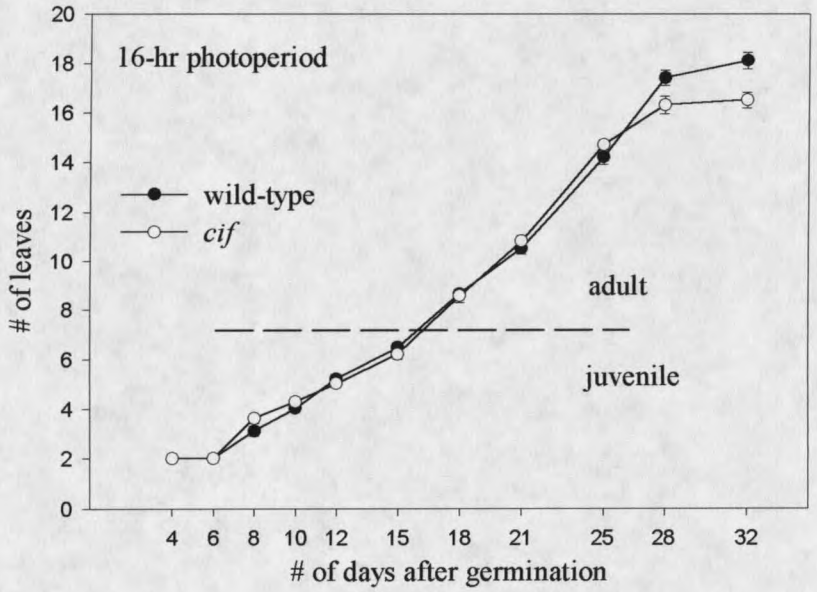

Figure 2.4. Leaf initiation rate in No-0 wild type and *cif*.
Leaf initiation rate was measured in 12 wild-type and 11 *cif* plants grown in a 16-hour photoperiod of fluorescent light. The dashed line indicates the change from juvenile to adult leaf morphology. The last two adult leaves of *cif* plants could not be detected at flowering.

leaves, the overall size of the rosette is not obviously dwarfed (Figures 2.1, 2.2d). At flowering, *cif* plants have on average 2.5 fewer adult leaves than wild-type plants (Figure 2.4). However, this discrepancy is likely due to the final two leaves in *cif* plants being too small to detect as elongation and expansion of the leaf blade are progressively compromised in *cif* mutants.

In a 24-hour photoperiod, No-0 wild-type and *cif* plants exhibit adult leaf characteristics beginning at leaf 6 (2 leaves earlier than in a 16-hour photoperiod) (Figure 2.3b). Again, it is at this transition to the adult phase of growth that the *cif* phenotype becomes apparent (Figure 2.3b). When grown in an 8-hour photoperiod, the transition to adult-phase growth is delayed, with wild-type and *cif* plants generating 16 juvenile

leaves. Although the *cif* phenotype is less pronounced in plants grown in short days, appearance of the *cif* trait again correlates with the onset of the adult vegetative phase (data not shown). Hence, either reducing or increasing the duration of vegetative development by altering the photoperiod results in a coordinate change in the onset of the *cif* phenotype such that it is observed at the juvenile to adult phase transition.

Reproductive Development
and Morphology of the *cif* Mutant

Wild-type and *cif* plants flower at the same time under various photoperiods (Table 2.1), and *cif* plants generate morphologically normal flowers that are fully fertile (inset, Figure 2.1). However, apical internodes of the *cif* inflorescence stem do not elongate properly and a cluster of flowers results rather than the wild-type raceme (Figure 2.1). Measurements of wild-type and *cif* plants are given in Table 2.2. These data show that the most basal inflorescence internodes of mutant plants exhibit significant elongation, although reduced as compared to wild-type plants, whereas expansion of more apical internodes is severely restricted or completely lacking. This results in a drastic reduction of overall height of *cif* plants. Wild-type and *cif* plants have the same number of cauline leaves on the primary inflorescence, although later formed *cif* cauline leaves are often small and underdeveloped (Table 2.2). Plants with the *cif* phenotype produce fewer flowers on their primary inflorescence than do wild-type plants, but *cif* flowers are morphologically normal, and develop into normal fruits. Silique length is the same in *cif* and wild-type plants, whereas pedicel length is slightly reduced in the mutant (Table 2.2).

Mature *cif* plants also exhibit reduced apical dominance, generating more than four times the number of secondary inflorescences arising from the rosette as compared to wild-type plants (Table 2.2). Whether this is a direct activity of the mutant *cif* genes, or alternatively, is a response to early arrest of growth in the primary inflorescence is not currently known. The decreased number of flowers produced on the primary shoot, coupled with the increased number of secondary inflorescences, results in wild-type and *compact inflorescence* plants producing similar seed sets (data not shown).

Table 2.2. Inflorescence measurements of No-0 wild-type and *cif* plants

	No-0	*cif*
Primary Inflorescence:		
Length of internodes subtending cauline leaves		
internode #1(basal-most) (mm)	41.4 ± 10.60 (*n*= 5)	15.0 ± 5.33 (*n*= 5)
internode #2 (mm)	45.2 ± 8.35 (*n*= 5)	8.4 ± 9.74 (*n*= 5)
internode #3 (mm)	22.6 ± 11.15 (*n*= 5)	0.1 ± 0.26 (*n*= 5)
internode #4 (mm)	22.4 ± 1.95 (*n*= 5)	0.0 ± 0.00 (*n*= 5)
Length of floral internodes		
internode #1 (basal-most) (mm)	7.4 ± 5.18 (*n*= 5)	0.0 ± 0.00 (*n*= 5)
internode #2 (mm)	8.9 ± 7.89 (*n*= 5)	0.0 ± 0.00 (*n*= 5)
Total length of inflorescence stem (cm)	34.8 ± 3.84 (*n*=22)	2.0 ± 1.33 (*n*=23)
Pedicel length (mm)	9.0 ± 1.06 (*n*= 5)*	7.6 ± 2.57 (*n*= 5)*
Silique length (mm)	12.1 ± 1.86 (*n*= 5)*	12.1 ± 1.29 (*n*= 5)*
Number of cauline leaves	4.2 ± 0.50 (*n*= 5)	4.1 ± 0.64 (*n*= 5)
Area of the 4th cauline leaf (mm^2)	41.3 ± 9.97 (*n*= 5)	8.1 ± 6.27 (*n*= 5)
Number of flowers	45.5 ± 3.69 (*n*=22)	17.7 ± 7.12 (*n*=21)
Number of secondary rosette inflorescences	2.5 ± 0.91 (*n*=22)	11.0 ± 2.95 (*n*=23)

All measurements were taken from plants grown in a 16-hour photoperiod for 47 days under fluorescent and incandescent light.
n, number of plants measured.
*, 10 pedicels and 10 siliques were measured from each of 5 plants for a total of 50 measurements.
±, standard deviation.

Histology of *cif* Inflorescence Internodes

Histological analysis of basal inflorescence internodes from wild-type and *cif* inflorescences demonstrates that *cif* internodes exhibit normal stem cell type specification and tissue organization, but that *cif* internode cells are significantly less elongated that wild-type internode cells. Stained transverse sections through basal internodes of wild-type and *cif* inflorescences, shown in Figure 2.5, exhibit an anatomy typical of a dicotyledon stem. Though histologically very similar, one difference between wild type and *cif* has been reproducibly observed in the cortical cell layer (c on Figure 2.5a). Wild-

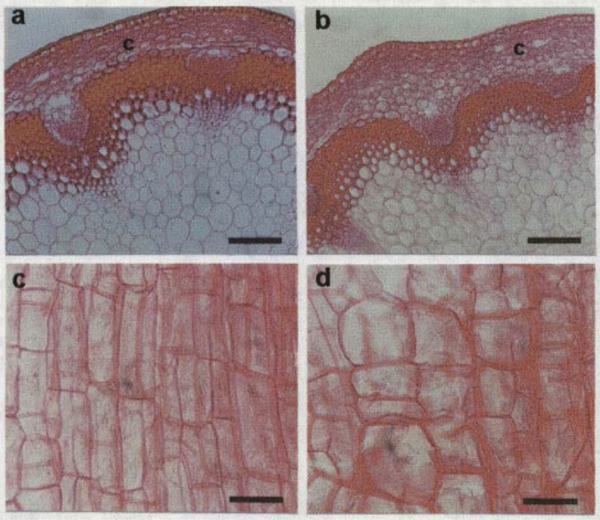

Figure 2.5. Histology of wild-type and *cif* inflorescence stems.
(a,b) Cross sections through basal internodes of wild-type (a) and *cif* (b) inflorescence stems. Both plants show normal cell type specification and tissue organization. Wild-type cortex (c on Figure a) is composed of rectangular parenchyma cells laid down in an orderly, brick-like fashion. In contrast, *cif* cortical cells (c on Figure b) have a rounder shape and are distributed more randomly. Bar = 100 μm. (c,d) Longitudinal sections of wild-type (c) and *cif* (d) inflorescence internodes showing lengths of parenchyma cells from the outer margin of the pith. Bar = 50 μm.

type cortex is composed of rectangular parenchyma cells laid down in an orderly, brick-like fashion. In contrast, *cif* cortical cells have a rounder shape and are distributed more randomly (c on Figure 2.5b). Longitudinal sections of wild-type and *cif* inflorescence internodes show a significant reduction in *cif* cell length as compared to wild-type (Figures 2.5c,d).

The *cif* Phenotype Is Inherited as a Two-Gene Trait

The *compact inflorescence* trait segregates as a simple recessive mutation in crosses done within the parental genetic background. In a cross of No-0 *cif* X No-0 wild type, ¼ of the F_2 progeny are true-breeding *cif* and ¾ are phenotypically wild-type (54:172, P=0.7). However, crosses of the *cif* mutant to other ecotypes such as Columbia (Col) and Landsberg *erecta* (L*er*) produce very different results in the F_2 and F_3 generations. F_1 plants from the cross of No-0 *cif* X Col wild-type are normal in inflorescence structure and, in a population of 152 F_2 plants, 29 show either a strong or "weak" but significant *cif* phenotype. Plants characterized as "weak" *cif* exhibit greater elongation of basal internodes and flower clusters form at more apical positions. Because two distinguishable phenotypic types were found in the F_2 progeny of this cross, and the statistical fit of 123:29 to the expected 3:1 is marginal (P<0.1), F_3 progeny of the *cif* F_2 plants were scored. Only 11 of the 29 *cif* F_2 plants from the cross to Col bred true in the F_3 generation, indicating that in crosses to divergent ecotypes, *compact inflorescence* is not inherited as a simple single-gene trait.

When F_2 plants from the No-0 *cif* X Col cross that had a "weak" *cif* phenotype were allowed to self, a 1:2:1 wild-type : "weak" *cif* : strong *cif* ratio was observed in the F_3 generation. Since the distinction between the strong and "weak" *cif* phenotypes is subtle, this segregation pattern (1 wild-type : 3 *cif*) indicates the involvement of a dominant or semi-dominant locus. Thus, in crosses to divergent ecotypes, *cif* is inherited as a two-gene trait requiring homozygosity for the recessive mutant allele (*cif1-1*) of one gene, *CIF1*, and either heterozygosity or homozygosity for a dominant allele ($CIF2^N$) of a second unlinked gene, *CIF2*. The dominant $CIF2^N$ allele is apparently a naturally occurring allele in the No-0 ecotype and the recessive allele, $CIF2^C$, is present in the Col ecotype. The expected and observed phenotypic ratios for the F_2 progeny of the cross between No-0 *cif* and a wild-type plant, ecotype Col, as well as their assigned genotypes are presented in Table 2.3.

We observed the F_3 segregation of all plants that had a strong or "weak" *cif* phenotype in the F_2 generation from the original No-0 *cif* X Col cross (classes I and II in Table 2.3). The observed numbers of true-breeding F_2 *cif* plants, and *cif* plants that segregate in the F_3 generation, fit well with the expected values (*P* values in Table 2.3). F_3 segregation ratios of a limited number of F_2 plants with a normal inflorescence phenotype (classes III, IV, and V) were also determined. All such plants exhibited an F_3 segregation ratio that corresponds to one of the possible genotypes listed in Table 2.3, and representatives for each of these three classes were identified.

Table 2.3. F_2 progeny classes from a No-0 *cif* to Col cross

class	genotype	phenotype	expected F_2 frequency	actual F_2 frequency	*P* value (χ^2)	F_3 segregation*
I.	*cif1/cif1, CIF2^N/CIF2^N*	strong *cif*	$^1/_{16}$	$^{11}/_{152}$	~.65	breeds true as *cif*
II.	*cif1/cif1, CIF2^N/CIF2^C*	weak *cif*	$^2/_{16}$	$^{18}/_{152}$	~.80	1:2:1 wild-type: weak *cif*: strong *cif*
III.	*CIF1/cif1, CIF2^N/CIF2^N*	wild-type	$^2/_{16}$	3 lines identified**	---	3:1 wild-type: strong *cif*
IV.	*CIF1/cif1, CIF2^N/CIF2^C*	wild-type	$^4/_{16}$	2 lines identified**	---	13:2:1 wild-type: weak *cif*:strong *cif*
V.	___, *CIF2^C/CIF2^C* and *CIF1/CIF1*,___	wild-type	$^7/_{16}$	4 lines identified**	---	breeds true as wild-type

*F_3 segregation was determined from 48 F_3 plants per F_2 line.
**A limited # of F_2 plants with a normal inflorescence were F_3 progeny-tested.

Preliminary Map Locations for the *CIF1* and *CIF2* Genes

In order to determine the chromosomal locations of the *CIF* genes, linkage analysis to simple sequence length polymorphisms (SSLPs) between the No-0 and Col ectoypes (Bell and Ecker, 1994; Cereon *Arabidopsis* Polymorphism Collection, www.arab.org/cereon/) was performed on the 29 *cif* progeny of the No-0 *cif* X Col cross described above. Linkage to a recessive gene suggests the *cif1-1* allele is located between the markers AthATPASE (BAC T4O12) and nga280 (BAC F14J16) on the bottom arm of chromosome 1. Linkage to a dominant locus was also detected, and places the *CIF2*^{N} allele between the markers AthSO392 (BAC F5I8) and T27K12-Sp6 (BAC F7F22) on the top arm of chromosome 1. In order to more finely map the *CIF2* gene, a

mapping population independently segregating the mutant allele of *CIF2* was developed. Linkage analysis places the $CIF2^N$ allele 1.28 cM centromeric to the SSLP marker CER458894 (BAC T19E23) (5 recombinants out of 388 chromosomes screened), and 0.51 cM distal to a dinucleotide repeat GA_n located at 30,246 nt on BAC F3C3 (2 recombinants out of 388 chromosomes screened). These recombination frequencies are in agreement with the physical distance between the two markers (www.Arabidopsis.org/).

Discussion

One of the most common conceptual frameworks for describing plant development postulates that postembryonic plant growth is divided into three major phases - juvenile vegetative, adult vegetative, and reproductive (Poethig, 1990). Although the genetic framework that regulates the timing and elaboration of plant growth phases has not been well defined, it likely comprises overlapping programs of gene expression that specify meristem and organ identities, control growth patterns, and are responsive to environmental cues including photoperiod, light quality, and nutritional status. In this report we describe a novel phase-specific phenotype in *Arabidopsis*. *compact inflorescence* (*cif*) plants exhibit abnormal growth of adult vegetative leaves and vegetative portions of the inflorescence including stem internodes and cauline leaves. The most striking feature of the *cif* trait is formation of floral clusters on all inflorescence stems. Development of *cif* juvenile vegetative organs is indistinguishable from that of wild type, and *cif* plants maintain normal floral meristem identity and are fully fertile.

The *cif* phenotype does not result from a simple deficiency in either auxin or gibberellin, as exogenous applications of these plant hormones do not reverse the *cif* trait (see Chapter 3).

The specificity of the *cif* trait to adult vegetative organs is unique in *Arabidopsis*. Other *Arabidopsis* mutants that show strongly reduced elongation growth, such as hormone mutants and dwarf mutants, are highly pleiotropic in their growth effects. The *cif* phenotype is inherited as a two-gene trait involving the action of a recessive *cif1* and dominant *CIF2* locus. These two *CIF* genes appear to encode key components of a growth regulatory pathway that responds to phase change and thus specifies critical aspects of plant development and architecture.

The rapid bolting of a flowering stalk represents a striking example of developmentally controlled plant cell division and expansion. Moreover, the genetic regulation of inflorescence structure and organization is critical to the specification of higher plant architectures and has implications for understanding the origins and evolution of plant mating strategies, pollination biology, and seed dispersal mechanisms. Attempts have previously been made to isolate mutants in *Arabidopsis* that maintain normal vegetative growth and normal floral meristem identity but do not properly elongate inflorescence internodes. Candidates for such mutations include *erecta*, which encodes a receptor-like protein kinase (Torii et al., 1996), *corymbosa* (Komeda et al., 1998), and *acaulis5,* which encodes a spermine synthase (Hanzawa et al., 1997; Hanzawa et al., 2000; Tsukaya et al., 1993). Although each of these mutants shows compromised internode elongation, each is also highly pleiotropic, affecting growth of juvenile

vegetative tissues, overall plant stature, and fruit development. Perhaps because it requires altered alleles of two independent genes, the very striking and specific effect of the *cif* trait on adult vegetative growth has not previously been described.

The *cif* Trait Supports a Model in Which Vegetative Plant Growth Is Divided into Two Relatively Discrete Phases

Development of juvenile vegetative leaves in *cif* mutant plants is indistinguishable from that of wild type, while the first leaf generated with adult characteristics exhibits compromised elongation and expansion. Appearance of the *cif* trait coincides with the onset of adult vegetative growth even if the juvenile to adult transition is shifted by altering the photoperiod. Hence the *cif* phenotype appears to be specific to an adult vegetative developmental program. Although the first leaf to exhibit the *cif* phenotype is transitional between the juvenile and adult phases of growth, as it often exhibits traits that are characteristic of both, the abrupt onset of the *cif* phenotype (Figure 2.3) supports a model of plant development that divides the vegetative phase into two discrete, but overlapping programs. Indeed, appearance of the *cif* trait may serve to more clearly define the developmental point at which the adult vegetative program is initiated.

Abaxial trichome formation has been used to mark the adult vegetative phase of *Arabidopsis* development (Telfer, et al., 1997). In the ecotype No-0, we found that abaxial trichome formation is preceded by the appearance of other adult morphological features when plants are grown in a 16-hour photoperiod under fluorescent light. Moreover, when plants are grown in continuous light, trichomes appear before the transition to adult vegetative growth on leaves that are otherwise juvenile in morphology.

Chien and Sussex (1996) showed that the onset of trichome formation in *Arabidopsis* is regulated by day length and gibberellin (GA). Telfer et al. (1997) showed that in wild-type Col plants, abaxial trichome formation could be triggered on juvenile leaves 3 or 4 by growing them in a 24-hour photoperiod, or by applications of GA. Hence, the onset of abaxial trichome formation is somewhat loosely correlated with the transition to adult phase growth and may be more sensitive to the light environment and hormonal fluctuations than other aspects of plant development associated with phase change. In contrast, the tight correlation of the onset of the *cif* phenotype with the transition to adult vegetative growth suggests that the *CIF* genes are components of a genetic pathway that is directly associated with *Arabidopsis* phase change.

The *cif* Trait Provides New Insight for a Model of Development in Wild-Type *Arabidopsis*

A standard sequence of events occurs during each of the juvenile, adult, and reproductive growth phases; organs are initiated, their identity is determined, secondary compounds specific to each phase are produced and characteristic growth patterns are manifested (Lawson and Poethig, 1995). The early events in this sequence appear to be intact during adult vegetative growth in *cif* plants, as organs are initiated at the wild-type rate, and the proper identity of organs is maintained. Thus, the *cif* mutant genotype affects the growth pattern of adult vegetative leaves without altering meristem identity or the timing of the vegetative phase transition. This is also the case in relation to development of vegetative structures associated with the inflorescence. In general, the initiation rate and identity of stem and leaf components of the inflorescence are

maintained, while their growth patterns are highly compromised. In these ways, the *cif* mutant is distinct from other phase-associated mutants in *Arabidopsis*, all of which affect the timing of the phase transitions, rather than the development of phase-specific organs. Most late flowering mutants in *Arabidopsis* extend the duration of both the juvenile and adult vegetative phases (Martinez-Zapater et al., 1995; Telfer et al., 1997). The early-flowering mutant, *hasty,* specifically abbreviates the juvenile vegetative phase (Telfer and Poethig, 1998). The early-flowering mutant *efs,* primarily abbreviates the adult vegetative phase (Soppe et al., 1999). Most phase mutants in maize also affect the timing of the phase transitions, including *glossy15, viviparous8*, and the *Teopod* mutants. Recessive mutations of *Glossy15* cause premature expression of some adult vegetative traits (Evans et al., 1994; Moose and Sisco, 1994), *viviparous8* plants are delayed in the juvenile to adult transition (Evans and Poethig, 1997), and the gain-of-function *Teopod* mutants exhibit constitutive expression of juvenile-phase traits (Evans and Poethig,1995; Poethig, 1988). A single mutant in maize, *Ragged1*(*Rg1*), exhibits altered development of phase-specific organs without affecting transition timing (Bongard-Pierce et al., 1996; Evans et al., 1994). The leaves of *Rg1* plants develop necrotic lesions in the lamina, and their appearance is correlated with the appearance of adult traits. Hence, *Rg1* has been used as a phase-specific marker in maize (Bongard-Pierce et al., 1996; Evans and Poethig, 1997).

The *cif* phenotype overlaps the development of the rosette and the inflorescence, and likely defines a growth regulatory pathway common to these structures. This overlap serves to emphasize the vegetative nature of the inflorescence stem and cauline leaves

and supports their portrayal as a scaffold of vegetative tissues that supports and presents the reproductive organs. The *cif* trait demonstrates that growth and development of these tissues is controlled by pathways associated with adult vegetative identity, rather than by pathways controlling reproductive identity. Although flower development is normal in the *cif* mutant, pedicel length is reduced. This suggests that even flower stalks are developmentally influenced by the adult vegetative developmental program.

Figure 2.6 shows a model of development in *Arabidopsis* that incorporates changing organ identities in relation to phase transition and the proposed activities of the *CIF* genes. The model presents plant development as directed by a series of discrete, but overlapping developmental programs that act in succession and determine organ identity and subsequent growth patterns. The initial developmental program confers juvenile identity and directs the production of juvenile leaves. This program is overlapped by a second developmental program that confers adult identity and directs production of adult rosette leaves and adult vegetative organs of the inflorescence. A third program confers reproductive identity, and directs the development of floral organs. In this model, the development of secondary shoots, including those that arise in the axils of rosette and cauline leaves, mimics that of the primary inflorescence. All of the observed phenotypic effects of mutation at the *CIF1* and *CIF2* genes indicate that their activities are restricted to and integral to the adult vegetative program (shown in black in Figure 2.6).

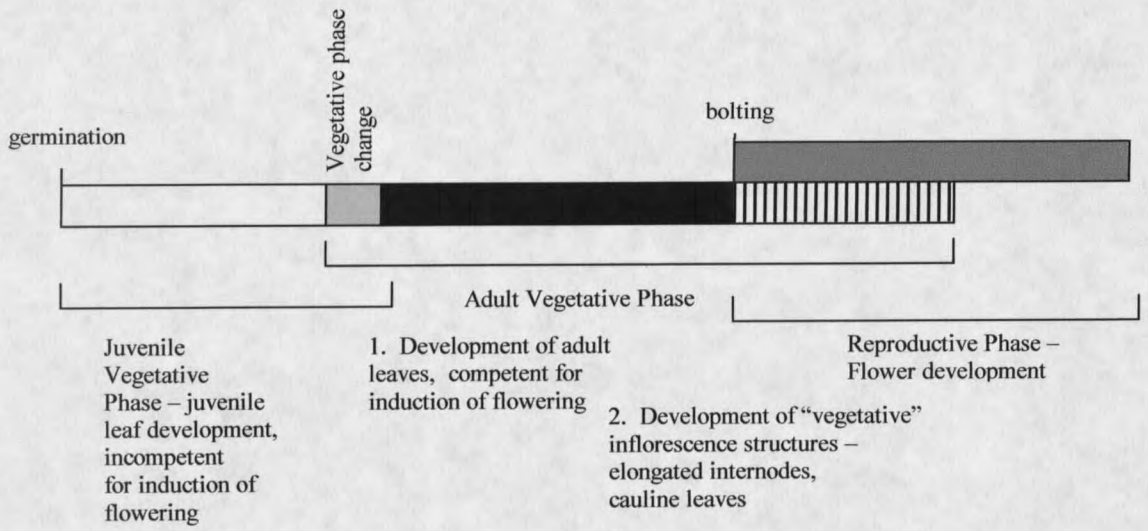

Figure 2.6. Diagram of *Arabidopsis* post-embryonic development. The *CIF* pathway is active throughout the Adult Vegetative Phase.

Materials and Methods

Genetic Stocks and Growth Conditions

The *cif* mutant was isolated in the ecotype Nossen (No-0). No-0 plants were used as wild-type in all developmental comparison studies. Seeds were surface-sterilized for 20 minutes in 15% bleach, rinsed 5 times with sterile water, and plated in 150 x 25 mm petri dishes containing GM medium (Valvekens et al., 1988). Plates were treated at 4°C in the dark for 2 days before being placed under white light. After approximately 10 days, seedlings were transferred to potting soil overlaid with vermiculite. Unless otherwise indicated, growth conditions for potted plants comprised a 16-hour photoperiod of white light supplied by fluorescent and incandescent bulbs, and a temperature of 22°C in a Conviron growth chamber. The No-0, Col, and Ler ecotypes were obtained from the *Arabidopsis* Biological Resource Center (Ohio State University).

Growth Analyses

For hypocotyl lengths, seedlings were planted on GM plates as described above, and measured after five days of growth for dark grown plants, and six days of growth for light grown plants. The rate of leaf initiation was determined by counting leaves and visible leaf primordia twice weekly under a dissecting microscope. Average leaf areas were determined using the Zeiss Interactive Digital Analysis System (ZIDAS) and were measured after 35 days of growth under a 16-hour photoperiod of fluorescent light. Flowering time was recorded as the number of days of growth until the first appearance of a recognizable flower bud.

Histological Analysis

For histological analyses, stem sections from basal inflorescence internodes of wild-type and *cif* plants grown in a 16-hour photoperiod of fluorescent and incandescent light for 35 days were fixed at room temperature in FAA (4% formaldehyde, 5% glacial acetic acid, 47.5% ethyl alcohol) for 24 hours, dehydrated through an ethanol series, transferred to xylene, and embedded in paraffin. 30μm microtome sections were mounted on slides and stained with safranin-fast green. Stained sections were photographed under a Leitz DMR microscope.

CHAPTER 3

THE EFFECTS OF PHOTOPERIOD, GA SUPPLEMENTATION, AND LIGHT QUALITY ON EXPRESSION OF THE *cif* TRAIT, AND THE ISOLATION OF NEW MUTANT *cif* LINES

Introduction

As described in the previous chapter, *compact inflorescence* (*cif*) is a mutant in *Arabidopsis* that exhibits aberrant elongation growth of adult vegetative tissues including adult leaves of the rosette, inflorescence internodes, and cauline leaves. Onset of the *cif* trait coincides tightly with the transition from juvenile to adult vegetative growth, the same transition wherein reproductive competency, or the ability to generate flowers, is gained. Photoperiod strongly influences the timing of the juvenile-to-adult vegetative phase change and therefore flowering time in *Arabidopsis* plants (Koornneef et al., 1998; Simpson et al., 1999). Photoperiod also strongly influences the determination of which, out of three genetic pathways, is used to make the transition to flowering (Reeves and Coupland, 2001). Although it is not currently known if reproductive competency, and possibly aspects of adult identity, occur through pathways related to those through which the floral transition occurs, the impact of variable photoperiods on the *cif* trait deemed investigation. The initial characterization of the *cif* phenotype was from mutants grown exclusively under long-day growth conditions (see Chapter 2). Here, the effects on the *cif* phenotype of growth under a short-day photoperiod are described.

A prominent feature of the *cif* phenotype is the compromised elongation of vegetative inflorescence structures, primarily inflorescence internodes. Internode

elongation, in particular the photoperiod-induced bolting of rosette plants, has been shown to be mediated by gibberellins (GAs). Light quality, specifically the red/far-red ratio is also known to impact floral transition and internode elongation as part of the shade avoidance syndrome in flowering plants. Preliminary experiments had indicated an effect of light quality on the severity of the *cif* trait. For these reasons, the effects of exogenous GA supplementation and end-of-day far-red (EODFR) treatment on the development of the *cif* phenotype were investigated. The impact of mutation in *PHYB*, the primary mediator of shade avoidance responses, is also reported.

Background

Flowering Promotion Pathways

Extensive analysis of late-flowering mutants has established a model for the activities of three main pathways in promoting the switch from vegetative to reproductive development in *Arabidopsis*: the long-day (LD), or photoperiod promotion pathway, the autonomous pathway, and the GA-dependent, or short-day (SD), pathway (Reeves and Coupland, 2001). Mutations in genes in the LD pathway, including *CONSTANS* (*CO*), delay flowering under LD but not SD conditions. *CO* encodes a zinc finger transcription factor (Putterill et al., 1995) and mediates the response to "inductive" LD photoperiods. Flowering under "non-inductive" SD conditions requires gibberellin synthesis, as shown by the inability of severely GA-deficient mutants to flower. However, these *ga* mutants are only slightly affected in flowering time under LD conditions and the GA-dependent pathway is thought to function principally in SDs (Reeves and Coupland, 2001). The

autonomous pathway is thought to promote flowering by reducing the expression of the *FLC* gene that encodes a repressor of flowering (Michaels and Amasino, 1999a, 2001; Sheldon et al., 1999). Mutations in genes in the autonomous pathway, including FCA, delay flowering under both LD and SD conditions.

Extended exposure to low temperatures soon after germination, or vernalization, can also promote flowering. This response is thought to occur through a different pathway from the three described above (Chandler et al., 1996; Simpson et al., 1999), but like the autonomous pathway leads to repression of *FLC* expression (Michaels and Amasino, 1999b; Sheldon et al., 1999).

Gibberellins

Gibberellins (GAs) are tetracyclic diterpene carboxylic acids and were identified more than 50 years ago from *Gibberella fujikuroi*, a fungus that infects rice plants and causes Bakanae disease (Takahashi et al., 1991). Nearly 100 different types of gibberellins have been identified from a range of plants and fungi, but only a few are known to be biologically active forms. Bioactive gibberellin species in higher plants include GA_1, GA_3, GA_4, and GA_7 (Olszewski et al., 2002). The remaining GAs are thought to be precursors of active GAs, deactivated forms of active GAs, or secondary metabolites that may lack any physiologic role.

GA Physiology and GA-Related Dwarf Mutants. Internode elongation is a primary physiologic role for gibberellins. Specifically, there is considerable evidence that the photoperiod-induced bolting of long-day rosette plants is mediated by GAs (Wu,

et al., 1996; Zeevaart et al., 1996). Numerous members of the Brassicacae, including *Arabidopsis*, grow vegetatively for a substantial period of time, generating a basal rosette of leaves separated by short internodes. Exposure to long-days induces reproductive phase change, which is accompanied by extensive internode elongation or bolting. It has been shown that photoperiod-induced bolting is accompanied by dramatic increases in the endogenous levels of active GAs (Talon et al., 1991a; Talon and Zeevaart, 1992). Additionally, application of GA to rosette plants grown under short day conditions will trigger reproductive phase change and bolting, mimicking exposure to long days, whereas treatment with inhibitors of GA biosynthesis suppresses bolting under long days (Zeevaart, 1971; Zeevaart et al., 1993).

An additional physiologic role for GA is the mobilization of stored food reserves following the germination of cereal grains. Depending on the plant species, GAs may also be required for seed germination, for floral induction and flower development, for seed and fruit development, and possibly for anthocyanin biosynthesis. (Takahashi et al., 1991; Hooley, 1994).

Much of what we know regarding GA physiology comes from the study of GA-related dwarf mutants in *Arabidopsis*, pea, and maize. These mutants typically exhibit a dwarf phenotype characterized by a strong reduction in internode length. In addition to reduced stature, organs such as leaves and fruits may also be reduced in size. GA-related dwarf mutants can be subclassified as GA response mutants or GA biosynthesis mutants. GA biosynthesis mutants have a reduced ability to carry out at least one step in the GA biosynthetic pathway and thus are GA deficient. The phenotype of GA boisynthesis

mutants can be corrected by the exogenous application of biologically active GAs. In *Arabidopsis*, GA deficient mutants have been identified at five distinct genetic loci: *GA1, GA2, GA3, GA4,* and *GA5* (Koornneef and van der Veen, 1980). *GA1* encodes *ent*-kaurene synthetase A, an enzyme that is involved in the early stages of GA biosynthesis (Sun and Kamiya, 1994), and *GA4* encodes a 2-oxoglutarate-dependent dioxygenase, which is likely to be a GA 3β-hydroxylase involved in the final step in the synthesis of bioactive GAs (Chiang et al., 1995).

GA response mutants typically display a phenotype that closely resembles that of GA biosynthesis mutants. (Koornneef et al., 1985; Wilson et al., 1992; Peng and Harberd, 1993; Ezura and Harberd, 1995; Putterill et al., 1995). However, GA response mutants are either unresponsive or weakly responsive to exogenous GA applications. The *Arabidopsis* GA response mutant, *gai*, is semidominant and associated with an accumulation of (rather than a deficiency for) bioactive GAs (Talon et al., 1990). *GAI* putatively encodes a transcriptional regulator that acts as a repressor of GA-regulated processes (Olszewski et al., 2002).

Red and Far-Red Photoreceptors: the Phytochromes

Ambient light conditions are among the most important environmental variables that control plant development. Accordingly, plants have evolved multiple photoreceptor systems for perceiving the quality and quantity of light in their surroundings. The most important plant photoreceptors are the red(R)/far-red(FR)-absorbing phytochromes, the blue/UV-A-absorbing cryptochromes, phototropins, and unidentified UV-B

photoreceptors (Quail et al., 1995; Fankhauser and Chory, 1997). The best-characterized photoreceptor, phytochrome, is a soluble chromoprotein which consists of an apoprotein of about 120 kDa and a covalently attached linear tetrapyrrole chromophore. The phytochrome holoprotein undergoes photoreversible conversion between two spectrally distinct forms, a biologically-active FR light-absorbing form (P_{FR}), and a R light absorbing form (P_R) that is either inactive or exhibits a different activity than P_{FR} (Reed et al., 1994; Liscum and Hangarter, 1993). Light acts as a signal to switch between the two forms and phytochrome-mediated responses that are induced with R light can often be reversed with FR light. Seed germination, hypocotyl and internode elongation, cotyledon expansion, leaf development, and floral initiation in plant species requiring long days to flower, are all phytochrome-regulated developmental processes (Reed et al., 1996). In natural environments, phytochromes act to both sense the presence or absence of R and FR light and under continuous irradiation, to monitor the R:FR ratio in light. A set of physiological responses to reduced R:FR, including increased elongation growth of leaf and stem tissues and accelerated flowering, comprise what is known as the shade avoidance response. Phytochromes are encoded by a small multigene family (Sharrock and Mathews, 1997), and in *Arabidopsis,* the complete family consists of five members, *PHYA-E* (Sharrock, and Quail 1989; Clack et al., 1994).

Mediation of shade avoidance responses constitutes one of the most prominent and important roles for phytochromes in higher plants. Light reflected off of neighboring plants or filtered through overhanging leaves is depleted in R wavelengths, resulting in a reduced R/FR ratio and a corresponding shift in the P_R/P_{FR} photoequilibrium of

phytochrome in the responding plant. Shade avoidance conditions are mimicked in the laboratory by growing plants under light of a low R/FR ratio or by treating plants with a pulse of FR light at the end of the day (end-of-day far-red treatment, or EODFR) (Smith, 1994). In *Arabidopsis*, the most noticeable FR induced responses are elongated growth of petioles, leaves and internodes, paler green pigmentation, reduced flowering time, and reduced leaf area. PHYB is the phytochrome form most active in regulating shade avoidance, and the *phyB* loss of function mutant of *Arabidopsis* constitutively exhibits elongated organs and paler pigmentation, flowers early, and displays attenuated responses to both a reduced R/FR ratio and EODFR (Reed et al., 1993).

It has been observed that phenotypes of GA-related mutants and phytochrome related mutants, or transgenics, can be strikingly similar. Over-expression of phytochromes A or B in transgenic plants confers a dark-green, somewhat dwarfed phenotype, which resembles that of GA-related mutant plants (Boylan and Quail, 1989, 1991; Kay et al., 1989). Experimental evidence shows that the levels of biologically active GAs in transgenic tobacco plants, which over-express oat phytochrome A, are substantially lower than that found in nontransgenic controls, and that foliar application of GA can partially suppress the phenotypic consequences of phytochrome A over-expression (Jordan et al., 1995). Phytochrome-deficient mutants display a pale-green, elongated phenotype with increased apical dominance (Reed et al., 1993). This phenotype is similar to that of *spy*, an *Arabidopsis* mutant that exhibits resistance to the GA biosynthesis inhibitor paclobutrazol, and is thought to constitutively express a GA signal transduction component (Jacobsen and Olszewski, 1993). In several different

species, mutants deficient for phytochrome B-like proteins have been shown to have elevated GA levels (Rood et al., 1990; Beall et al., 1991; Childs et al., 1992; Devlin et al., 1992), or to exhibit an increased responsiveness to applied GAs (Reed et al., 1996).

Results

Gibberellins (GAs) and the *cif* Trait

The reduced internode elongation seen in *cif* mutant plants suggests the possible involvement of plant hormones including auxin, gibberellins (GAs), or brassinosteroids. Because GAs are known to play a prominent role in regulating internode elongation in plant species that exhibit separate vegetative and reproductive growth phases (Wu, et al., 1996; Zeevaart et al., 1991, 1993), these hormones were studied first. Table 3.1 shows the effects on the wild type and the *cif* mutant of applications of GA_3 and GA_{4+7} for three weeks beginning 12 days after germination.

Table 3.1. Wild-type and *cif* plants treated with exogenous GAs.

	WT	*cif*	WT+GA_3	WT+GA_{4+7}	*cif*+GA_3	*cif*+GA_{4+7}
Days to flower	32.2(1.64)	31.7(1.50)	27.2(0.40)	26.8(0.75)	27.3(0.51)	26.7(0.82)
Length of the fourth juvenile leaf (cm)	1.9(0.07)	1.9(0.05)	2.0(0.05)	2.5(0.08)	2.0(0.05)	2.5(0.11)
Length of primary inflorescence (cm)	28.3(2.99)	0.8(0.22)	34.8(1.81)	47.8(4.14)	1.2(0.32)	4.2(1.70)
# of elongated inflorescence internodes	7.0(0.00)	1.0(0.00)	10.7(1.03)	11.8(1.17)	2.2(0.45)	3.2(1.30)

As expected, GA-treated wild-type plants flower early, exhibit paler green pigmentation and increased elongation of juvenile rosette leaves, have an increased number of inflorescence internodes and increased elongation of those internodes as compared to non-treated plants (Table 3.1). GA-treated *cif* plants also flower early and exhibit paler pigmentation and elongated juvenile rosette leaves as compared to non-treated mutants (Table 3.1). However, as shown in Figure 3.1, adult vegetative leaves of GA-treated *cif* plants do not elongate normally, and a strong *cif* mutant leaf phenotype remains. Treated *cif* plants show a small increase in the number and length of elongated basal inflorescence internodes, and like the wild type, the *cif* mutant exhibits a greater response with respect to these parameters when treated with GA_{4+7} as compared to GA_3 (Table 3.1). This is not unexpected, as GA_4 has been shown to be more effective at stimulating elongation growth, particularly in inflorescence internodes, than have other GA species (Talon et al., 1990). Although *cif* mutant plants show a GA-induced increase in elongation of basal inflorescence internodes, upper inflorescence internodes do not elongate significantly and a strong *cif* phenotype remains (Table 3.1). These data indicate that *cif* is neither a GA deficiency mutant, nor a typical GA response mutant (see Discussion). In preliminary experiments the *cif* phenotype was also unresponsive to exogenous applications of auxin (data not shown). The possible effects of brassinosteroids have not yet been investigated.

Figure 3.1. Exogenous GA applications do not rescue wild-type leaf development in mutant *cif* plants.
At 25 days, adult leaves are emerging in wild-type (a) and *cif* (b) rosettes. Wild-type plants treated with exogenous application of GA_{4+7} (c) are flowering early and exhibit paler green pigmentation and elongated leaves. *cif* plants treated with GA_{4+7} (d) are also flowering early, and exhibit paler green pigmentation and elongated juvenile rosette leaves. Adult leaves in treated *cif* plants do not elongate however, such that a strong mutant leaf phenotype remains. The arrows in panels a-d point to adult vegetative leaves of the rosette.

Light Quality and the *cif* Trait

As shown in Chapter 2, *cif* plants that are grown in a 16-hour day of fluorescent light develop normally during the generation of juvenile rosette leaves. However, as shown in Figure 3.2, adult vegetative leaves exhibit a dramatic reduction in the elongation and expansion of the lamina as compared to wild-type plants. The inflorescence of *cif* plants grown under such conditions also exhibits a severe *cif* mutant phenotype with the basal-most internode elongating only slightly (usually less than 5mm) and no elongation of the remaining internodes, such that a cluster of flowers/fruits forms within the rosette (Figure 3.2c). In contrast, *cif* plants grown in a 16-hour day of fluorescent light supplemented with light from incandescent bulbs show a reduction in the severity of the mutant phenotype. They develop normally during both the juvenile

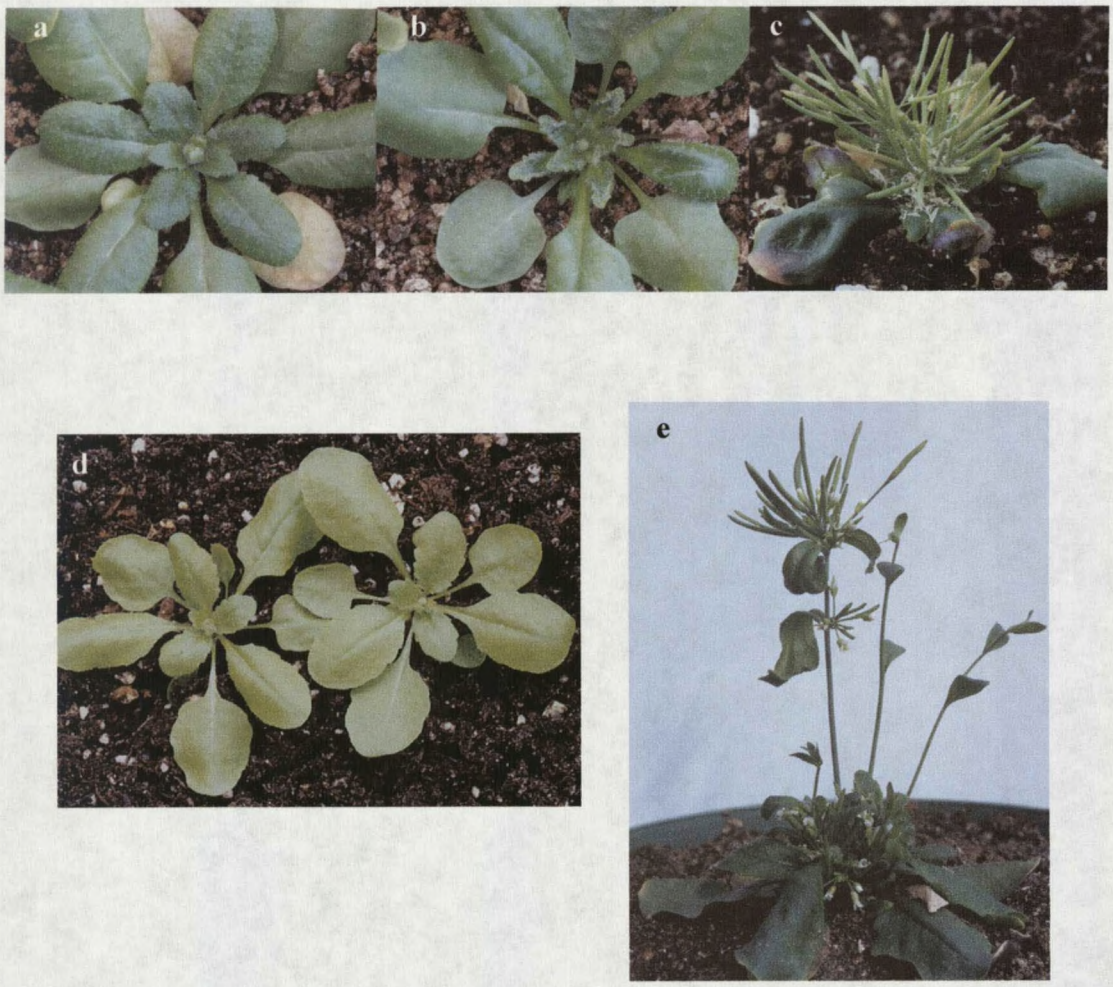

Figure 3.2. Severity of the *cif* trait is sensitive to light quality.
In a 16-hour photoperiod of fluorescent light, *cif* plants at flowering exhibit a dramatic reduction in the elongation of adult rosette leaves (b) as compared to wild-type plants (a). Long fluorescent days also generate a strong inflorescence phenotype in *cif* plants with little or no elongation of inflorescence internodes and a cluster of flowers/fruits formed within the rosette (c). In a 16-hour photoperiod of fluorescent light supplemented with incandescent, *cif* plants at flowering (d-right) are indistinguishable from wild-type plants (d-left). Incandescent supplementation also generates a less severe inflorescence phenotype with significant elongation of the most basal two or three inflorescence internodes (e).

and adult phases of rosette growth, and are indistinguishable from wild type at the initiation of flowering (Figure 3.2d). During generation of the inflorescence, considerable elongation of the 2 or 3 basal-most inflorescence internodes occurs, but little or no elongation of upper internodes. This results in the generation of a floral cluster at the apex of a somewhat elongated stem (Figure 3.2e). This variation in severity of the *cif* phenotype under different light conditions was initially a confounding factor in studying the *cif* trait.

The inclusion or removal of incandescent light alters the ratio of R/FR light, a parameter known to regulate elongation growth as part of the phytochrome-regulated shade avoidance response (Smith and Whitelam, 1997; Smith, 2000). To test whether the FR light supplied by the incandescent bulbs was acting to moderate the *cif* phenotype, an EODFR experiment was performed and is shown in Figure 3.3. Control plants received a 16-hour day supplied by fluorescent light, and experimental plants received a 16-hour day supplied by fluorescent light with a 30 min. pulse of far-red at the end of the day. Fifteen days after flowering, wild-type plants in the control group exhibit a normal raceme inflorescence, while *cif* plants exhibit a severe phenotype with greatly compromised elongation of adult vegetative leaves and little or no elongation of any vegetative inflorescence components (Figure 3.3a,b). When treated with EODFR, wild type again develop a normal raceme inflorescence, whereas *cif* plants exhibit a much milder *cif* mutant phenotype with little effect on adult leaves of the rosette and significant elongation of the most basal two or three inflorescence internodes (Figure 3.3c,d). Both the incandescent supplementation and EODFR experiments demonstrate that the *cif* trait

is responsive to R/FR light quality and suggest that the *CIF* gene products function in a pathway that is influenced by light signaling (see Discussion).

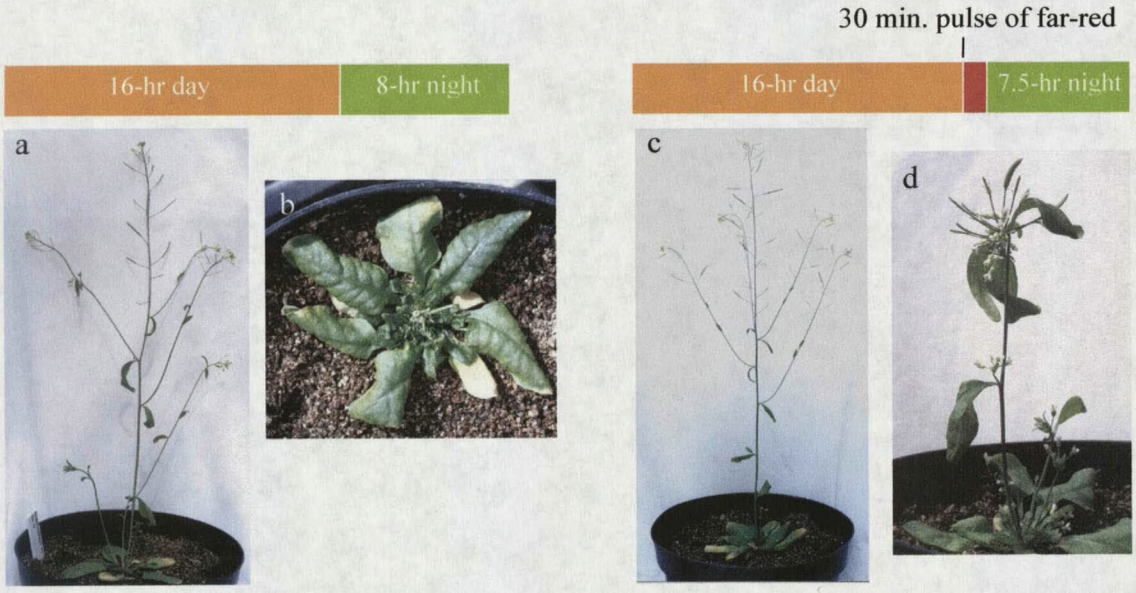

Figure 3.3. EODFR treatment reduces the severity of the *cif* trait.
After 42 long, fluorescent days, wild-type plants (a), exhibit the typical elongated raceme. *cif* plants exhibit a severe phenotype (b), with minimal elongation of inflorescence internodes. When treated with 30 min. of FR at the end of the day, wild type (c), and *cif* plants (d) flower approximately 7 days earlier and thus at 35 days exhibit a comparable developmental stage to that shown in (a) and (b). EODFR treatment has little effect on the morphology of wild-type plants, but reduces the severity of the *cif* trait. Mutant plants treated with EODFR develop normally during the generation of the rosette, and show significant elongation of 2 or 3 basal inflorescence internodes (d).

The *cif* Phenotype in a *phyB* Background

Observation of an EODFR effect on the *cif* phenotype (Figure 3.3) implicates a phytochrome in regulation of CIF signaling activity. Among the five *Arabidopsis* phytochromes, PHYB is the most likely candidate for this regulation as it is the main R/FR receptor that controls shade-avoidance/EODFR responses (Aukerman et al., 1997;

Smith and Whitelam, 1997; Devlin et al., 1998). To test the role of PHYB in the responsiveness of *cif* plants to changes in light quality, we generated a line [*cif1-1/cif1-1/CIF2^N/CIF2^N/phyB/phyB*] which has a genotype specifying the *cif* mutant and *phyB* mutant traits. This line will be referred to as the *cif/phyB* double mutant. Under a 16-hour day of fluorescent light (no incandescent supplementation), the *phyB* mutant and the *cif/phyB* double mutant flower 4 days earlier than wild-type and *cif* plants (23 days and 27 days, respectively) as expected for lines showing a *phyB* mutant constitutive shade avoidance phenotype. Figure 3.4 shows the phenotypes of wild-type and *phyB* rosettes at 30 and 26 days respectively, with the mutant having pale green pigmentation and elongated leaves compared to the wild type. In a *phyB* background, the *cif* mutant also exhibits lighter green pigmentation and more elongated juvenile rosette leaves, as compared to *cif* control plants (Figure 3.4c,d). However, the adult vegetative leaves of the *cif/phyB* double mutant do not elongate properly and still show a severe *cif* phenotype (Figure 3.4d). Inflorescence internodes in the *cif/phyB* mutant also fail to elongate such that at 37 days, flowers are opening within the rosette, similar to the situation in *cif* control plants (Figure 3.4g,h). In contrast, wild-type plants generate the typical *Arabidopsis* compound raceme and the *phyB* mutant produces a similar, but more elongated inflorescence (Figure 3.4e,f). These data show that although the *cif* phenotype is sensitive to the R/FR ratio, this sensitivity is not likely mediated through PHYB.

Figure 3.4. The *cif* phenotype in a *phyB* null background.
After 30 days in a 16-hour photoperiod of fluorescent light, wild-type plants (a) exhibit a compact, dark green rosette. The *phyB* mutant flowers early and at 26 days (b) exhibits an elongated, pale green rosette. The *cif* mutant (c) flowers with wild type and exhibits wild-type pigmentation and elongation of juvenile rosette leaves. Elongation of adult rosette leaves is reduced in the mutant. The *cif/phyB* double mutant (d) flowers early and exhibits reduced pigmentation and elongated juvenile leaves. Like in *cif*, adult vegetative leaves of the double mutant do not elongate. At 37 days, wild-type plants (e) exhibit the typical compound raceme, the *phyB* mutant (f) exhibits an elongated compound raceme, and both *cif* (g) and the *cif/phyB* double mutant (h) lack internode elongation such that flowers are formed within the rosette.

Photoperiod and the *cif* Trait

The transition to flowering in higher plants can occur through at least three distinct genetic pathways depending to a large degree on photoperiod. Because of the correlation between *cif* phenotypic onset and the transition to reproductive competency, the effects of different photoperiods on the severity of the *cif* trait were investigated. As shown in Figure 3.5, *cif* plants grown in a 16-hour photoperiod of fluorescent light exhibit a severe phenotype. A similar phenotype is observed under a 24-hour day. However, when grown in an 8-hour photoperiod, the mutant phenotype of *cif* plants is greatly reduced and occasionally completely repressed. Figure 3.5b-d show two examples of *cif* plants and a No-0 wild-type plant grown in a short fluorescent day. Under these conditions, the adult leaf phenotype in *cif* plants is strongly reduced and requires the measurement of adult leaves in *cif* and wild-type plants for detection. 85% of *cif* plants grown in this photoperiod develop between 4 and 6 elongated internodes on the primary inflorescence, with a single cluster of flowers at its apex (Figure 3.5b). Most coflorescence internodes elongate normally on these plants such that no floral clusters form on lateral branches and a modified compound raceme is generated (Figure 3.5b). In 15% of *cif* plants grown in SDs, the mutant inflorescence phenotype is completely suppressed (Figure 3.5c) and plants closely resemble the wild type. These results have strong implications for the relation of the *CIF* genes to different floral promotion pathways (see Discussion).

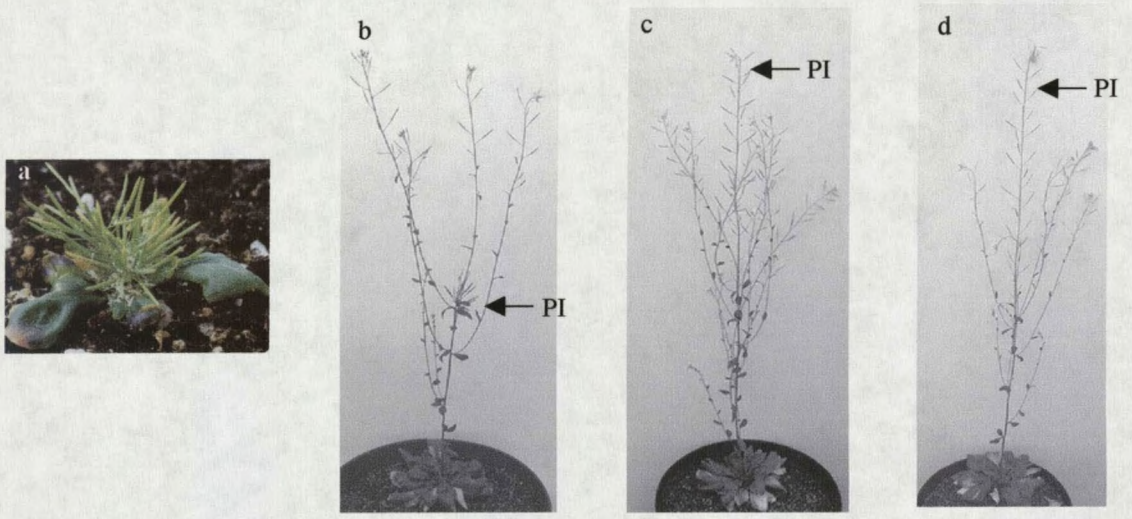

Figure 3.5. Severity of the *cif* trait is reduced under SDs.
cif plants grown in a 16-hour fluorescent day (a) develop a severe phenotype with no significant elongation of inflorescence internodes. Grown in an 8-hour fluorescent day, 85% of *cif* plants develop a mild phenotype (b) with elongation of 4 to 6 internodes on the primary inflorescence and normal internode elongation on lateral branches. In 15% of *cif* plants the mutant phenotype is completely suppressed (c), and plants closely resemble the wild type (d).

Isolation of Additional Mutant Lines That Exhibit the *cif* Trait

Seeds of an *Arabidopsis* mutant that exhibits aberrant development very similar to *cif* were obtained from the laboratory of Sarah Hake at the Plant Gene Expression Center. This mutant was identified in the progeny of a T-DNA mutagenesis experiment that was performed in the ecotype No-0 for an unrelated project. The mutant phenotype segregates as a recessive single-gene trait in crosses to No-0 wild type; out of 30 F2 plants from a backcross of the mutant to a wild-type No-0 plant, 7 exhibited a *cif*-like phenotype (P value = 0.8). A complementation assay was performed by crossing this mutant to our original *cif1* mutant, and all of the F_1 plants exhibited a wild-type phenotype. Hence, this mutation appears to be in a different gene than the recessive *cif1*

locus, and we have designated it *cif3*. The phenotype of a *cif3* mutant plant is shown in Figure 3.6. The *cif3* allele appears to be tagged by a T-DNA insert, as the phenotype co-segregates with Kanamycin resistance; 8 F2 *cif* plants from a backcross of the mutant to No-0 all exhibit Kanamycin resistance in the F3 generation. Southern blot analysis also confirms the absence of a T-DNA tag (data not shown).

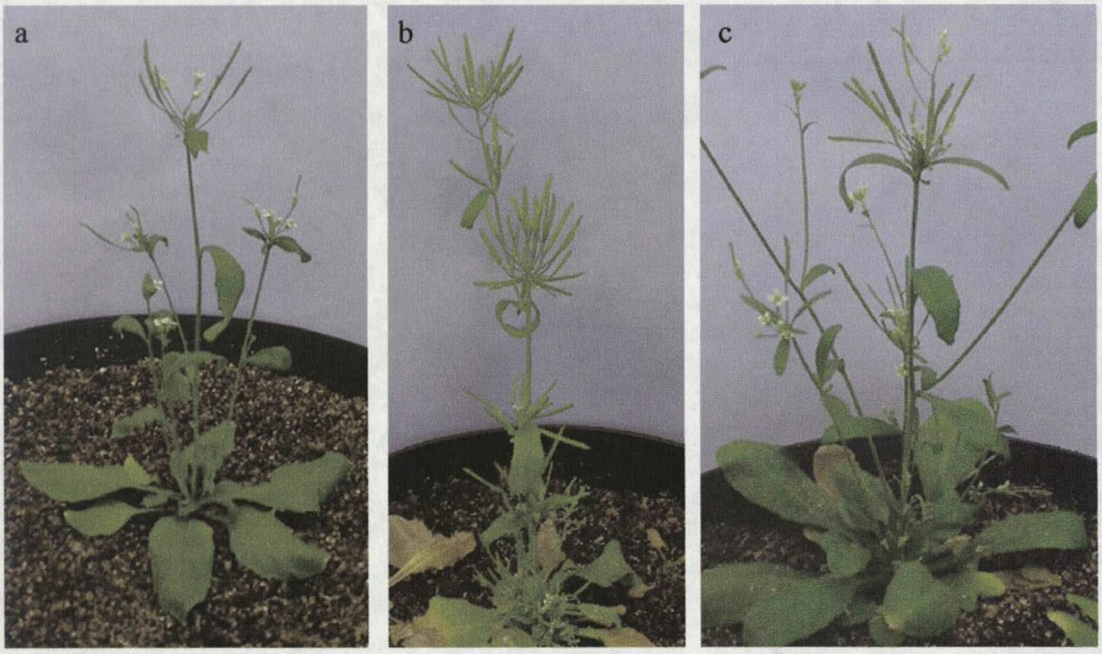

Figure 3.6. Additional *cif* mutants.
The T-DNA mutant *cif3* (a) is not allelic to *cif,* but exhibits a similar phenotype. Two mutants obtained from an EMS mutagenesis screen (b and c) also exhibit a *cif*-like phenotype. Initial experiments indicate that the mutant shown in panel c is allelic to *cif1-1.* All plants pictured were grown in a 16-hr photoperiod of fluorescent light supplemented with incandescent bulbs.

In addition to *cif3*, we have also isolated two new mutants from an EMS-mutagenesis screen of approximately 1500 M3 generation No-0 plants (Figure 3.6b,c). Both mutants exhibit a phenotype that is very similar to *cif.* The mutant pictured in panel c appears to involve a recessive gene that is allelic to *cif 1-1,* as F1 plants from a cross of

this mutant to *cif* are not phenotypically complemented. Once confirmed, this new recessive allele will be designated *cif1-3*.

As mentioned above, the original *cif* phenotype was isolated in the ecotype No-0 and requires the presence of the $Cif2^N$ gene, a naturally occurring allele within the No-0 background. *cif3*, as well as the two new *cif* mutants, were also isolated in the No-0 ecotype. That no *cif* mutants have been found through mutagenesis screens within the more commonly used ecotypes Columbia and Landsberg *erecta*, and the relative ease with which we were able to isolate *cif*-like mutants in No-0 suggest that the dominant $Cif2^N$ allele is a prerequisite for generation of the phenotype. That we've isolated a number of mutants in a relatively short period of time further suggests that the genetic target size for the *cif* trait is considerable, likely involving numerous genes.

Discussion

The activities of plant hormones, notably GA and auxin, are critical to many elongation growth responses and were clear candidates for involvement in the *cif* trait. In *Arabidopsis*, GA biosynthesis mutants, including *ga1* and *ga4*, display a dwarfed growth-habit throughout development, impaired seed germination, and reduced fertility (Peng and Harberd, 1997). In these mutants, the wild-type phenotype can be rescued by exogenous application of active GAs. The impaired elongation growth seen in *cif* is restricted to adult vegetative tissues, and *cif* exhibits normal seed germination and is fully fertile. That the *cif* phenotype is distinct from known GA biosynthesis mutants in these ways, and that it cannot be corrected by the exogenous application of active GAs indicate

that the *cif* trait does not result from a simple deficiency in GA biosynthesis. We show here that *cif* mutant plants are also not generally lacking in GA responses. They are as responsive to applied GAs as the wild type with respect to elongation growth in juvenile leaves and reducing the time to flowering. *cif* plants also show a GA-induced stem elongation response and like the wild type, *cif* plants are more reactive to GA_{4+7} in this respect than to GA_3. The data presented here clearly show that *cif* is distinct from GA biosynthesis mutants and known GA response mutants. These data do not rule out the possibility that the *cif* phenotype results in part from an alteration in GA levels in specific tissues or from an alteration in subtle aspects of GA signaling.

EODFR treatment provides a low R/FR ratio such that P_R/P_{FR} photoequilibrium is shifted toward the less active P_R conformation for the duration of the night phase. A low R/FR ratio induces shade avoidance traits including elongated leaves and internodes. On the other hand, non-shade avoidance traits, such as reduced leaf length and shorter internodes, result from a high R/FR ratio and thus are associated with increased phytochrome activity (P_{FR} conformation). Since we had observed a reduction in severity of the *cif* trait with EODFR treatment, we felt that completely knocking out the expression of *PHYB*, the primary phytochrome associated with the regulation of shade avoidance responses, might be more effective at rescuing wild-type development in *cif* than decreasing the activity of *PHYB* through altering the R/FR ratio. That the severity of the *cif* trait is not reduced in a *phyB* background strongly suggests that *PHYB* does not contribute to the generation of a severe *cif* phenotype under high R/FR conditions. Since phytochromes are the only photoreceptors known to mediate R/FR responses (Smith,

1994), a phytochrome other than *PHYB* is implicated. This is quite possibly *PHYA* as over-expression of this receptor, like *PHYB*, confers a somewhat dwarfed phenotype (Boylan and Quail, 1989, 1991; Kay et al., 1989). *PHYC,D,* and *E* function in a somewhat redundant fashion to *PHYB* in control of shade avoidance responses, and thus are also good candidates for mediating the mild suppression of the *cif* phenotype that is observed under low R/FR conditions.

The observed effect of EODFR on the severity of the *cif* phenotype is not unlike the effect of exogenous GA application. Under both conditions, mutant plants exhibit increased elongation of basal inflorescence internodes and an increased number of internodes that elongate. In both conditions upper internodes remain compact such that a cluster of flowers and fruits is formed. As mutants deficient for different phytochromes have been shown to exhibit elevated gibberellin levels (Rood et al., 1990; Beall et al., 1991; Childs et al., 1992; Devlin et al., 1992), the observed EODFR effect on *cif* may represent a FR induced down regulation of phytochrome activity and subsequent increase in GA levels. If the EODFR effect on *cif* is truly mediated through GAs, manipulation of phytochrome genes or their activity is not likely to have a greater effect at rescuing wild-type development than the application of exogenous GAs.

Photoperiod strongly influences the timing of the juvenile-to-adult vegetative phase change and, therefore, flowering time in *Arabidopsis* plants (Koornneef et al., 1998); Simpson et al., 1999). The suppression of the *cif* phenotype under SDs has important implications for how the CIF pathway may be integrated with and regulated by known floral promotion pathways. As outlined in the introduction, the switch from

vegetative to reproductive development in *Arabidopsis* can occur through three primary genetic pathways: the long day pathway, the autonomous pathway, and the GA-dependent or SD pathway. A strong *cif* phenotype is observed when mutant plants are grown under LD conditions and strong suppression of the *cif* phenotype is observed under SDs. These results suggest that the *CIF* genes are components of a developmental pathway that directs development of adult vegetative tissues under LD conditions, and that growing mutant plants in SDs routes development through a different genetic pathway, one in which the *CIF* genes are not active or are not required.

As described above, three different developmental pathways are known to direct the transition to flowering in *Arabidopsis*. It seems plausible that these same developmental pathways may influence growth slightly earlier, during the development of adult vegetative leaves. An adult developmental status, as opposed to a juvenile status, is associated with reproductive competency, or the capacity to be induced to produce flowers. This fact would seem to increase the likelihood that developmental pathways governing floral transition might also be influencing the development of a reproductively competent, but still vegetative meristem. The increased severity of the *cif* trait seen under LD growth conditions suggests that the *CIF* genes are active in the LD flowering time pathway. The gene *CONSTANS* (*CO*), a zinc finger transcription factor, is known to mediate the floral transition response to LD photoperiods. To test the involvement *CO* in influencing the *cif* phenotype, I am currently generating the *cif1-1/cif1-1/CIF2*$^{No-0}$*/CIF2*$^{No-0}$*/co/co* triple mutant. Suppression of the *cif* phenotype in a *co/co* background

under long-day conditions, would confirm a connection between the *CIF* genes and the long day developmental pathway.

Materials and Methods

GA Treatments

For the exogenous application of GAs, No-0 wild-type and *cif* plants were sprayed twice weekly with 100 uM solutions of either GA_3 or GA_{4+7} beginning 12 days after germination. Control plants were sprayed with water. Plants were grown at 20°C in a 16-hour day of fluorescent light at an intensity of 4 mW/cm^2.

EODFR Experiment

For the EODFR experiment, a Conviron growth chamber (CMP 3244) was maintained at 20°C and divided in half with foam boarding. Both sides were illuminated with fluorescent light at an intensity of 2.6-2.7 mW/cm^2. A bracket fitted with a FR light source was mounted in the experimental side of the chamber. Because this bracket slightly shadowed the surface below it from the above fluorescent lights, a bracket fitted with a FR light source was also mounted in the control side of the chamber, but was not connected to a power source. Control plants received a 16-hour day and an 8-hour night. Experimental plants received a 16-hour day, a 30-minute pulse of FR after the 16-hour day, and a 7.5-hour night.

Experiments Involving the *phyB* Mutant

To generate the *cif1-1/cif1-1/CIF2^N/ CIF2^N/phyB/phyB* triple mutant, the *phyB* null line *Bo64* (Koornneef et al., 1980) that exhibits an elongated hypotcotyl phenotype was crossed to the *cif1-1* mutant. The *Bo64* line had been previously introgressed into the No-0 ecotype and was presumed to be homozygous for the *CIF2^N* allele. The F_1 plants, being heterozygous for both the *cif1* and *phyB* mutations, exhibited intermediate hypocotyl lengths and were complemented for the *cif* phenotype. 180 F_2 seeds were planted on GM plates (Valvekens et al., 1988). ¼ of the germinated seedlings exhibited a long-hypocotyl phenotype and were presumed to be homozygous for the *phyB* mutation. 40 tall seedlings were transferred to pots and maintained through flowering. Approximately ¼ of these tall seedlings developed a *cif* phenotype. F_3 seeds were harvested from these long-hypocotyl/*cif* lines and 2 individual lines were planted on solid GM medium. 30 out of 30 seedlings from both of these lines exhibited a long hypocotyl phenotype as well as the *cif* mutant phenotype. These lines (*Bo64 X cif* F_3 #'s 1-1-1 and 1-1-2) were used for the *cif/phyB* double mutant experiment. Plants were grown in a 16-hour photoperiod of fluorescent light at an average intensity of 4 mW/cm^2.

Photoperiod Experiments

To test the effect of varying day lengths on the *cif* phenotype, three Conviron growth chambers (CMP 3244) were used with photoperiods of 8, 16, and 24 hours. All chambers were illuminated by fluorescent lights with an average intensity of 4 milliwatts/cm^2, and were maintained at 20°C.

Mutagenesis Screen

For the isolation of additional *cif* mutants, seeds of the ecotype No-0 were sent to Lehle Seeds (Round Rock, TX) for mutagenesis with ethylmethane sulfonate (EMS). For planting, approximately 1500 M_3 generation mutagenized seeds were suspended in a .15% agar solution and distributed with a pipette onto prepared pots. Growth conditions comprised a 16-hour photoperiod of fluorescent light supplemented with incandescent bulbs, and a temperature of 20°C.

CHAPTER 4

ISOLATION OF THE *CIF1* GENE AND A REFINED MAP LOCATION FOR *CIF2*

Introduction

In a forward genetic screen, mutagenized plants are screened for a phenotype of interest, and map-based cloning is used to identify the genetic basis of the phenotypic trait. In contrast to reverse genetics, forward genetic screens are unbiased with regard to the likelihood of a particular gene being involved in a specific developmental pathway; the researcher is essentially looking at all of the genes in the genome simultaneously to find those that affect the phenotype of interest (Jander et al., 2002). Forward genetics is a process that allows for the discovery of mutations anywhere in the genome, including intergenic regions and within the 40% of *Arabidopsis* genes that do not resemble any gene with known or inferred function.

Sequencing of the 125 megabase *Arabidopsis* nuclear genome was completed in the year 2000. The subsequent availability of tens of thousands of molecular markers has facilitated map-based cloning to the extent that a single researcher can now find a gene of interest in approximately 1 year by scanning for linkage to markers with a known physical location (Jander et al., 2002). Previous to this, map-based cloning relied on "chromosome walking", a process wherein the researcher constructed a map of overlapping genomic clones to narrow in on candidate genes. The approach required the construction of a genomic library and the development of numerous molecular markers. The "walk" was followed by cloning, complementation testing through transformation,

and sequencing of a relatively large refined region without an available wild-type reference sequence for comparison.

Saturation of the *Arabidopsis* genome with molecular markers was accomplished through the sequencing efforts of the Arabidopsis Genome Initiative (AGI) and Cereon Genomics. While the AGI provided high fidelity sequencing of the entire genome of the Arabidopsis Columbia (Col) ecotype, Cereon provided low coverage (~70%) shotgun sequencing of Landsberg *erecta* (L*er*), a second, commonly used ecotype. The resulting sequence data from the two slightly different genomes facilitated the development of a database of DNA polymorphisms, primarily single nucleotide polymorphisms (SNPs) and small insertions/deletions (INDELs), that can be used as genetic markers (http://www.arab.org/cereon/).

This report describes the map-based isolation of two recessive alleles in *Arabidopsis*, *cif1-1* and *cif1-2*, to mutations within ACA10, a gene that encodes a P-type IIB calcium ATPase. The abundance of Cereon molecular markers on chromosome 4 was instrumental in the efficient mapping of these alleles. When combined with $CIF2^{No\text{-}0}$, *cif1-1* or *cif1-2* causes the elaboration of a phenotype previously designated *compact inflorescence* (*cif*). The *cif* trait was isolated out of a T-DNA transformation, but is not tagged, and as described in chapter 2, mutant *cif* plants exhibit a novel, phase-specific phenotype with all organs generated during the adult vegetative phase of growth being malformed. Here we also describe the cloning of *CIF1*, and show that transformation of *cif* plants with a T-DNA construct containing the *CIF1* allele of the ACA10 Ca^{2+}-ATPase gene rescues wild-type development.

Signal transduction pathways comprise cascades of molecular events through which living organisms respond to environmental and internal stimuli, and make developmental decisions. Plant cells use a variety of messengers in signaling pathways including Ca^{2+}, lipids, pH, and cyclic GMP. No single plant-signaling messenger however, has been demonstrated to respond to more stimuli, both biotic and abiotic, than has cytosolic free Ca^{2+} (Sanders et al., 1999). Growing evidence indicates that the profile of a Ca^{2+} wave, including its amplitude and frequency, encodes specific signaling information. Ca^{2+} wave attributes are determined not only by the dynamics of Ca^{2+} influx through ion channels, but also by the active transport of Ca^{2+} out of the cell.

P-Type IIB Ca^{2+} ATPases

A primary class of active Ca^{2+} transporters in plant membranes is the P-type IIB Ca^{2+}-ATPases. These Ca^{2+} pumps are characterized by the formation of a phospho-aspartate enzyme intermediate during the reaction cycle. Upon phosphorylation of a specific aspartic acid residue, a conformational change occurs that propels two $Ca2+$ ions through the pump to be released on the exoplasmic surface. P-type IIB Ca^{2+}-ATPases have a similar molecular structure in plant and animal systems and, as shown in Figure 4.1, are predicted to contain 10-membrane-spanning segments with the N- and C-termini both located on the cytosolic side of the membrane (Geisler et al., 2000a). The bulk of the protein mass faces the cytosol, and consists of three major parts: the intracellular loop between transmembrane segments 2 and 3, the large intracellular unit between membrane-spanning domains 4 and 5, and an extended intracellular tail located at the N-terminus in plants (left in Figure 4.1), or at the C-terminus in animals (right in Figure

4.1). In animal systems it has been shown that the first intracellular loop between membrane-spanning domains 2 and 3 corresponds to the "transduction domain" thought to play an important role in the long-range transmission of conformational changes occurring during the transport cycle. The large cytosolic region of ~400 residues between membrane-spanning domains 4 and 5 contains the major catalytic domain including the ATP binding site and the invariant aspartate residue that forms the acyl-phosphate intermediate during ATP hydrolysis. Lastly, the extended terminal tail corresponds to the major regulatory domain of the protein (Strehler and Zacharias, 2001).

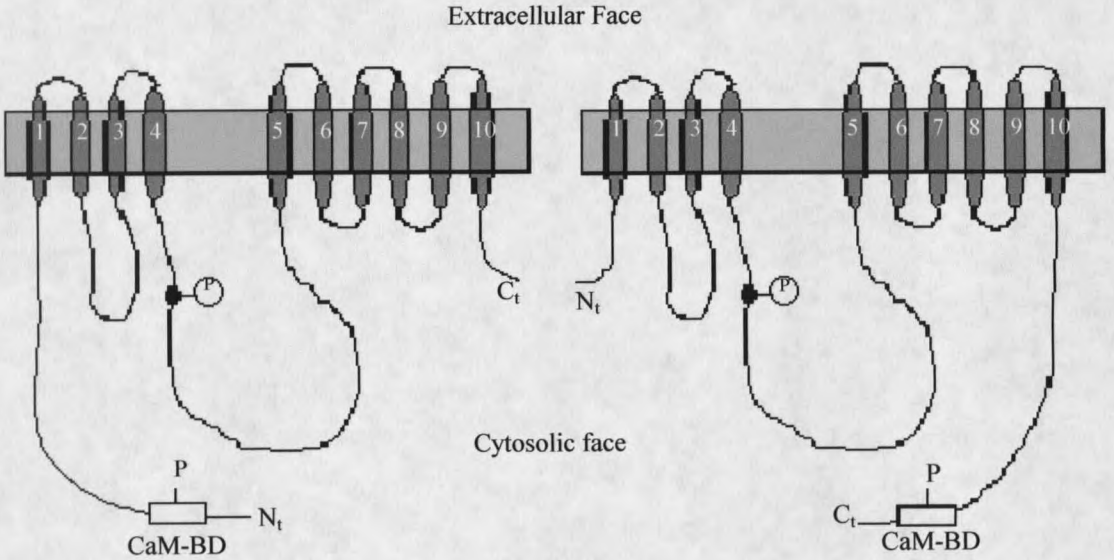

Figure 4.1. A model of P-type IIB Ca^{2+}-ATPases in plants and animals.
The membrane is shown as a light gray bar; the phosphorylated aspartate residue is marked (encircled P). The autoinhibitory/CaM-binding domain is boxed and is situated at the N-terminus in plants (left) or at the C-terminus in animals (right). Phosphorylation of regulatory domains is indicated. CaM-BD, calmodulin binding domain; P, phosphate; N_t, N-terminus; C_t, C-terminus. Adapted from Geisler et al., 2000, and Strehler and Zacharias, 2001.

The current model for regulation of plant P-type IIB Ca^{2+} -ATPases is partly derived from work done in mammalian systems (Strehler and Zacharias, 2001). Here, P-type IIB Ca^{2+} pumps are inhibited by a C-terminal inhibitory sequence, the calmodulin-binding domain (CaM-BD), within the pump molecule (Figure 4.1). As shown in Figure 4.2 (left), in the absence of Ca^{2+}-CaM, this sequence acts as an autoinhibitory domain by interacting intramolecularly with two regions of the pump; one located in the first cytosolic loop and the other in the major catalytic unit between the phosphorylation and ATP binding sites. In the absence of Ca^{2+}-CaM, the autoinhibitory domain is thought to prevent catalytic turnover, keeping the pump in an inactive state. An elevation in cytoplasmic Ca^{2+} results in an increase in Ca^{2+}-CaM, which binds with high affinity to the autoinhibitory domain of the pump, thereby releasing inhibition and stimulating pump activity to near maximal potential (Figure 4.2, right). CaM-binding and autoinhibitory domains are not necessarily synonymous but are usually overlapping (Geisler et al., 2000a). C-terminal CaM-binding/autoinhibitory domains regulate animal type IIB Ca^{2+}-ATPases through a fine balance between internal autoinhibition and activation through CaM binding. Release of autoinhibition can also be achieved by phosphorylation of the autoinhibitory domain by protein kinase A and/or C, resulting in a drop in the affinity of the domain for the active site. Irreversible activation of the Ca^{2+}-ATPase can be achieved through the action of proteases like calpain, which cleave off the autoinhibitory domain entirely (Geisler, 2000a).

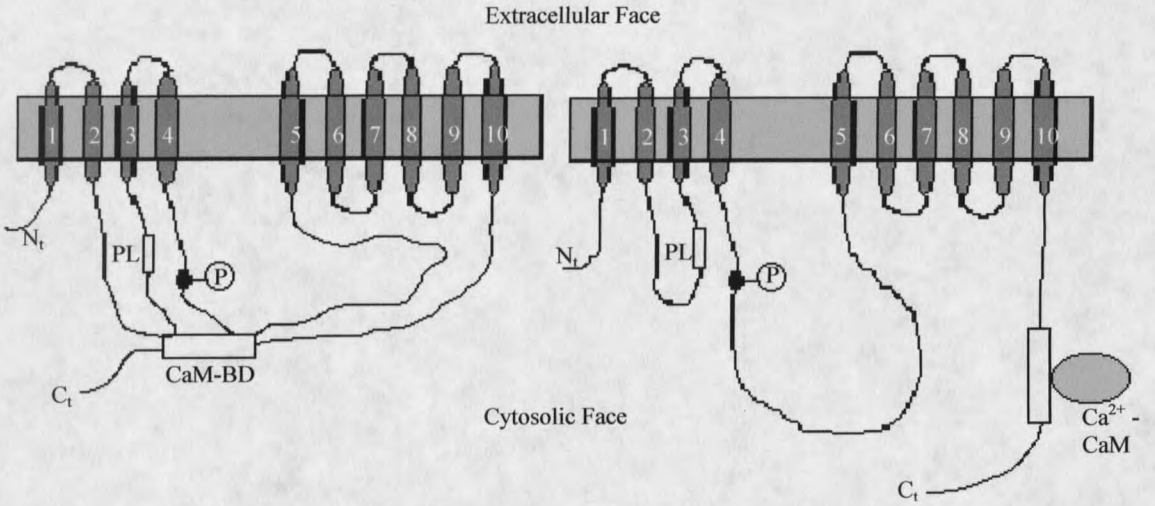

Figure 4.2. Regulation of P-type IIB Ca^{2+}-ATPases in mammalian systems. In the absence of Ca^{2+}-CaM a C-terminal autoinhibitory domain (CaM-BD) interacts with two regions of the pump; one located in the first cytosolic loop and the other in the major catalytic unit between the phosphorylation and ATP binding sites (left). Autoinhibition prevents catalytic turnover, keeping the pump in an inactive state. Binding of Ca^{2+}-CaM to the autoinhibitory domain releases the autoinhibition and stimulates the pump to near maximal velocity (right). Acidic phospholipids also stimulate mammalian P-type IIB Ca^{2+}-ATPases and bind at a domain (PL) located in the first intracellular loop. Other designations are as in Figure 1. Adapted from Strehler and Zacharias, 2001.

Unlike the C-terminal localization of the CaM-binding domain in animal Ca^{2+}-ATPases, plant Ca^{2+} pumps employ an N-terminal CaM-binding region (Figure 4.1, left) (Geisler, 2000a). Domain swapping has been used to demonstrate that the C-terminal autoinhibitory domain of a human plasma membrane Ca^{2+} -ATPase can be relocated to the N-terminus without loss of function (Adamo and Grimaldi, 1998). Thus the different localization of the autoinhibitory domain in plant and animal P type IIB Ca^{2+} -ATPases does not greatly detract from their overall similarity. On the basis of sequence analyses, CaM-binding domains have been identified in the first 50 amino acids of all *Arabidopsis* P-type IIB Ca^{2+}-ATPases (Axelsen and Palmgren, 2001). Experimental evidence has

also illustrated the presence of CaM-binding sequences in the N-terminal regions of ACA2, ACA4, and ACA8 (Harper et al., 1998, Geisler et al., 2000b, Bonza et al., 2000).

In animal systems, acidic phospholipids, polyphosphoinositides in particular, have been shown to act as more potent stimulators of P-type IIB Ca^{2+}-ATPases than CaM (Strehler and Zacharias 2001). Data showing that the fully Ca^{2+}-CaM-stimulated pump (or a truncated pump lacking the COOH-terminal autoinhibitory, CaM-BD) can be further stimulated by phospholipids, indicates that a region(s) other than the COOH-terminal domain must also be involved in lipid stimulation. Work with different proteolytic fragments of animal Ca^{2+}-ATPases and with synthetic peptides has shown that there are indeed two separate phospholipid binding regions in the pump: one corresponding to the previously mentioned COOH-terminal CaM-binding domain and the other situated in the first cytosolic loop immediately preceding the third membrane-spanning domain (Figure 4.2) (Strehler and Zacharias, 2001). The mechanism by which acidic phospholipids activate mammalian Ca^{2+}-ATPases is not known. A phospholipid binding domain has not yet been identified in plant Ca^{2+}-ATPases, and there is currently no evidence that plant P-type IIB Ca^{2+}-ATPases are stimulated by acidic phospholipids.

In *Arabidopsis* there are 10 genes encoding P-type IIB Ca^{2+}-ATPases and they form three clusters within a phylogenetic tree; ACA1, ACA2, ACA4, ACA7, and ACA11 form one cluster, ACA12 and ACA13 form a second cluster, and ACA8, ACA9 and ACA10 form a third cluster (Geisler, 2000a). Four of these; ACA1, ACA2, ACA4, and ACA8, have been cloned and characterized in some detail (Huang et al., 1993; Harper et al., 1998; Bonza et al., 2000; Geisler et al., 2000b). The enzyme encoded by each of

these genes seems to be present in a specific membrane such as the vacuolar membrane (ACA4), the chloroplast envelope (ACA1), and the plasma membrane (PM) (ACA8) (Geisler et al., 2000b; Huang et al., 1993; Bonza et al., 2000). Due to their high molecular masses and similarity to ACA8 (~70% at the amino acid level), ACA9 and ACA10 are also very likely PM pumps. This report describes the map-based isolation of two recessive alleles, *cif1-1* and *cif1-2*, to ACA10, an *Arabidopsis* gene that encodes a P-type IIB Ca^{2+}-ATPase that is likely localized to the PM.

Results

Isolation of the CIF1 Gene

As described in Chapter 2, preliminary data from recombinant frequency mapping using SNPs and INDELs between the No-0 and Col ecotypes (Cereon Arabidopsis Polymorphism Collection, http://www.arab.org/ereon/) on an F_2 population of a No-0*cif* to Col cross, indicated that the *cif1-1* allele was linked to markers on the lower arm of chromosome 1. For higher resolution mapping, a population segregating the No-0 *cif1-1* allele and the wild-type Columbia allele in a background homozygous for $CIF2^{No-0}$ was generated. Linkage to a recessive allele on the lower arm of chromosome 1 was again detected. However, between two markers that flank a 15 cM region, AthATPASE and CER448712, only 1 recombination event was observed at AthATPASE and 3 at CER448712 out of a total of 214 recombinant chromosomes. Within an approximate 5 cM region no recombinants were found. This almost complete absence of

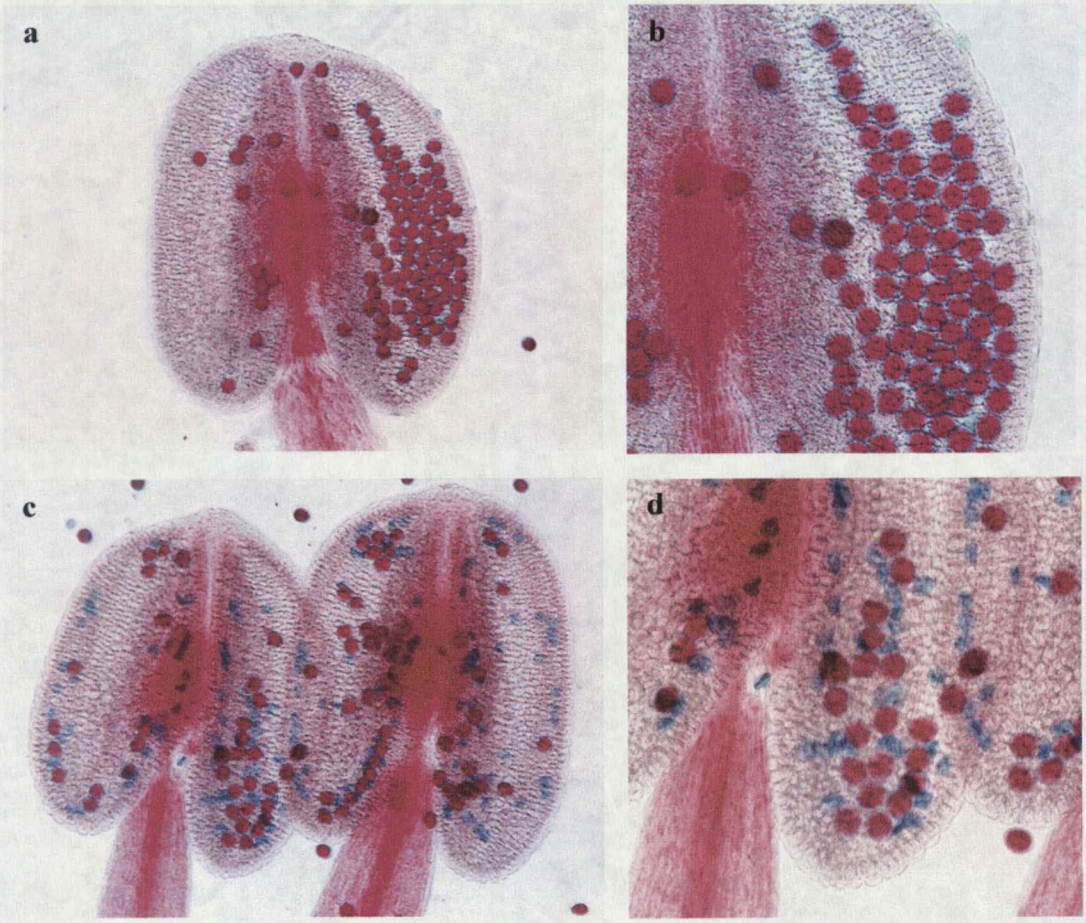

Figure 4.3. Aborted pollen in a *cif* X No-0 F_1 progeny plant.
Stained anthers from a *cif* control plant show viable pollen in (a) (100x), and (b) (200x). Stained anthers from a *cif* X No-0 F_1 progeny plant in (c) (100x), and (d) (200x) show an approximate 50% reduction in pollen viability. Viable pollen stains pink, and aborted pollen stains blue.

recombination around *cif1-1* suggested that *cif1* might be associated with a chromosomal rearrangement. An approximate 50% reduction in pollen viability was also observed in pollen from a *cif1-1/CIF1* heterozygote by differential staining of aborted and nonaborted pollen (Alexander, 1969). Figure 4.3 shows stained anthers and pollen from a *cif* plant (a and b), and from an F_1 progeny plant from a No-0*cif* to Columbia cross (c and d). The

abundance of aborted pollen grains in the heterozygote further indicates the presence of a large genetic aberration. That the *cif1-1* allele might be associated with such a genetic change is not surprising as the mutant was isolated out of a T-DNA transformation, a process that has been shown to induce chromosomal rearrangements (Nacry et al., 1998).

Mutations involving chromosomal rearrangements are not easily cloned by recombinant frequency mapping. In hopes of quickly identifying a second *cif1* allele, a comprehensive search through the mutant seed stock database at TAIR (The Arabidopsis Information Resource, www.arabidopsis.org) was initiated. The line CS253, *pseudoverticillata* or *psv*, a mutant in the ecotype S96 that was described as having an umbellate inflorescence (Relichova, 1976) was identified. Seeds of this line were obtained from the Arabidopsis Biological Resource Center and the phenotype of *psv* was found to be very similar to that of *cif*. The *psv* mutant was crossed to Columbia and the F_2 generation observed for segregation of the *psv* phenotype. Out of 520 F_2 plants, 93 or 3/16 (p-value = 0.3), exhibited the *psv* trait. This segregation ratio fit nicely with the hypothesis that, in crosses to genetically distinct ecotypes, *psv*, like *cif*, is inherited as a two-gene trait involving the action of both a recessive and a dominant locus (see Chapter 2). A complementation test was then performed between our No-0 *cif* mutant and the S96 *psv* mutant. Out of 25 F_1 plants, 0 showed complementation, indicating that our original *cif1* mutation and the recessive *psv* mutation are allelic. To determine whether the dominant loci required for phenotypic expression of *cif1* or *psv* and present in, respectively, the No-0 and S96 ecotypes, are allelic, the F_1 plants from the *cif* to *psv* cross

were selfed and the F_2 phenotypes observed. Out of 30 F_2 plants from two separate F_1's, none showed complementation. These data indicate that the dominant genes involved in the *cif* and *psv* phenotypes are also allelic. To confirm this model, an F_2 line from the S96 *psv* X Col cross was identified that segregated the dominant gene (i.e., wild-type: *psv* phenotypic ratio of 1:3) and this line was used to roughly map the dominant locus. It was found to be linked to the same markers as $CIF2^{No\text{-}0}$ (see Mapping of the *CIF2* Gene below), confirming that they are very likely the same gene.

The *cif* and *psv* mutants appear to represent very similar genetic entities, independent recessive mutations in the same gene, which require the activity of naturally occurring dominant alleles of the same gene at a second, unlinked locus. This presents a problem in gene nomenclature. Although *psv* was isolated in 1976 by Jirina Relichova, the phenotype of the mutant was only very briefly described in a survey of 64 new mutant lines and no information regarding segregation or linkage was provided. Also, no work has since been published on *psv*. Because our lab has already published an extensive phenotypic and genetic characterization of this mutant phenotype (Goosey and Sharrock, 2001), we propose to continue to use the *compact inflorescence* or *cif* nomenclature. We propose the following nomenclature for *cif* mutants and *CIF* genes and such designation will be used throughout this work.

Allele designations:

reference	wild-type allele		mutant allele	
	old	new	old	new
Goosey and Sharrock (2001)	*CIF1*	*CIF1*	*cif1*	*cif1-1*
Relichova (1976)	*PSV*	*CIF1*	*psv*	*cif1-2*
Goosey and Sharrock (2001)	*CIF2*	$CIF2^{Col}$	$CIF2^{N}$	$CIF2^{No\text{-}0}$
This work			--	$CIF2^{S96}$

Mutant designations:	mutant name	
	old	new
Goosey and Sharrock (2001)	*cif*	*cif1-1*
Relichova (1976)	*psv*	*cif1-2*
This work – further *cif* lines	--	start with *cif 3*

Recombinant Frequency Mapping of the *cif1-2* Allele. After determining that the recessive loci involved in the generation of the *cif* and *psv* phenotypes were allelic, mapping of the *cif1-2* allele was initiated. This allele was generated by MNU mutagenesis and thus was likely to be a point mutation. Initially, F_2 progeny of the S96 *cif1-2* X Col cross were analyzed and, unlike the *cif1-1* mutation, no linkage of the *cif1-2* phenotype to markers on the bottom arm of chromosome 1 was detected. However, further analysis indicated the presence of the recessive *cif1-2* allele on the top arm of chromosome 4. Subsequent analysis using the same chromosome 4 markers on the original *cif1-1* mapping population showed tight linkage of these chromosome 4 markers to both the *cif* phenotype and also to chromosome 1 molecular markers. These data strongly suggest that our original *cif1-1* phenotype resulted from a rearrangement between chromosomes 1 and 4, and that the wild-type *CIF1* gene is in fact located on the top arm of chromosome 4. In the *cif1-2* mapping population, recombination frequencies between markers surrounding the gene were in agreement with the physical distances between those markers. In consideration of these appropriate recombination frequencies, and that the *cif1-2* mutant was isolated out of an MNU chemical mutagenesis, it seemed likely that the *cif1-2* allele was a simple point mutation that could be efficiently mapped by recombinant frequency mapping. To simplify the mapping process, a parental mapping line that was homozygous for the dominant $CIF2^{S96}$ allele, and heterozygous for

the recessive *cif 1-2* allele was generated. This population segregates nicely in a 3:1 non*cif*: *cif* phenotypic ratio (1472:464, *P* value = ~0.3). In March of 2002, a large growth room with the capacity to grow 4,000 individual plants was obtained. This corresponds to a mapping population of 500 individuals and 1000 recombinant chromosomes per planting. After 2 plantings, the *cif1-2* allele was isolated to an 80kb region containing 20 candidate genes.

A PCR walking strategy was first used in an attempt to determine which of these genes harbored the *cif1-1* and *1-2* mutations. Primers were designed that amplified 7kb overlapping PCR products spanning the 80kb region shown to harbor the *cif1* mutations. Presuming that *cif1-1* is associated with a chromosomal rearrangement, it was anticipated that an abnormal amplification pattern in one of these 7kb products amplified out of the *cif1-1* allele, most likely the lack of a product indicating the translocation of primer sequence in the mutant, would be observed. However, amplification products out of the *cif1-1* mutant were obtained across the entire region shown to harbor the recessive allele and no detectable size differences were observed between mutant and wild-type products (data not shown). Although I have shown that *cif1-1* plants harbor a relatively large chromosomal rearrangement, these data show that the *cif1-1* allele is not directly associated with this rearrangement, and suggest that instead, *cif1-1* is likely tightly linked to it. After the PCR walking strategy failed, individual genes within the 80kb region shown to harbor the *cif1-1* allele were sequenced out of the *cif1-1* mutant (ecotype No-0), and compared to the wild-type sequence of the ecotype Columbia available at Genbank (www.NCIhomepage.com). No polymorphisms that were likely candidates for the

disruption of gene function were found within numerous genes including those encoding a MAP kinase, a G-protein beta-subunit, a LRRP, a predicted transmembrane protein, and a predicted transcription factor (sequence data not shown). However, as shown in Figure 4.4, a 23 bp deletion (nt 6617-6639) was found within the coding sequence of ACA10, a gene encoding a P-type IIB Ca^{2+}-ATPase. This deletion was not only not present in the Columbia sequence at Genbank, but was also not found to be present in the ACA10 gene of the parental ecotype No-0.

To confirm the association of *cif1* with mutations in ACA10, the ACA10 Ca^{2+} ATPase gene from *cif1-2* was sequenced. Since this mutant allele is in the ecotype S96, sequence polymorphisms relative to the No-0 and Col ACA10 sequences were anticipated, but it was hoped that an obvious alteration such as a nonsense mutation corresponding to *cif1-2* would be found. Surprisingly, no sequence differences that seemed likely to disrupt gene function were found. 16 single nucleotide polymorphisms within intron sequence were identified and 2 silent mutations within coding regions. To determine whether any of these polymorphisms was the *cif1-2* allele, rather than representing naturally occurring variation within different ecotypes, the wild-type Ca^{2+}-ATPase ACA10 gene from the *cif1-2* parental ecotype S96 was sequenced. As shown in Figure 4.5, a single sequence difference, an adenine to guanine transition in the first base of an intron near the 5′ end of the gene, remained when comparing the *cif1-2* mutant and parental S96 sequences. The proximity of this nucleotide difference to the exon/intron boundary suggested that it might represent a mutation that interfered with processing of the Ca^{2+}-ATPase pre-mRNA in the *cif1-2* mutant.

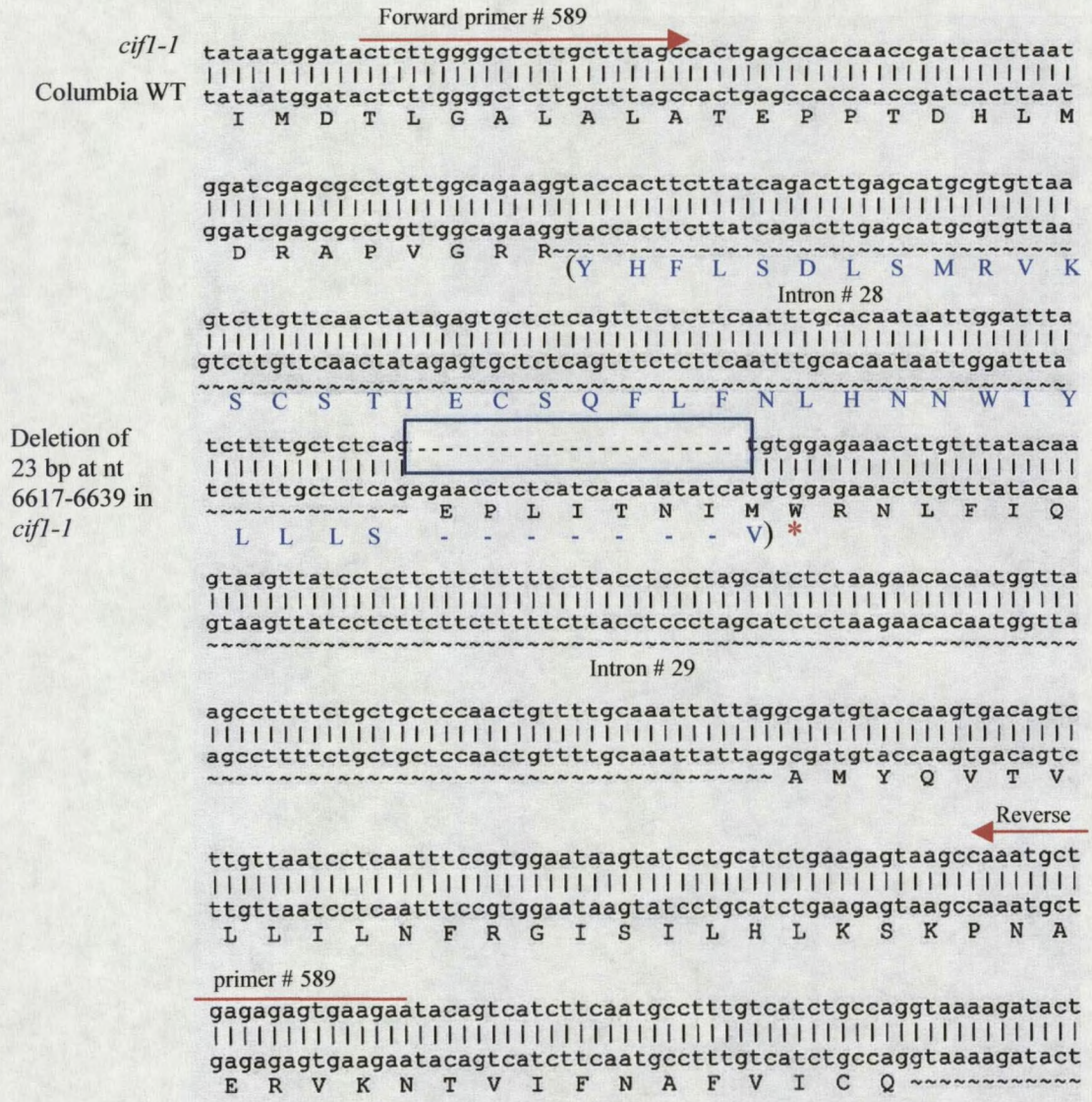

Figure 4.4. Sequencing of the ACA10 gene in *cif1-1*.
The *cif1-1* allele harbors a 23 bp deletion from nt 6617-6639 (shown as a blue box) in ACA10, a gene that encodes a P-type IIB Ca^{2+}-ATPase. RT-PCR and cDNA sequencing shows that this deletion likely results in the loss of 8 amino acids. In much of the *cif1-1* transcript, the intron immediately preceding the 23-bp deletion is also retained such that 37 incorrect amino acids are inserted (shown in blue lettering). The correct reading frame is regained at Trp945 (shown as a red asterisk). Red arrows represent primer sequences used to amplify DNA fragments from *cif1-1* cDNA for sequencing.

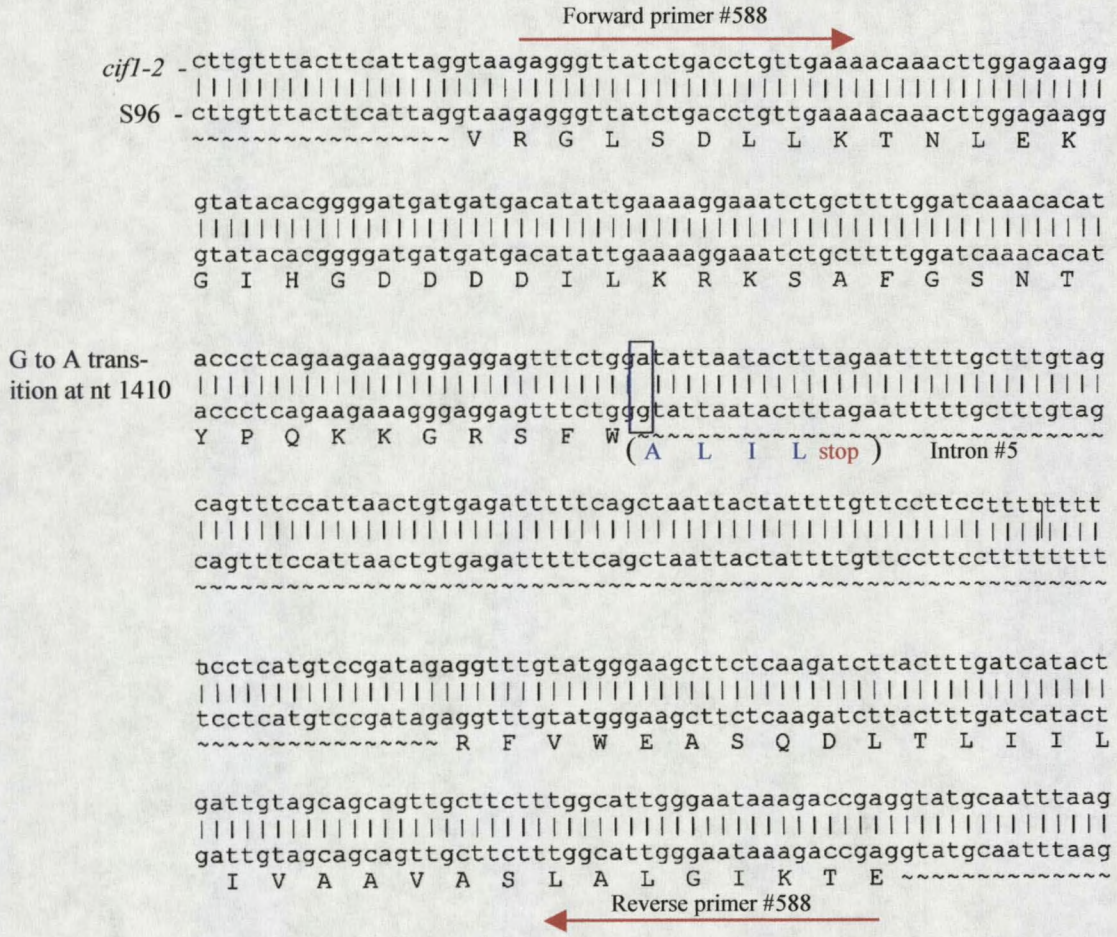

Figure 4.5. Sequencing of the ACA10 gene in *cif1-2*.
The *cif1-2* allele harbors a point mutation, a G to A transition, in the first nt of intron # 5 at bp position 1410 (shown as a blue box) in ACA10, a gene that encodes a P-type IIB Ca^{2+} -ATPase. RT-PCR shows that this mutation prevents splicing of intron # 5 in almost all *cif1-2* transcripts. A stop codon is encountered after reading 4 amino acids into the intron (shown in blue and red lettering). Red arrows represent primer sequences used to amplify DNA fragments from *cif1-2* cDNA for sequencing.

Both the *cif1-1* and *cif1-2* mRNA Transcripts Are Processed Incorrectly. To test the hypothesis that the *cif1-2* ACA10 transcript is processed incorrectly, and to test whether the *cif1-1* deletion alters processing of the ACA10 mRNA, primers were designed that flanked the point mutation found in *cif1-2*, as well as the 23-bp deletion found in *cif1-1* (Figures 4.4, 4.5). cDNA samples synthesized from No-0 and S-96 wild type total RNA and from *cif1-1* and *cif1-2* total RNA were used as templates. Figure 4.6 shows RT-PCR products amplified from the No-0 and S-96 wild types, and the *cif1-1* and *cif1-2* mutants. The primer sets amplify products of the expected size for fully processed mRNAs from No-0 and S96. When used with cDNA from *cif1-2* mutant plants, primers that flank the *cif1-2* point mutation generate a predominant band that is approximately 120 bp larger than control products, and a faint band of control size (Figure 4.6). The large band is consistent with amplification of an unprocessed mRNA. Surprisingly, primers that flank the *cif1-1* deletion generate 3 bands when run on cDNA from *cif1-1* plants; a band approximately 115 bp larger than control products, a larger band, and a band that is slightly smaller than control products (Figure 4.6). Hence, both the *cif1-1* and *cif1-2* mutations alter processing of specific introns in the ACA10 mRNA.

The large *cif1-2* RT-PCR band, and the central *cif1-1* RT-PCR band (Figure 4.6) were cloned and sequenced. As expected, the mutant mRNA fragment amplified from *cif1-2* retains intron #5 in which the G to A transition is the first base. This intron contains a stop signal 5 codons into the intron (Figure 4.5). As only a very small amount of message appears to be processed correctly in the *cif1-2* mutant, represented by a faint

band of wild-type size in lane 4 of Figure 4.6, *cif 1-2* likely represents a strong loss of function allele.

Sequencing of the central *cif1-1* band confirmed that, in much of the mutant message, 23 bp of coding sequence are deleted, from positions 6617 – 6639 which putatively corresponds to a small intracellular loop between membrane spanning domains 6 and 7, and that intron # 28, immediately preceding the deletion, is not excised (Figure 4.4). Despite the intron insertion and 23-bp deletion, this transcript regains the correct reading frame at Trp945 (indicated with a red asterisk in Figure 4.4) after the insertion of 37 amino acids. The larger *cif1-1* band of approximately 400 bp was not cloned but likely represents a portion of the message in which the downstream intron (intron #29) is also retained (see Figure 4.4). As the *cif1-1* deletion removes almost half of the exon sequence and strongly reduces splicing of the preceding intron, an effect on downstream splicing may not be unexpected. The smaller *cif1-1* band of approximately 194 bp was also cloned and sequenced, revealing that some of *cif1-1* message is processed correctly. However, this fraction of the message still harbors the 23-bp deletion which, when combined with the removal of both the preceding and proceeding introns, alters the reading frame such that a stop codon is encountered after the inclusion of 32 incorrect residues. The *cif1-1* deletion occurs at nt 6617 of the 7,551 bp ACA10 gene, which leaves most of the coding sequence for the ACA10 Ca^{2+} pump intact. These data do not rule out the possibility that some *cif1-1* transcript is translated into a partially functional protein containing a 37 amino acid insertion and 8 amino acid deletion.

However, that the severity of the *cif1-1* phenotype is extremely similar to that of *cif1-2*, suggests that like *cif1-2*, little functional ACA10 enzyme is likely generated.

Primer set	Predicted size of PCR product
588	218bp (processed)
	324bp (unprocessed)
589	217bp (processed, no deletion)
	194 bp (23bp deletion, processed)
	315bp (23bp deletion, 1st intron unprocessed)
	400bp (23bp deletion, both introns unprocessed)

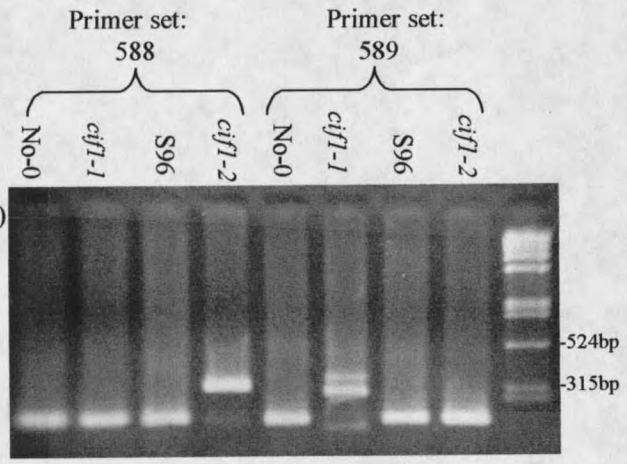

*Primer set 588 flanks the *cif1-2* point mutation
*Primer set 589 flanks the *cif1-1* 23bp deletion

Figure 4.6. Incorrect processing of ACA10 mRNA occurs in both *cif1-2* and *cif1-1*. In *cif1-2* plants, PCR amplification of cDNA fragments that span the *cif1-2* point mutation yields a predominant band that is approximately 120 bp larger than control products. In *cif 1-1* plants, PCR amplification of cDNA fragments that span the *cif1-1* 23-bp deletion yields 3 bands; a central band of approximately 315 bp, a larger band, and a band that is slightly smaller than control products.

Cloning of the *CIF1* Gene and Transgenic Complementation of the *cif1-1* Mutation

That both *cif1-1*and *cif1-2* produce altered mRNA transcripts for ACA10, a 7,551-bp gene encoding a P-type IIB Ca^{2+} ATPase, strongly indicates that *CIF1*is ACA10. For final confirmation of the *CIF1* identity, a 9.5 kb DNA fragment from the Columbia ecotype containing the wild-type allele of ACA10, as well as ~1500 bp preceding the 5′ end of the gene and 300 bp following the 3′ end, was generated by PCR. This PCR product was cloned into a binary plant transformation vector (see Materials and

Methods) and the vector shuttled into *Agrobacterium tumefaciens*. *cif1-1* plants were transformed with this bacterial strain and two Kanamycin resistant lines, both shown to harbor a copy of the transgene, show complementation of both the mutant *cif* leaf phenotype, and the mutant inflorescence phenotype. This experiment provides the most conclusive data yet that *CIF1* is ACA10. Figure 4.7 shows the complemented leaf phenotype of two *cif1-1* plants transformed with the ACA10 T-DNA, as well as the uncomplemented leaf phenotype of a *cif1-1* plant that was transformed and is kanamycin resistant, but did not receive an intact copy of the entire ACA10 gene (see below). Figure 4.7 also shows the wild-type inflorescence development of the two transformed *cif1-1* lines, and the uncomplemented inflorescence phenotype of the transformed *cif1-1* line that did not receive an intact copy of the wild-type ACA10 gene.

Figure 4.8 shows PCR products from a No-0 wild type plant, a *cif1-1* plant, the transformed, but uncomplemented *cif1-1* plant shown in Figure 4.7, and the two complemented transformed *cif1-1* lines also shown in Figure 4.7. Primer sequences used in the amplification process flank the *cif1-1* 23-bp deletion, and in No-0 wild-type and *cif* plants generate bands of 124 and 101 bp respectively (Figure 4.8, lanes 1 and 2). In complemented *cif1-1* plants, PCR amplification with these primers generates two bands, a 101-bp band corresponding to the endogenous *cif1-1* allele, and a 124-bp band corresponding to the wild-type ACA10 gene located in the T-DNA construct (Figure 4.8, lanes 4 and 5). The lack of a 124-bp band in the transformed and kanamycin-resistant, but uncomplemented *cif* plant (Figure 4.8, lane 3), shows that this line did not receive an intact copy of the ACA10 gene during transformation. Kanamycin resistance in this line

Figure 4.7. Wild-type leaf and inflorescence development are rescued in *cif1-1* plants transformed with a T-DNA construct containing the wild-type allele of the ACA10 gene.
A *cif1-1* plant that was transformed with the ACA10 T-DNA and is kanamycin resistant, but did not receive an intact copy of the entire ACA10 gene (see Figure 4.8) shows a strong mutant leaf and inflorescence phenotype (a). In contrast, two *cif1-1* plants that received an intact copy of the ACA10 transgene (see Figure 4.8) show wild-type adult leaf development (b,c) as well as normal development of the inflorescence (d,e). All plants shown are of the T_1 generation.

suggests that a portion of the T-DNA, a region containing the neomycin phosphotransferase gene, was successfully transferred.

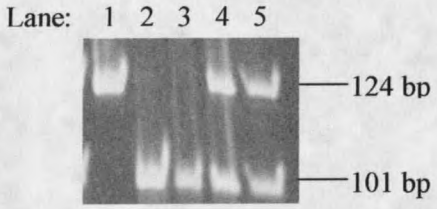

Figure 4.8. PCR analysis of *cif1-1* mutant plants transformed with a T-DNA construct containing the wild-type allele of the ACA10 gene.
PCR primers flank the 23 bp deleted in the *cif1-1* mutant, and generate a band of 124 bp in wild-type plants (lane 1) and a band of 101 bp in *cif1-1* plants (lane 2). Lane 3 shows that a single 101-bp band is amplified from a *cif1-1* plant that was transformed with the ACA10 T-DNA and is kanamycin resistant, but does not show complementation of the mutant phenotype. This line likely received only a part of the T-DNA construct. Lanes 4 and 5 show that two bands are amplified from *cif1-1* plants that were transformed with the ACA10 T-DNA and show complementation of the mutant phenotype. In these lines, the 101 bp band corresponds to the endogenous *cif1-1* allele containing the 23-bp deletion, and the124-bp band corresponds to the wild-type allele contained in the T-DNA construct.

RT-PCR Expression Analysis of
the ACA10 Gene

Onset of the *cif* mutant phenotype correlates tightly with the juvenile to adult vegetative phase transition. To determine whether the onset of the *cif* phenotype also correlates with expression of the ACA10 gene, an RT-PCR analysis using cDNA synthesized from seedling, juvenile leaf, and adult leaf tissue from both wild-type and *cif1-1* plants was performed. Primers used for the PCR analysis flank the 23 bp that are deleted in *cif1-1*mutant plants (Figure 4.4) and amplify a 217bp fragment from wild-type cDNA and 3 bands from *cif1-1* cDNA (see Isolation of the *CIF1* Gene). As shown in

Figure 4.9, the ACA10 mRNA is present in all three tissue types in both wild-type and *cif1-1* plants. To determine if the ACA10 transcript is present in similar quantities in these different tissues, an RT-PCR dilution curve was performed using cDNA synthesized from wild-type seedlings, juvenile leaves, and adult leaves. The curve, as shown in Figure 4.10, indicates that the ACA10 mRNA is present in similar quantities in the three different tissue types. The apparent constitutive and equal nature of ACA10 expression contrasts the tissue-specific nature of the *cif* phenotype. One possible explanation for this apparent discrepancy involves the potential for alternative splicing of the ACA10 pre-mRNA (see Discussion).

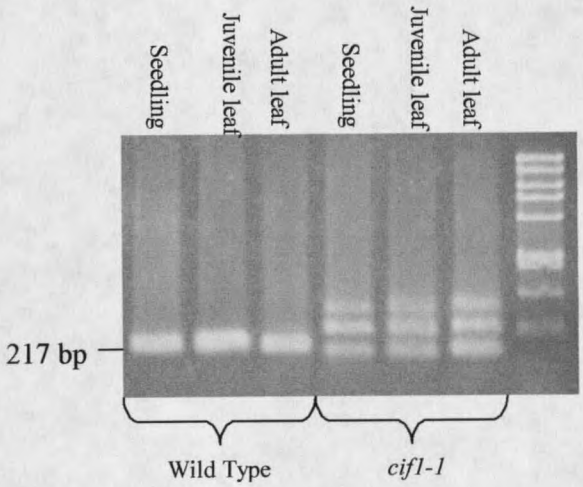

Figure 4.9. The ACA10 mRNA is present in tissue from three separate developmental stages.
In contrast to the specificity of the *cif* trait to adult vegetative tissues, the ACA10 mRNA is present in tissue from seedlings, juvenile leaves, and adult leaves in both wild-type and *cif1-1*plants. cDNA was synthesized from total RNA, and the primers used for PCR amplification are the same as in Figure 4.4.

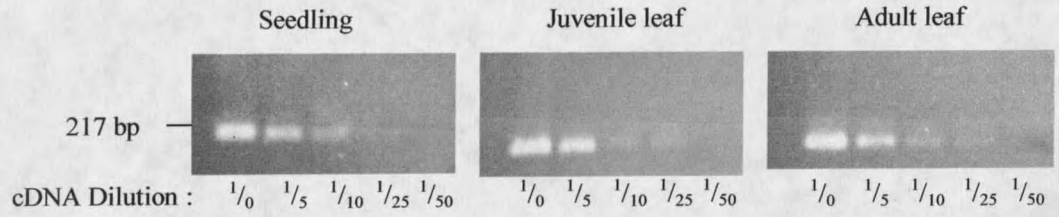

Figure 4.10. The quantity of ACA10 mRNA is similar in seedling, juvenile leaf and adult leaf tissue.
To roughly compare the quantity of ACA10 mRNA in different types of wild-type tissue, PCR products were amplified from a dilution series of the ACA10 cDNA from seedling, juvenile leaf, and adult leaf tissue. cDNA was synthesized from total RNA, and the primers used for PCR amplification are the same as in Figure 4.4.

High Resolution Mapping of the *CIF2* Gene

To map the dominant *CIF2* allele, which is required for expression of the *cif* phenotype in *cif1/cif1* homozygotes, a line was generated from a *cif*No-0 X Col cross that was homozygous for the recessive *cif1-1* allele and heterozygous for the Col and dominant No-0 alleles of *CIF2*. The progeny of this line segregated 3*cif*:1wild type (313:100, *P* value = ~ 0.7) and the plants showing a wild-type inflorescence, having a homozygous $CIF2^{Col}$/ $CIF2^{Col}$ genotype, were used for recombinant frequency mapping. At present, 1058 recombinant chromosomes have been assayed, isolating the *CIF2* gene to a 120kb region spanned by two overlapping BAC clones, T12O21 and F3C3, on chromosome 1. This region contains 22 candidate genes including a putative G-box binding protein, an RNA helicase, a heat shock transcription factor, and multiple genes with unknown function. This progress was made in spite of three delaying factors. First, the $CIF2^{No-0}$ allele exhibits some incomplete dominance. Approximately 5% of plants that are *cif1cif1*/$CIF2^{No-0}$ $CIF2^{Col}$ fail to develop a significant *cif* phenotype. For this

reason, all wild-type plants that are potential recombinants must be progeny tested to determine their true genetic status at the *CIF2* locus. Progeny testing takes approximately 8 weeks per round of mapping. Second, the *CIF2* gene lies within a highly repetitive region of DNA with numerous stretches that contain multiple small-sequence repeats, mini-satellites, or are AT rich. An approximate 30% reduction in recombination was observed in this region, possibly due to the presence of repetitive DNA. Third, the absence of Cereon markers on the BAC clone T12O21 necessitated the independent development of molecular markers in this region. Although final isolation of the *CIF2* gene was not accomplished, having delimited *CIF2* to a 120kb region on chromosome 1 will greatly facilitate the future cloning of this gene.

Discussion

Ca^{2+} is a much-studied second messenger in animal and plant cell signaling pathways. Until recently, a steady state rise in intracellular Ca^{2+} was presumed to activate cellular processes. Growing evidence now indicates that Ca^{2+} signals are propagated as waves of Ca^{2+} release and uptake, and that specific information is encoded in the amplitude and frequency of these oscillations within the cytosol (Sanders et al., 2002; Evans et al., 2001). To date, the best understood calcium signal transduction pathway in plants controls the opening and closing of stomata by guard cells within the epidermis of higher plants (Geisler, 2000). In wild-type plants, a variety of hormone or stress treatments trigger a series of Ca^{2+} oscillations in guard cells that result in prolonged closure of stomata. In contrast, mutants that show a steady state rise in Ca^{2+} (*det3*) or an

increased frequency of Ca^{2+} oscillations (*gca2*) in response to these same triggers fail to exhibit stomatal closure (Allen et al., 2000, 2001). Loss of stomatal closure in these mutants provides experimental evidence that signaling information is encoded in the amplitude and frequency of a calcium wave and that these parameters are interpreted by the cell to trigger a defined physiological response.

In the recent past, Ca^{2+} pumps were thought to provide a housekeeping role with regard to Ca^{2+} signal transduction; the Ca^{2+} signal was presumed to be the influx of Ca^{2+} through ion channels, and Ca^{2+} pumps were thought to function in reestablishing resting Ca^{2+} levels. Recent work shows that efflux attributes, including the Ca^{2+} affinity, activation threshold, and maximal velocity of a Ca^{2+} pump, help determine the size and frequency of Ca^{2+} oscillations, in addition to influx pathways (Sanders et al., 2002). Research in Xenopus oocytes demonstrates that overexpression of sarco-endoplasmic reticulum Ca^{2+} ATPases increases Ca^{2+} wave frequency and amplitude. This effect is attributed to an increased removal of cytoplasmic Ca^{2+} and more efficient refilling of Ca^{2+} stores (Lechleiter et al., 1998). This work and others (Camacho and Lechleiter, 1995; Roderick et al., 2000), show that efflux mechanisms, including Ca^{2+} ATPases, help determine the dynamic profile of a Ca^{2+} wave. Here it is shown that reducing the amount of normal transcript for ACA10, an *Arabidopsis* P-type IIB Ca^{2+}-ATPase, affects the elaboration of plant organs specific to a single plant developmental growth phase. That the *cif* phenotype is not pleiotropic, but rather is restricted to adult vegetative tissues, strongly suggests that ACA10 is a component of a defined Ca^{2+} signal transduction pathway required for the development of adult vegetative organs.

The Ca^{2+}-ATPases ACA8, ACA9, and ACA10 share approximately 70% identity at the amino acid level, and the genes for these pumps contain 32, 31, and 33 introns respectively (www.ncbi.nlm.nih.govl). This is a very high number compared to the other P-type IIB Ca^{2+}-ATPases which all contain between 6 and 8 introns. Pre-mRNAs for mammalian P-type IIB Ca^{2+}-ATPases that contain a high number of introns (22 or 23) have been shown to be alternatively spliced (Brandt and Vanaman, 1998). In mammalian P-type IIB Ca^{2+}-ATPase genes, one alternative splice junction is localized within the CaM-binding domain, and the isoforms arising from alternative splicing exhibit different CaM-binding affinities (Carafoli, 1994; Brandt and Vanaman, 1998). A second alternative splice site is located within the first intracellular loop between the phospholipid binding domain and the sequence involved in autoinhibitory interactions. It is speculated that alternative splicing at this site affects the phospholipid regulation of mammalian P-type IIB Ca^{2+}-ATPase isoforms by altering the accessibility of the phospholipid-binding domain to acidic phospholipids.

In this report it is shown that ACA10 is expressed constitutively in seedlings, juvenile vegetative leaves, and adult vegetative leaves, and that the amount of ACA10 transcript present in these different tissue types is similar. This is somewhat surprising in light of the specificity of the *cif* trait to adult vegetative organs. The possibility that differentially processed isoforms of ACA10 are specific to different tissue types is a potential explanation for this apparent discrepancy. In mammalian systems, it has been shown that numerous different Ca^{2+}-ATPase isoforms, generated through alternative splicing, are expressed in a tissue-specific manner (Zylinska et al., 2002; Strehler and

Zacharias, 2001; Carafoli and Stauffer, 1994). Although alternative splicing has not yet been addressed in plant P-type IIB Ca^{2+}-ATPases, the structural similarity of *Arabidopsis* Ca^{2+} pumps ACA8, ACA9, and ACA10 to those in animal systems, and their high number of introns suggests that differential splicing may play a role in the regulation of these plant enzymes. An interesting note is that the genes for both ACA8 and ACA10 contain an intron that lies roughly in the middle of the CaM-binding domain, a similar configuration to that in mammalian systems where differential splicing has been demonstrated (www.ncbi.nlm.nih.gov1).

It was shown in Chapter 2 that *cif* is inherited as a two gene trait involving the action of a recessive and a dominant locus; *cif1-1* and $CIF2^{No-0}$ respectively, and that the *cif1-1* allele is silent as a single gene mutation. One possible explanation for this two-gene requirement is that a second Ca^{2+}-ATPase provides a redundant function to ACA10 and that the expression of this second pump must also be reduced to see a phenotypic effect. The region on chromosome 1 to which $CIF2^{No-0}$ maps does not contain a gene encoding a second Ca^{2+}-ATPase. However, a less obvious possibility is that $CIF2^{No-0}$ encodes a gene that regulates the expression or activity of a redundant pump. The RNA helicase gene that lies within the defined $CIF2^{No-0}$ map region is a possible candidate for the regulation of a second P-type IIB Ca^{2+}-ATPase. Numerous RNA helicases have been shown to play a role in pre-mRNA splicing (Schwer and Meszaros, 2000; Liu,. 2002), and these enzymes have also been shown to regulate alternative splicing of exons containing AC-rich exon enhancer elements (Honig et al., 2002). Although we currently have no data indicating that $CIF2^{No-0}$ regulates the expression of a redundant

Ca^{2+}-ATPase, or that alternative splicing contributes to the regulation of P-type IIB Ca^{2+}-ATPases in higher plants, the possibility that *CIF2* encodes an RNA helicase that is involved in the pre-mRNA splicing of a calcium pump that provides redundant function to ACA10 is quite compelling. This is only one model for the potential role of *CIF2* in generation of the *cif* phenotype, and many other activities for *CIF2* within Ca^{2+} signal transduction pathways are also possible.

Calcium is a ubiquitous second messenger in eukaryotic signal transduction cascades. Different calcium sensors recognize specific calcium signatures and transduce them into downstream effects, including altered protein phosphorylation and gene expression patterns. In plants, intracellular Ca^{2+} levels are modulated in response to various signals, including hormones, light, mechanical disturbances, abiotic stress, and pathogen elicitors (Cheng et al., 2002). Stimulus-triggered calcium oscillations are also known to regulate stomatal closure in higher plants, and a wide variety of growth and developmental processes are thought to be regulated by Ca^{2+} fluxes including pollen tube growth in maize (Estruch et al., 1994), potato tuberization (MacIntosh et al., 1996), and nodulation in soybean (Weaver and Roberts, 1992). Other developmental processes likely involving Ca^{2+} signaling include embryogenesis, seed development and germination in sandalwood (Anil et al., 2000).

Although Ca^{2+} signaling has been implicated in numerous response and developmental pathways, in general little is known regarding the specific mechanisms that contribute to the generation of different calcium profiles and other mechanisms that contribute to stimulus specificity. Calcium-permeable channels have been investigated

with electrophysiological, biochemical, and molecular approaches, and these studies are now beginning to yield insight into the nature and control of these Ca^{2+} influx routes that underlie the generation of Ca^{2+} signals. *TPC1* is a unique gene in *Arabidopsis* that encodes a plasma membrane Ca^{2+} permeable channel (Sanders et al., 2002). Although there are indications that TPC1 forms a depolarization-activated Ca^{2+} channel, there are as yet no indications as to the physiological role(s) of TPC1. Additionally, the *Arabidopsis* genome appears to encode 20 members of a plasma membrane, cyclic nucleotide-gated channel (CNGC) family (Sanders et al., 2002). Although it is likely that CNGCs provide an essential link between cyclic nucleotides and Ca^{2+} signaling, to date there are no reports of cyclic nucleotide-activated channel activity in planta. Additionally, no genes encoding endomembrane Ca^{2+} release channels have yet been identified (Sanders et al., 2002). Of the ten P-type IIB Ca^{2+}-ATPases in Arabidopsis, only four have been cloned and characterized, and no mutants for these enzymes have previously been described. Functional redundancy has likely made it difficult to assign individual physiologic roles for these Ca^{2+} pumps. Although calcium dependent protein kinases (CDPKs) have been implicated biochemically to act as key mediators of calcium induced responses, very little is known about which particular CDPK acts as the calcium sensor in each case (Cheng, 2002).

Hence, in spite of the primary role that calcium signaling plays with regard to plant physiology and development, much remains to be learned regarding the specifics of Ca^{2+} driven signal transduction pathways. *cif1-1* is the first P-type IIB calcium pump mutant to be described in a higher plant and its phenotypic association with a single plant

developmental growth phase provides new insight into the possible roles that Ca^{2+} pumps may play in Ca^{2+} mediated developmental responses. That altered development in *cif* plants is restricted to adult vegetative tissues, supports a model for Ca^{2+} signaling in which individual Ca^{2+}-ATPases act as components of defined Ca^{2+} signal transduction cascades that mediate progression through specific plant developmental pathways. Further studies of the *cif1-1* mutant, including the cloning of *CIF2*, will undoubtedly shed further light on the regulation of Ca^{2+} signaling in higher plants. The isolation of other, non-allelic *cif* mutants should identify additional genes that are players in the same *cif* developmental pathway as ACA10. Second site suppressor screens in *cif* should allow for the elucidation of specific Ca^{2+} response elements that act downstream from ACA10. Lastly, expression profiling of the *cif* mutant using microarray analysis or SAGE might identify genes specifically regulated by a Ca^{2+} signal transduction pathway involving ACA10. These contributions would mark great advances toward a more complete understanding of Ca^{2+} signaling in higher plants.

Materials and Methods

Differential Staining of Aborted and Nonaborted Pollen

The stain used for differential staining of aborted and nonaborted pollen was prepared by adding the following constituents in the order given, mixing after each addition, and storing in a colored bottle:

95% ETOH; 10 ml
Malachite green; 10 mg (1 ml of a 1% solution in 95% ETOH)
Distilled H_20; 50 ml
Glycerol; 25 ml
Phenol; 5 gm
Chloral hydrate; 5 gm
Acid fuchsin; 50 mg (5 ml of a 1% solution in H_20)
Orange G; 5 mg (0.5 ml of a 1% solution in H_20)
Glacial Acetic acid; 1 ml

The staining procedure is described in Alexander, 1969.

Map-Based Cloning of the
CIF1 Gene and Plant Transformation

Linkage analysis to INDELS that were polymorphic between the S-96 and Col ecotypes (Bell and Ecker, 1994; Cereon *Arabidopsis* Polymorphism Collection, http://www.arab.org/cereon/) was performed on 29 F_2 *cif* progeny from a *S96cif1-2* X Col cross to determine a rough map location for the *cif1-2* allele. For high resolution mapping, a parental mapping line that was homozygous for the dominant $CIF2^{S96}$ allele, and heterozygous for the recessive *cif 1-2* allele was generated. This population segregated in a 3:1 non*cif*:*cif* phenotypic ratio (1472:464, *P* value = ~0.3) and *cif* plants, being homozygous for the *cif1-2* allele were screened by PCR for recombination. DNA from these plants was extracted and amplified using the REDExtract-N-Amp Plant PCR Kit (Sigma). The PCR cycle for most INDEL markers included a 94°C-denaturing step for 30 seconds, a 55°C-annealing step for 1 minute, and a 72°C extension step for 30 seconds. This cycle was repeated 29 times for a total of 30 cycles in a Mastercycler Gradient Thermal Cycler (Eppendorf Scientific). Analysis of ~1220 recombinant chromosomes delimited the *cif 1-2* allele to a region spanning 80 kb on the overlapping

BAC clones T16L4 and F27B13 on chromosome 4. PCR amplification of 700 bp fragments and direct sequencing was then used to scan individual genes for loss of function mutations. Sequencing was performed by Northwoods DNA, Inc. (Becida, MN). Cloning of ACA10 was accomplished by PCR amplification of a 9.5kb DNA fragment from the Columbia ecotype containing the wild-type allele of ACA10, as well as ~1500bp preceding the 5′ end of the gene and 300bp following the 3′ end. This DNA fragment was generated using Herculase Enhanced DNA Polymerase (Stratagene), and the cycling conditions outlined in the Herculase reference protocol for amplifying targets ≤ 10 kb. A *Sal*I restriction site was engineered into the 5′gene primer. The amplified ACA10 product was end polished with T_4 DNA polymerase and subsequently cut with *Sal*I. The GUS expression vector pBI101 (Jefferson et al., 1987) was modified by removing the GUS coding sequence at the *Xba*I and *Sst*I sites and substituting the corresponding portion of the polylinker from plasmid pGEM-7Zf$_{(+)}$ (Promega). The polished, *Sal*I cut PCR product was cloned into this modified pBI vector cut with *Sal*I and *Sma*I. The pBIACA10 plasmid was introduced into electrocompetent *E. coli* by direct transformation (An et al., 1988) and sub-cloned into *Agrobacterium tumefaciens* GV3101 using the same method. Mutant *cif1-1* plants were transformed with the pBIACA10 T-DNA by the floral dipping protocol described by Clough and Bent (1998).

RNA Preparation

All RNA preparation procedures were carried out on ice, using baked glassware and solutions treated with diethylpyrocarbonate. Phenol/chloroform/isoamyl alcohol (phenol/CIAA) (25:24:1) was equilibrated 3 times with 100 mM Tris-HCl (pH 8.3) and

10 mM EDTA (TE 10:10). For RTPCR analysis of the No-0, *cif1-1*, S96 and *cif1-2* mRNA transcripts, RNA was prepared from seedlings grown under continuous fluorescent light in liquid GM (Valvekens et al., 1988) for 14 days. For RT-PCR expression analysis, No-0 and *cif1-1* seedlings were grown on GM plates (Valvekens et al., 1988) overlaid with sterile filter paper for 7 days, and juvenile and adult leaves were harvested from No-0 and *cif1-1* plants grown on pots in a 16-hour photoperiod of fluorescent light for approximately 30 days. 3 grams of fresh weight tissue were ground to a powder in liquid N_2 in a mortar and pestle, transferred to a 30-ml Corex tube containing 10 ml of extraction buffer [50mM Tris-HCl (pH 8.3), 150 mM NaCl, 10 mM EDTA, 1% lauryl sarcosine] and 10 ml phenol/CIAA, and mixed with a polytron at low speed for 10 seconds, and at high speed for 10 seconds. Samples were then vortexed for 10 minutes. After centrifugation, the aqueous phase was extracted three more times with phenol/CIAA, and the nucleic acids precipitated with Na acetate/ethanol. The precipitates were dissolved in 3 ml TE 10:10 and precipitated twice with 8 M LiCl, the first time overnight on ice in a total volume of 4 ml and the second time for 4-5 hrs in a volume of 2 ml. The RNA pellet was dissolved in 1.5 ml H_2O and ethanol-precipitated. RNA yields were 470-690 ug of RNA per gram of tissue for seedling and adult leaf tissue, and 230-245 ug of RNA per gram of tissue for juvenile leaves.

cDNA Synthesis and Dilutions for RT-PCR

For RT-PCR analysis, cDNA was synthesized from 1μg of total RNA using the ThermoScript RT-PCR System (dT primer) (Invitrogen). To compare the amount of ACA10 transcript present in seedlings, juvenile leaves and adult leaves, 1 ul of cDNA

was diluted in 5, 10, 25, and 50 ul of H_20 and 2 ul of these dilutions were amplified by PCR. Primers used to amplify cDNA fragments flanked the *cif1-1* 23bp deletion and *cif1-2* point mutation as outlined in Figures 4.4 and 4.5.

References Cited

Adamo, H.P., and Grimaldi, M.E. (1998). Functional consequences of relocating the C-terminal calmodulin-binding autoinhibitory domains of the plasma membrane Ca2+ pump near the N-terminus. *Biochem. J.* **331**, 763-766.

Alexander, M.P. (1969). Differential staining of aborted and nonaborted pollen. *Stain Technology* **44**(3), 117-122.

An, G., Ebert, P.R., Mitra, A. and Ha, S.B. (1988) Binary vectors. *Plant Mol Biol. Manual,* **A3**, 1-19.

Anil, W.S., Harmon, A.C., and Rao, K.S. (2000). Spatio-termporal accumulation and activity of calcium-dependent kinases during embryogenesis, seed development and germination in sadalwood. *Plant Physiol.* **122**, 1035-1043.

'The Arabidopsis Genome Initiative' (2000). Analysis of the genome sequence of the flowering plant *Arabidopsis thaliana. Nature* **408**, 796-813.

Axelsen, K.B., and Palmgren, M.G. (1998). Evolution of substrate specificities in the P-type ATPases superfamily. *J. Mol. Evol.* **46**, 84-101.

Axelsen, K.B., and Palmgren, M.G. (2001). Iventory of the superfamily of P-Type ion pumps in Arabidopsis. *Plant Physiol.* **126**, 696-706.

Bagnall, D.J., King, R.W., Whitelam, G.C., Boylan, M.T., Wagner, D., and Quail, P.H. (1995). Flowering responses to altered expression of phytochrome in mutants and transgenic lines of Arabidopsis thaliana (L.) Heynh. *Plant Physiol.* **108**, 1495-1503.

Beall, F.D., Morgan, P.W., Mander, L.N., Miller, F.R., and Babb, K.H. (1991). Genetic regulation of development in *Sorgum bicolor*. V. The ma_3R allele results in gibberellin enrichment . *Plant Physiol.* **95**, 116-125.

Bell, C. J., and Ecker, J. R. (1994). Assignment of 30 microsatellite loci to the linkage map of *Arabidopsis. Genomics* **19**, 137-144.

Berger, B. (1965). The taxonomic confusion within *Arabidopsis* and allied genera. In *Arabidopsis* Research (G. Röbbelen, ed.), Report of an International Symposium, Arab. Inf. Serv, Göttingen, 19-25.

Bongard-Pierce, D. K., Evans, M. M. S., and Poethig, R. S. (1996). Heteroblastic features of leaf Anatomy in maize and their genetic regulation. *Int. J. Plant Sci.* **157**, 331-340.

Bonza, M.C., Morandini, P., Luoni, L., Geisler, M., Palmgren, M.G., and De Michelis, M.I., (2000). At-ACA8 encodes a plasma membrane-localized calcium-ATPase of Arabidopsis with a calmodulin-binding domain at the N terminus. *Plant Physiol.* **123**, 1495-1506.

Bowling, S.A. et al. (1994) A mutation in *Arabidopsis* that leads to constitutive expression of systematic acquired resistance. *Plant Cell* **6**, 1845-1857.

Boylan, M.T., and Quail, P.H. (1989). Oat phytochrome is biologically active in transgenic tomatoes. *Plant Cell* **1**, 765-773.

Boylan, M.T., and Quail, P.H. (1991) Phytochrome A overexpression inhibits hypocotyls elongation in transgenic *Arabidopsis. Proc. Natl. Acad. Sci. USA* **88**, 10806-10810.

Bradley, D., Carpenter, R., Copsey, L., Vincent, C., Rothstein, S. and Coen, E. (1996a). Control of inflorescence architecture in *Antirrhinum. Nature* **379**, 791-797.

Bradley, D., Vincent, C., Carpenter, R. and Coen, E. (1996b). Pathways for inflorescence and floral induction in *Antirrhinum. Development* **122**, 1535-1544.

Brandt, P.C., and Vanaman, T.C. (1998). Calmodulin and ion flux regulation. In Calmodulin and Signal Transduction (L Van Eldik, DM Watterson, eds.) Academic Press, San Diego, 397-471.

Butler, W.L., Norris, K.H., Siegelman, H.W., and Hendricks, S.B. (1959). Detection, assay, and preliminary purification of the pigment controlling photoresponsive development of plants. *Proc. Natl. Acad. Sci. USA* **45**, 1703-1708.

Camacho, P., and Lechleiter, J.D. (1995). Spiral calcium waves: implications for signaling. *Ciba. Found. Symp.* **188**, 66-84.

Carafoli, E. (1994). Biogenesis: plasma membrane calcium ATPase: 15 years of work on the purified enzyme. *FASEB J.* **8**, 993-1002.

Carafoli, E., and Stauffer, T. (1994). The plasma membrane calcium pump: functional domains, regulation of the activity, and tissue specificity of isoform expression. *J Neurobiol.* **25**(3), 312-324.

Carol, P., Peng. J., and Harberd, N.P. (1995). Isolation and preliminary characterization of *gas1-1*, a mutation causing partial suppression of the phenotype conferred by the gibberellin-insensitive (*gai*) mutation in *Arabidopsis thaliana* (L.) Heyhn. *Planta* **197**, 414-417.

Chandler, J., Wilson, A., and Dean, C. (1996). Arabidopsis mutants showing an altered response to vernalization. *Plant J.* **10**, 637-644.

Cheng, S.H., Willmann, M.R., Chen, H.C., and Sheen, J. (2002). Calcium signaling through protein kinases. The Arabidopsis calcium-dependent protein kinase gene family. *Plant Physiol.* **129**, 469-485.

Chiang, H-H, Hwang, I., and Goodman, H.M. (1995). Isolation of the *Arabidopsis GA4* locus. *Plant Cell* **7**, 195-201.

Chien, J. C. and Sussex, I. M. (1996). Differential regulation of trichome formation on the adaxial and abaxial leaf surfaces by gibberellins and photoperiod in *Arabidopsis thaliana* (L.) Heynh. *Plant Physiol.* **111**, 1321-1328.

Childs, K.L., Cordonnier-Pratt, M.M., Pratt, L.H., and Morgan, P.W. (1992). Genetic regulation of development in *Sorgum bicolor*. VII. Ma_3R flowering mutant lacks a phytochrome that predominates in green tissue. *Plant Physiol.* **99**, 765-770.

Clack, T., Mathews, S., and Sharrock, R.A. (1994). The phytochrome apoprotein family in *Arabidopsis* is encoded by five genes: the sequences and expression of *PHYD* and *PHYE*. *Plant Mol.Biol.* **25**, 413-427.

Clough, S.J., and Bent, A.F. (1998). Floral dip: a simplified method for *Agrobacterium*-mediated transformation of *Arabidopsis thaliana*. *Plant J.* **16**(6), 735-743.

Coen, E.S., and Meyerowitz, E.M. (1991). The war of the whorls: genetic interactions controlling flower development. *Nature* **353**, 31-37.

Crivici, A., and Ikura, M. (1995). Molecular and structural basis of target recognition by Calmodulin. *Annu. Rev. Biophys. Biomol. Struct.* **24**, 85-116.

Desfeux, C., Clough, S.J. and Bent, A.F. (2000). Female reproductive tissues are the primary target of *Agrobacterium*-mediated transformation by the Arabidopsis floral-dip method. *Plant Physiol.* **123**, 895-904.

Devlin, P.F., Rood, S.B., Somers, D.E., Quail, P.H., and Whitelam, G.C. (1992). Photophysiology of the elongated internode (*ein*) mutant of *Brassica rapa*. *ein* mutant lacks a detectable phytochrome B-like polypeptide. *Plant Physiol.* **100**, 1442-1447.

Doebley, J., Stec, A., and Hubbard, L. (1997). The evolution of apical dominance in maize. *Nature* **386**, 485-488.

Estruch, J.J., Kadwell, S., Merlin, E., and Crossland, L. (1994). Cloning and characterization of a maize pollen-specific calcium-dependent calmodulin-independent protein kinase (abstract no. J6-430). *J. Cell Biochem.* Suppl. **21A**, 507.

Evans, D.E. (1994). Calmodulin-stimulated calcium pumping ATPases located at higher plant intracellular membranes: a significant divergence from other eukaryotes? *Physiol. Plant* **90**, 420-426.

Evans, M. M. S., Passas, H. J. and Poethig, R. S. (1994). Heterochronic effects of *glossy15* mutations on epidermal cell identity in maize. *Development* **120**, 1971-1981.

Evans, M. M. S. and Poethig, R. S. (1995). Gibberellins promote vegetative phase change and reproductive maturity in maize. *Plant Physiol.* **108**, 475-487.

Evans, M. M. S. and Poethig, R. S. (1997). The *viviparous8* mutation delays vegetative phase change and accelerates the rate of seedling growth in maize. *Plant J.* **12**, 769-779.

Evans, D.E., and Williams, L.E. (1998). P-type calcium ATPases in higher plants: biochemical, molecular and functional properties. *Biochim. Biophys. Acta* **1376**, 1-25.

Evans, N.H., McAinsh, M.r., and Hetherington, A.M. (2001). Calcium oscillations in higher plants. *Curr. Opin. Plant Biol.* **4**(5), 415-420.

Ezura, H., and Harberd, N.P. (1995). Endogenous gibberellin levels influence *in vitro* shoot regeneration in *Arabidopsis thaliana* (L.) Heyhn. *Planta* **197**, 301-305.

Fankhauser, C., and Chory, J. (1997). Light control of plant development. In Annual review of Cell and Developmental Biology (JA Spudich, J Gerhart, SL McKnight, R Schekman, eds.) Annual Reviews, Palo Alto, CA, 203-229.

Geisler, M. Axelsen, K.B., Harper, J.F. and Palmgren, M. (2000a). Molecular aspects of higher plant P-type Ca^{2+}-ATPases. *Biochimica et Biophysica Acta* **1465**, 52-78.

Geisler, M., Frangne, N., Gomes, E., Martinoia, E., and Palmgren, M.G. (2000b). The *ACA4* gene of Arabidopsis encodes a vacuolar membrane calcium pump that improves salt tolerance in yeast. *Plant Physiol.* **124**, 1814-1827.

Goebel, K. (1900). *Organography of Plants. Part 1. General Organography.* Transl. IB Balfour. Oxford: Clarendon (from German).

Goosey, L., and Sharrock, R. (2001). The *Arabidopsis compact inflorescence* genes: phase-specific growth regulation and the determination of inflorescence architecture. *The Plant Journal* **26**(5), 549-559.

Guo, H., Yang, H., Mockler, T.C., and Lin, C. (1998). *Science* **279**, 1360-1363.

Hanzawa, Y., Takahashi, T. and Komeda, Y. (1997). *ACL5*: an *Arabidopsis* gene required for internodal elongation after flowering. *The Plant Journal* **12**, 863-874.

Hanzawa, Y., Takahashi, T., Michael, A.J., Burtin, D., Long, D., Pineiro, M., Coupland, G. and Komeda, Y. (2000). *ACAULIS5*, an *Arabidopsis* gene required for stem elongation, encodes a spermine synthase. *EMBO J.* **19**, 4248-4256.

Harmon, A.C., Yoo, B-C, and McCafferey, C. (1994). Pseudosubstrate inhibition of CDPK, a protin kinase with a calmodulin-like domain. *Biochem.* **33**, 7278-7287.

Harper, J.F., Huang, J-F, and Lloyd, S.J. (1994). Genetic identification of an autoinhibitor in CDPK, a protein kinase with a calmodulin-like domain. *Biochem.* **33**, 7267-7277.

Harper, J.F., Hong, B., Hwang, I., Guo, I.Q., Stoddard, R., Huang, J.F., Palmgren, M.G., and Sze, H. (1998). A novel calmodulin-regulated Ca^{2+} ATPase (ACA2) from Arabidopsis with an N-terminal autoinhibitory domain. *J. Biol. Chem.* **273**, 1099-1106.

Horsch, R.B., Klee, H.J., Stachel, S., Winans, S.C., Nester, E.W., Rogers, S.G., and Fraley, R.T. (1986). Analysis of Agrobacterium tumefaciens virulence mutants in leaf discs. *Proc Nat Acad Sci U S A.* **83**(8):2571-2575.

Hooley, R. (1994). Gibberellins: perception, transduction and responses. *Plant Mol. Biol.* **26**, 1529-1555.

Huang L., Berkelman, T., Franklin, A.E., and Hoffman, N.E. (1993). Characterization of a gene encoding a Ca^{2+} ATPase-like protein in the plastid envelope. *Proc. Natl. Acad. Sci. USA.* **90**, 10066-10070.

Hwang, I., Harper, J.F., Liang, F., and Sze, H. (2000a). Calmodulin activation of an endoplasmic reticulum-located calcium pump involves an interaction with the N-terminal autoinhibitory domain. *Plant Physiol.* **122**, 157-168.

Hwang, I., Sze, H., and Harper, J.F. (2000b). A calcium-dependent protein kinase can inhibit a calmodulin-stimulated Ca^{2+} pump (ACA2) located in the endoplasmic reticulum of *Arabidopsis. Proc. Natl. Acad. Sci. USA* **97**, 6224-6229.

Jacobsen, S.E., and Olszewski, N.E. (1993). Mutations at the *SPINDLY* locus of Arabidopsis alter gibberellin signal transduction. *Plant Cell* **5**, 887-896.

James, P., Vorherr, T., and Carafoli, E., (1995). *Trends Biochem. Sci.* **20**, 38-42.

Jander, G., Norris, S.R., Rounsley, S.D., Bush, D.F., Levin, I.M., and Last, R.L. (2002). Arabidopsis map-based cloning in the post-genome era. *Plant Physiol.* **129**(2), 440-50.

Jefferson, R.A., Kavanaugh, T.A., and Bevan, M.W. (1987). GUS fusions: Beta-glucuronidase is a sensitive and versatile gene fusion marker in higher plants. *EMBO J.* **6**, 3901-3907.

Jordan, E.T., Hatfield, PlM., Hondred, D., talon, M., Zeevaart, J.A.D., and Vierstra, R.D. (1995). Phytochrome A overexpression in transgenic tobacco. Correlation of dwarf phenotype with high concentration of phytochrome in vascular tissue and attenuated gibberellin levels. *Plant Physiol.* **107**, 797-805.

Kay, S.A., Nagatani, A., Deith, B., Deak, M., Furuya, M., and Chua, N-H (1989). Rice phytochrome is biologically active in transgenic tobacco. *Plant Cell* **1**, 775-782.

Kerstetter, R.A., and Poethig, R.S., (1998). The specification of leaf identity during shoot development. *Annu. Rev. Cell Dev. Biol.* **14**, 373-398.

Komeda, Y., Takahashi, T. and Hanzawa, Y. (1998). Development of inflorescences in Arabidopsis thaliana. *J. Plant Res.* **111**, 283-288.

Koornneef, M., Elgersma, A., Hanhart, C.J., van Loenen-Martinet, E.P., van Rijn, L., and Zeevaart, J.A.D. (1985) A gibberellin insensitive mutant of *Arabidopsis thaliana. Physiol. Plant* **65**, 33-39.

Koornneef, M., Rolff, E., and Spruit, C.J.P. (1980). Genetic control of light-inhibited hypocotyl elongation in *Arabidopsis thaliana* (L.) Heynh. *Z. Pflanzenphusiol.* **100**.S, 147-160.

Koornneef, M., and van der Veen, J.H. (1980). Induction and analysis of gibberellin sensitive mutants in *Arabidopsis thaliana* (L.) Heyhn. *Theor. Appl. Genet.* **58**, 257-263.

Laval, V., Masclaux, F., Serin, A., Carriere, M., Roldan, C., Devie, M., Pont-Lezica, R.f., and Galaud, J.P. (2003). Seed germination is blocked in Arabidopsis putative vacuolar sorting receptor (atbp80) antisense transformants. *J. Exp. Bot.* **54**(381), 213-21.

Lawson, E. and Poethig, R. S. (1995). Shoot development in plants: time for a change. *Trends Genet.* **11**, 263-268.

Lechleiter, J.D., John, L.M., and Camacho, P. (1998). Ca^{2+} wave dispersion and spiral wave entrainment in *Xenopus laevis* oocytes overexpressing Ca^{2+} ATPases. *Biophys. Chem.* **72**, 123-129.

Leutwiler, L.S., Hough-Evans, B.R. and Meyerowitz, E.M. (1984). The DNA of *Arabidopsis thaliana. Mol. Gen. Genet.* **194**, 15-23.

Liscum, E, and Hangarter, R.P. (1993). Genetic evidence that the Pr form of phytochrome B mediates gravitropism in *Arabidopsis thaliana. Plant Physiol.* **103**, 15-19.

MacIntosh, G.C., Ulloa, R.M., Raíces, M., and Téllez-Iñón, M.T. (1996). Changes in calcium-dependent protein kinase activity during in vitro tuberization in potato. *Plant Physiol.* **112**, 1541-1550.

Martinez-Zapater, J.M., Jarillo, J.A., Cruz-Alvarez, M., Roldan, M. and Salina, J. (1995). *Arabidopsis* late-flowering *fve* mutantsare affected in both vegetative and reproductive development. *Plant J.* 7, 543-551.

Matzke, M., Matzke, A.J.M. and Kooter, J.M. (2001). RNA: guiding gene silencing. *Science* **293**, 1080-1083.

McAinish, M.R. and Hetherington, A.M. (1998). Encoding specificity in Ca^{2+} signaling systems. *Trends Plant Sci.* **3**, 32-36.

McCallum, C.M., Comai, L., Greene, E.A. and Henikoff, S. (2000). Targeted screening for induced mutations. *Nat. Biotechnol.* **18**(4), 455-457.

McDaniel, C. N., Singer, S. R. and Smith. S. M. E. (1992). Developmental states associated with the floral transition. *Dev. Biol.* **153**, 59-69.

McPhalen, C.A., Strynadka, N.C., and James, M.N.G. (1991). Calcium-binding sites in proteins: A structural perspective. *Adv. Prot. Chem.* **42**, 77-144.

Meier, C. et al. (2001) Gibberellin response mutants identified by luciferase imaging. *Plant J.* **25**, 509-519.

Meinke, D.W., Cherry, J.M., Dean, C., Rounsley, S.C. and Koorneef, M. (1998) *Arabidopsis thaliana*: A Model Plant for Genome Analysis. *Science* **282**, 662-682.

Michaels, S.D., and Amasino, R.M. (1999a). FLOWERING LOCUS C encodes a novel MADS domain protein that acts as a repressor of flowering. *Plant Cell* **11**, 949-956.

Michaels, S.D., and Amasino, R.M. (1999b). The gibberellic acid biosynthesis mutant *ga1-3* of *Arabidopsis thaliana* is responsive to vernalization. *Dev. Genet.* **25**, 194-198.

Michaels, S.D., and Amasino, R.M. (2001). Loss of FLOWERING LOCUS C activity eliminates the late-flowering phenotype of *FRIGIDA* and autonomous pathway mutations, but not responsiveness to vernalization. *Plant Cell* **13**, 935-941.

Miller, A.J., Straume, M., Chory, J., Chua, N.-H. and Kay, S.A. (1995) Circadian clock mutants in *Arabidopsis* identified by luciferase imaging. *Science* **267**, 1161-1164.

Moose, S. P. and Sisco, P. H. (1994). *Glossy15* Controls the Epidermal Juvenile-to-Adult Phase Transition in Maize. *The Plant Cell* **6**, 1343-1355.

Napoli, C., Lemieux, C. and Jorgensen, R. (1990). Introduction of a chimeric chalonce synthase gene into petunia results in reversible co-suppression of homologous genes *in trans*. *Plant Cell* **2**, 279-289.

Olszewski, N., Sun, T., and Gubler, F. (2002). Gibberellin signaling: biosynthesis, catabolism, and response pathways. *Plant Cell* Supplement 2002, S61-S80.

O'Neil, K.T., and DeGrado, W.F., (1990). *Trends Biochem. Sci.* **15**, 59-64.

Page, D.R., and Grossniklaus, U. (2002) The art and design of genetic screens: *Arabidopsis thaliana. Nature Reviews Genetics* **3**, 124-136.

Peng, J., and Harberd, N.P. (1997). Gibberellin deficiency and response mutations suppress the stem elongation phenotype of phytochrome-deficient mutants of Arabidopsis. *Plant Physiol.* **113**(4), 1051-8.

Pennisi, E. Plants Join the Genome Sequencing Bandwagon. *Science* **290**, 2054-2057.

Poethig, R. S. (1988). Heterochronic mutations affecting shoot development in maize. *Genetics* **119**, 959-973.

Poethig, R. S. (1990). Phase change and the regulation of shoot morphogenesis in plants. *Science* **250**, 923-930.

Poethig, R.S., Coe, E.H., and Johri, M.M. (1986). Cell lineage patterns in maize embryogenesis: a clonal analysis. *Dev. Biol.* **117**, 392-404.

Pruitt, R.E. and Meyerowitz, E.M. (1986). Characterization of the genome of *Arabidopsis thaliana. J. Mol. Biol.* **187**, 169-183.

Putterill, J., Robson, F., Lee, K., Simon, R., and Coupland, G. (1995). The *constans* gene of Arabidopsis promotes flowering and encodes a protein showing similarities to zinc finger transcription factors. *Cell* **80**, 847-858.

Quail, P.H., Boylan, M.T., Parks, B.M., Short, t.W., Xu, Y., and Wagner, D. (1995). Phytochromes: Photosensory perception and signal transduction. *Science* **268**, 675-680.

Rédei, G.P. (1992) In Methods in *Arabidopsis* Research (eds Koncz, C., Chua, N.-H., and Schell, J.) World Scientific, Singapore, 1-15.

Rédei, G.P. (1970). *Arabidopsis thaliana* (L.) Heynh. A review of the genetics and biology. *Bibliog. Genet.* **20**, 1-151.

Reed, J.W., Foster, K.R., Morgan, P.W., and Chory, J. (1996). Phytochrome B affects responsiveness to gibberellins in Arabidopsis. *Plant Physiol.* **112**, 337-342.

Reed, J.W., Nagatani, A., Elich, T.D., Fagan, M., and Chory, J. (1994). Phytochrome A and phytochrome B have overlapping but distinct functions in *Arabidopsis* development. *Plant Physiol.* **104**, 1139-1149.

Reed, J.W., Nagpal, P., Poole, D.S., Furuya, M., and Chory, J. (1993). Mutations in the gene for the red/far-red light receptor phytochrome B alter cell elongation and physiological responses throughout *Arabidopsis* development. *Plant Cell* **5**, 147-157.

Reeves, P.H., and Coupland, G. (2001). Analysis of flowering time control in Arabidopsis by comparison of double and triple mutants. *Plant Physiol.* **126**, 1085-1091.

Roderick, H.L., Lechleiter, J.D. and Camacho, P. (2000). Cytosolic phosphorylation of calnexin controls intracellular Ca^{2+} oscillations via an interaction with SERCA2b. *J.Cell Biol.* **149**, 1235-1248.

Rood, S.B., Willians, P.H., Pearce, D., Murofushi, N., Mander, L.N., and Pharis, R. (1990). A mutant gene that increases gibberellin production in *Brassica. Plant Physiol.* **93**, 1168-1174.

Ruban, A.V., Wentworth, M., Yakushevska, A.E., Andersson, J., Lee, P.J., Keegstra, W., Dekker, J.P., Boekema, E.J., Jansson, S., and Horton, P. (2003). Plants lacking the main light-harvesting complex retain photosystem II macro-organization. *Nature* **421**, 648-652.

Sanders, D., Pelloux, J., Brownlee, C. and Harper, J.F. (2002). Calcium at the crossroads of signaling. *Plant Cell* Supplement 2002, S401-S417.

Sanders, D., Brownlee, C., and Harper, J.F. (1999). Communicating with calcium. *Plant Cell* **11**, 691-706.

Schell, J. (1987). Transgenic plants as tools to study the moleuclar organization of plant genes. *Science* **237**, 1176-1187.

Shannon, S. and Meeks-Wagner, D. R. (1991). A mutation in the *Arabidopsis TFL1* gene affects inflorescence meristem development. *Plant Cell* **3**, 877-892.

Sharrock, R.A., and Quail, P.H. (1989). Novel phytochrome sequences in *Arabidopsis Thaliana:* structure, evolution, and differential expression of a plant regulatory photoreceptor family. *Genes Dev.* **3**, 1745-1757.

Sheldon, C.C., Burn, J.E., Perez, P.P., Megzger, J., Edwards, J.A., Peacock, W.J., and Dennis, E.S. (1999). The *FLF* MADS box gene: a repressor of flowering in *Arabidopsis* regulated by vernalization and methylation. *Plant Cell* **11**, 445-458.

Simpson, G.G., and Dean, C. (2002). Arabidopsis, the rosetta stone of flowering time? *Science* **296**, 285-289.

Simpson, G.G., Gendall, A.R., and Dean, C. (1999). When to switch to flowering. *Annu. Rev. Cell Dev. Biol.* **99**, 519-550.

Smith, H. (1994). Sensing the light environment: the functions of the phytochrome family. In Photomorphogenesis in Plants – 2nd Edition (R.E. Kendrick, and G.H.M. Kronenberg, eds.), (Boston: Kluwer Academic Publishers), 377-416.

Somerville, C. and Dangl, J. (2000). Plant Biology in 2010. *Science* **290**, 2077-2078.

Soppe, W.J., Bentsink, L. and Koorneef, M. (1999). The early-flowering mutant *efs* is involved in the autonomous promotion pathway of *Arabidopsis thaliana. Development* **126**, 4763-4770.

Sparrow, A.H., Price, H.J., Underbrink, A.G. (1972). A survey of DNA content per cell and per chromosome of prokaryotic and eukaryotic organisms: some evolutionary considerations. *Brookhaven Symp. Biol.* **23**, 451-494.

Steeves, T.A., and Sussex, I.M. (1989). Patterns in Plant Development. Cambridge University Press, Cambridge, UK.

Strehler, E.E., and Zacharias, D.A. (2001). Role of alternative splicing in generating isoform diversity among plasma membrane calcium pumps. *Physiol. Rev.* **81**(1), 21-50.

Sun, T-P, and Kamiya, Y. (1994). The Arabidopsis *GA1* locus encodes the cyclase *ent*-kaurene synthetase A of gibberellin biosynthesis. *Plant Cell* **6**, 1509-1518.

Swain, S.M., and Olszewski, N.E. (1996). Genetic analysis of gibberellin signal transduction. *Plant Physiol.* **112**, 11-17.

Takahashi, N., Phinney, B.O., MacMillan, J. (1991). Gibberellins. Springer-Verlag, NewYork.

Talon, M., Koornneef, M., and Zeevaart, J.A.D. (1990). Accumulation of C19-gibberellins in the gibberellin-insensitive dwarf mutant *gai* of *Arabidopsis thaliana* (L.) Heyhn. *Planta* **182**, 501-505.

Talon, M., Tadeo, F.R., and Zeevaart, J.A.D. (1991a). Cellular changes induced by exogenous and endogenous gibberellins in shoot tips of the long-day plant *Silene armeria. Planta* **185**, 487-493.

Talon, M., and Zeevaart, J.A.D. (1992). Stem elongation and changes in the levels of gibberellins in shoot tips induced by different photoperiodic treatments in the long-day plant *Silene armeria. Planta* **188**, 457-461.

Telfer, A., Bollman, K. M. and Poethig, R. S. (1997). Phase change and the regulation of trichome distribution in *Arabidopsis thaliana. Development* **124**, 645-654.

Telfer, A. and Poethig, R. S. (1994). Leaf development in *Arabidopsis*. In *Arabidopsis*. (eds. E.M. Meyerowitz and C.R. Somerville), pp. 379-401. Cold Spring Harbor. Cold Spring Harbor Press.

Telfer, A. and Poethig, R. S. (1998). *HASTY*: a gene that regulates the timing of shoot maturation in *Arabidopsis thaliana. Development* **125**, 1889-1898.

Torii, K. U., Mitsukawa, N., Oosumi, T. Matsuura, Y., Yokoyama, R., Whittier, R. F. and Komeda, Y. (1996). The Arabidopsis *ERECTA* gene encodes a putative receptor protein kinase with extracellular leucine-rich repeats. *Plant Cell* **8**, 735-746.

Tsukaya, H., Naito, S., Redei, G. and Komeda, Y. (1993). A new class of mutants in *Arabidopsis thaliana, acaulis1*, affecting the development of both inflorescences and leaves. *Development* **118**, 751-764.

Valvekens, D., Van Montagu, M. and Van Lijsebettens, M. (1988). *Agrobacterium tumefaciens*-mediated transformation of *Arabidopsis thaliana* root explants by using kanamycin selection. *Proc. Natl. Acad. Sci. USA* **85**, 5536-5540.

Vongs, A., Kalkutani, T., Martienssen, R.A. and Richards, E.J. (1993). *Arabidopsis thaliana* DNA methylation mutants. *Science* **260**, 1926-1928.

Weaver, C.D., and Roberts, D.M. (1992). Determination of the site of phosphorylation of nodulin 26 by the calcium-dependent protein kinase from soybean nodules. *Biochemistry* **31**, 8954-8959.

Weigel, D., and Meyerowitz, E.M. (1994). The ABCs of floral homeotic genes. *Cell* **78**, 203-209.

Weising, K., Schell, J. and Kahl, G. (1988). Foreign genes in plants: transfer, structure, expression, and applications. *Annu. Rev. Genet.***22**, 421-477.

Wilson, R.N., Heckman, J.W., and Somerville, C.R. (1992). Gibberellin is required for flowering in *Arabidopsis thaliana* under short days. *Plant Physiol.* **100**, 403-408.

Wilson, R.N., and Somerville, C.R. (1995). Phenotypic suppression of the gibberellin-insensitive mutant (*gai*) of Arabidopsis. *Plant Physiol.* **108**, 495-502.

Wu, K., Li, L., Gage, D.A., and Zeevaart, J.A.D. (1996). Molecular cloning and photoperiod-regulated expression of gibberellin 20-oxidase from the long-day plant spinach. *Plant Physiol.* **110**, 547-554.

Xiong, L. et al. The *Arabidopsis LOS5/ABA3* locus encodes a molybdenum cofactor sulfurase and modulates cold stress- and osmotic stress-responsive gene expression. *Plant Cell* **13**, 2063-2083.

Zambryski, P. (1988). Basic processes underlying Agrobacterium-mediated DNA transfer to plant cells. *Annu. Rev. Genet.* **22**, 1-30.

Zeevaart, J.A.D. (1971). Effects of photoperiod on growth rate and endogenous gibberellins in the long-day rosette plant spinach. *Plant Physiol.* **47**, 821-827.

Zeevaart, J.A.D., Gage, D.A., and Talon, M. (1993). Gibberellin A_1 is required for stem elongation in spinach. *Proc. Natl. Acad. Sci. USA* **90**, 7401-7405.

Zeevaart, J.A.D., Talon, M., and Wilson, T.M. (1991) Stem growth and gibberellin metabolism in spinach in relation to photoperiod. In Gibberellins (Takahashi, N., Phinney, B.O., and MacMillan, J., eds), 273-288. Springer-Verlag, New York.

Zylinska, L., Kawecka, I., Lachowicz, L., and Szemraj, J. (2002). The isoform- and location-dependence of the functioning of the plasma membrane calcium pump. *Cell Mol. Bio. Lett.* 7(4), 1037-45.